A STUDY TO INVESTIGATE RADIATION-INDUCED AND NON-RADIATION-INDUCED CAROTID ATHEROSCLEROSIS AND ENDOTHELIAL DYSFUNCTION

LI YUANXI

Ph.D

The Hong Kong Polytechnic University

2021

The Hong Kong Polytechnic University

Department of Health Technology and Informatics

A STUDY TO INVESTIGATE RADIATION-INDUCED AND NON-RADIATION-INDUCED CAROTID ATHEROSCLEROSIS AND ENDOTHELIAL DYSFUNCTION

LI Yuanxi

A thesis submitted in partial fulfilment of the requirements for

the degree of Doctor of Philosophy

August 2020

CERTIFICATE OF ORIGINALITY

I hereby declare that this thesis is my own work and that, to the best of my knowledge and belief, it reproduces no material previously published or written, nor material that has been accepted for the award of any other degree or diploma, except where due acknowledgement has been made in the text

_____ _____ (Signed)

_____LI Yuanxi_____ (Name of student)

Abstract

Both radiation and cardiovascular risk factors (CVRF) can lead to carotid atherosclerosis. The unstable carotid plaques are highly associated with cerebrovascular events. Therefore, detection and evaluation of carotid atherosclerosis and plaques characteristics are essential for individuals.

Endothelial dysfunction is the primary injury for both radiation-/hyperglycaemia-induced carotid atherosclerosis. However, the underlying mechanism is unclear.

This project aimed to investigate the feasibility of using a computer-assisted method to evaluate and differentiate the carotid plaque characteristics in radiation-/non-radiation-induced carotid atherosclerosis, and investigated the effects of radiation and high glucose on endothelial dysfunction and the possible signalling pathways involved.

In human study, 107 post-RT nasopharyngeal carcinoma (NPC) patients and 110 CVRF subjects were recruited. The carotid intima-media thickness (CIMT) and carotid plaque characteristics (plaque formation, detailed plaque texture analysis) were assessed. The correlation of risk factors and carotid plaque characteristics was evaluated by multivariate model. Study results showed post-RT NPC patients had significantly higher CIMT ($p=0.001$), plaque formations ($p<0.001$) and locations ($p<0.001$) than CVRF subjects. Besides, radiation-induced carotid plaques had significantly more calcification ($p=0.012$), but lesser lipids ($p=0.034$) than non-radiation-induced carotid plaques. Moreover, age, radiation and number of CVRF were significantly associated with carotid atherosclerosis burden ($p<0.001$). Age was significantly associated with the amount of lipid and calcification within carotid

plaques ($p<0.001$). In conclusion, post-RT NPC patients were more susceptible to carotid plaque formation, whereas CVRF subjects had carotid plaques with more lipids.

In cell line study, the cell viability, tube formation ability and various protein expressing levels of HUVECs were detected at high/low glucose level, with/without 8Gy radiation. The results found that radiation suppressed cell viability ($p<0.001$), and the combined effects of radiation and high glucose increased angiogenesis. In conclusion, caspase-promoted apoptosis and increased angiogenesis are the main cellular responses in radiation-induced endothelial dysfunction.

Publications

Scientific Journal Papers

Yuanxi Li, Vincent WC Wu, Yuan Chuang, Michael Ying et al. Ultrasound Computer-assisted Ultrasound Assessment of Plaque Characteristics in Radiation-induced and Non-radiation-induced Carotid Atherosclerosis. (Accepted by Quantitative Imageing in Medicine and Surgery, ID: QIMS-20-1012-R3).

Yuanxi Li, Michael Tin-Cheung Ying, Helen Ka-Wai Law, An Investigation of the Effects of Radiation and High Glucose on Endothelial Dysfunction (Submitted to Biochemical and Biophysical Research Communications, ID:BBRC-20-10366).

Conference Presentation

Yuanxi Li, Vincent WC Wu, Yuan Chuang, Doral LW Kwong, Shea Ping Yip, Helen KW Law, Shara WY Lee, Michael Ying. Ultrasound Assessment of Plaque Characteristics in Radiation-induced and Non-radiation-induced Carotid Atherosclerosis, the 47th Annual Scientific Meeting of the Australasian Society for Ultrasound in Medicine (ASUM) 2017, Melbourne, Australia, 6th – 8th October 2017 (Abstract, poster presentation)

Yuanxi Li, Vincent WC Wu, Dora LW Kwong, Shea Ping Yip, Michael Ying.Computer-asisted Ultrasound Assessment of Plaque Characteristics in Radiation-induced and Non-radiation-induced Carotid Atherosclerosis, the 4th Hong Kong Radiographers and Radiation Therapists Conference cum the 1st Guangdong-Hong Kong-Macau Greater Bay Area Forum on Radiological Imaging and technology, Hong Kong, China, 14th – 16th June 2019 (Abstract, oral presentation)

Acknowledgements

This work was supported by a research postgraduate studentship of the Hong Kong Polytechnic University (G.55.56. RUAS) and was carried out at the Hong Kong Polytechnic University.

Throughout my PhD journey, I owe sincere gratitude to many people. The greatest gratitude goes to my chief supervisor, Prof. Michael, Tin Cheung YING. His profound knowledge, abundant research experience and patient guidance are the great supports to me. His professional guidance in ultrasound enables me to master the carotid artery scanning from zero start. He is of great patience to conduct numerous in-depth discussions with me during the past years. His judicious insight leads me to the core questions, and always brings me one step closer to solve the problems by his constructive critical comments. His succinctly precise expression and strict attitude on manuscripts enable me a progress in scientific writing. By working and studying with him, I understand that calmness on difficulties, meticulous work attitude, and rigorous logical thinking are the substantial bricks of scientific research. It is my great honor and fortunate to be his student, obtaining the systemic and standardized guidance.

I would like to acknowledge Dr. Vincent, Wing Cheung WU, my co-supervisor. His kind concern and crucial support enable the collaboration with the Department of Clinical Oncology of Queen Mary Hospital smoothly in the data collection.

I would like to acknowledge Prof. YIP, Shea Ping, my co-supervisor. His valuable advice, everlasting passion towards research and kindly sharing of his research experience inspire me and encourage me in front of the research problem.

I sincerely thank Dr. Helen, Kai Wai LAW. She is a delicate supervisor, who understands my merits and demerits, and supports me in all aspects with her warm concern. She guides me the in vitro study of this project, spending her weekends to train my experimental techniques and habits. Her kindness, enthusiasm and hard work have impact on me in both research study and daily life.

I would also like to thank Prof. Dora KWONG, my clinical advisor, for her kind arrangement in data collection and patient recruitment in Queen Mary Hospital. Thanks are also extended to other colleagues in Queen Mary Hospital, especially to Ms. Tiffany MA and Mr. Gary WONG, for their kind assistance in patient recruitment.

I would like to acknowledge the professors from the Department of Health Technology and Informatics, PolyU, especially to Dr. Tony S. S. TO, Dr. Polly H. M. LEUNG, Prof. Jing CAI, Dr. Xiang, ZHOU, Dr. Fiona, X.Y.CHEN, Dr. Shara W. Y. LEE, Dr. Jung Sun YOO, Dr. Patrick Y. M. LAI, for their valuable comments of my study. I also appreciate the technical and administrative assistance from Mr. Bobby S. P. SHIU, Dr. Raymond K. H. HUI, Ms. Nicki W. M. KWAN., Ms. Julia P. S. YEUNG, Ms. Alison W. H. SIN, Ms. Pamela Y. N. MUI, and Mr. David W. L. LAU.

I would like to thank all the colleagues and friends in our department. They are brilliant, industrious and helpful. Discussions with them delight my daily routine, and also evoke my creative thinking. Many thanks to my roommates, Yu Hang, Li, Chen Chen and Ya Jing, for their help and caring. Grateful thanks to my best friend, Yu Ting in Beijing, for her consistent support and genuine encouragement with love and tenderness.

Finally, I would like to express my deepest gratitude to my parents, for their endless love and understanding. Special thanks go to my husband, Dr. LI, for his accompany, encouragement and support.

Table of Contents

List of Figures

List of Tables

List of Abbreviations

18F-FDG	18F-fluorodeoxyglucose
5-HT	5-hydroxytryptamine
AHA	American Heart Association
Ang II	Angiotensin II
APOL3	Apolipoprotein L3
ARFI	Acoustic radiation force impulse
ASR	Age-standardized Rate
ATCC	American Type Culture Collection
ATM	Ataxia telangiectasia mutated
bFGF	fibroblast growth factor
BM	Basement membrane
BSA	Bovine serum albumin
cAMP	cyclic adenosine 3, 5'-monophosphate
Caspases	Cysteinyl aspartate-specific proteases
CC	Common carotid
CCA	Common caroid artery
CCK8	Cell Counting Kit-8
CHD	Coronary heart disease

CI	Confidence interval
CIMT	Carotid intima-media thickness
cNH	Circulating nucleosome/histone
cNOS	Constitutive NOS
CRP	C-reactive protein
CT	Computed tomography
CTA	Computed tomography angiography
CVDs	Cardiovascular diseases
CVRF	Cardiovascular risk factor
DM	Diabetes mellitus
DMEM	Dulbecco's Modified Eagle Medium
DNA-PK	DNA-dependent protein kinase
DPTA	Digital detailed plaque texture analysis
DSBs	Double-strand breaks
EBNA1	EBV nuclear antigen 1
EBV	Epstein-Barr virus
ECA	External carotid artery
ECGS	Endothelial Cell Growth Supplement
ECM	Endothelial Cell Medium
ECST	European Carotid Surgery Trial
EGFR	Epidermal growth factor receptor
EndMT	Endothelial to mesenchymal transition
eNOS	endothelial NOS

FAK	Focal adhesion kinase
FoxO1	Forkhead box O1
GSM	Grey-scale median
HG	High glucose
HI	Heterogeneity index
HLA	Human leukocyte antigen
HMEC	Human microvascular endothelial cells
HMG-CoA	3-hydroxy-3-methylglutaryl–coenzyme
HRP	Horseradish peroxidase
HSP90	Heat shock protein 90
HUVECs	Human umbilical endothelial cells
ICA	Internal carotid artery
IL-1β	Interleukin-1β
IMPT	Intensity-modulated proton therapy
iNOS	inducible NOS
IOD	Integrated of density
IPH	Intraplaque hemorrhage
IVUS	Intravascular ultrasound
LDL	Low-density lipoprotein
LG	Low glucose

LMP1	Latent membrane protein 1
LRNC	Lipid-rich necrotic core
MCP-1	Monocyte chemotactic protein 1
MRA	MR angiography
MRI	Magnetic resonance imaging
MSC	Mesenchymal stem cells
MVA	Modified vaccinia ankara
NASCET	North American Symptomatic Carotid Endarterectomy
NF-κB	Nuclear factor-κB
nNOS	neuronal NOS
NO	Nitric oxide
NOS	Nitric oxide synthesis
NPC	Nasopharyngeal carcinoma
P/S	Penicilli/streptomycin
PAF	Platelet-activating factor
PD-L1	Programmed death-ligand 1
PET	Positron emission tomography
p-FAK	phospho-FAK
PGI2	Prostacyclin
PKC-βII	Protein kinase C- βII
p-NOS	phospho-NOS
PVDF	Polyvinylidene difluoride

p-VEGFR2	phospho-VEGFR2
RF-QIMT	Radiofrequency-based quality intima-media thickness
ROI	Region of interest
ROS	Reactive oxygen species
RT	Radiotherapy
SCC	Squamous cell carcinoma
SDS-PAGE	Sodium Dodecyl Sulfate PolyAcrylamide Gel Electrophoresis
Sema7A	Semaphorin 7A
SH2	Src homology 2
TIA	Transient ischemic attack
TIL	Tumor infiltrating lymphocyte
TOF	Time of flight
TOF-MRA	Time-of-flight MR angiography
t-PA	tissue-type plasminogen activator
UCNT	Undifferentiated carcinomas of the nasopharyngeal type
VEGF	Vascular endothelial growth factor
VEGFR2	Vascular endothelial growth factor receptor 2
vWF	von Willebrand factor

WHO	World Health Organization

Chapter One

Introduction

Nasopharyngeal carcinoma (NPC) is common in South-eastern Asia including Hong Kong. According to the WHO's report in 2018, the incidence of NPC ranked 23rd among all the cancers. However, 84.6% of the cases were found in Asia Bray et al. (2018).

Lymph node metastasis is common in NPC patients. Nasopharyngeal area is abundance of lymphatic plexus, and the epithelium is usually infiltrated by lymphocytes. Therefore, about 85% of NPC patients presented with lymphoid metastases, and neck lymph node metastasis is common in NPC patients (Ho et al., 2012).

Radiotherapy (RT) has been widely accepted to be an effective therapeutic approach for treating both the primary tumour and metastatic neck lymph nodes of NPC patients. In addition, chemotherapy may be used in conjunction with RT for patients in advanced disease stages (Lee et al., 2015). Since carotid arteries are in close proximity to the neck lymph nodes, they are inevitably irradiated during RT of neck lymph nodes. Carotid atherosclerosis is thus a common post-RT complication NPC patients received external beam irradiation to the neck. (**Figure 1.1**)

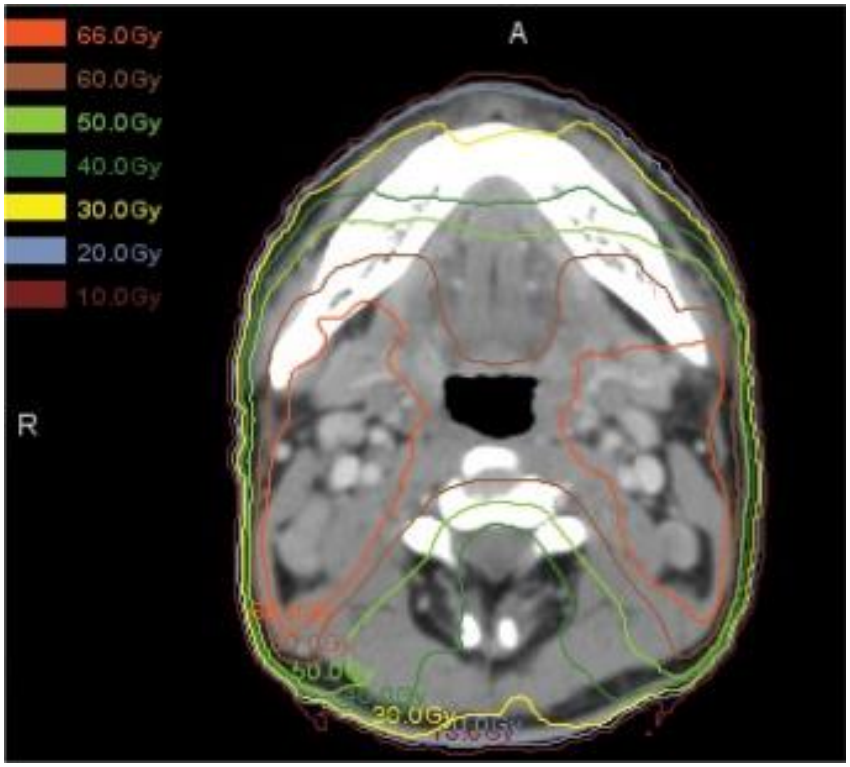

Figure 1.1 Radiologic images of dosemetric distribution in a NPC patient during the course of IMRT. (Lu et al., 2014)

Atherosclerosis is an inflammatory, chronic and systemic disease. In ancient Greek, athero means porridge, while sclerosis means indurate (Damjanov, 2012), which concisely concludes the characteristics of atherosclerosis - a soft-filled and fibrous-cap atheroma. Carotid atherosclerosis can be induced by having cardiovascular risk factors (CVRFs) and previous exposure to radiation. CVRFs can be classified into changeable factors, such as lipid metabolism-relevant factors, hypertension and cigarette smoking; and unchangeable factors, such as gender, age and heredity.

Carotid atherosclerosis is a progressive and long-term post-RT complication in NPC patients. Early detection and regular screening of carotid atherosclerosis is essential for these patients so that timely treatment and management can be provided. Subclinical atherosclerosis can be identified by the increased carotid intima-media thickness (CIMT) and the formation of carotid atherosclerotic plaque (Naqvi & Lee, 2014; Touboul et al., 2007). Previous studies showed that post-RT NPC patients had significant higher CIMT and higher prevalence of carotid plaque (Huang T. L. et al., 2013; Lam et al., 2001). As the development process of carotid atherosclerosis is complex, different characteristics of carotid plaque implicate the different degrees of atherosclerosis development (Insull, 2009). It is widely accepted that higher degree of carotid artery stenosis is associated with patients who are symptomatic of transient ischemic attack (TIA) or stroke. Moreover, the presence of vulnerable (or unstable) carotid plaque is considered a risk factor for future TIA or ischemic stroke. Therefore, carotid atherosclerosis, especially with the presence of carotid plaque, increases the risk of cerebrovascular diseases (Cheng et al., 2002; Lam et al., 2001; Lusis, 2000; Stein et al., 2008; Yuan et al., 2017). Clinically, detection of carotid atherosclerosis, regular monitoring of the progression of atherosclerosis, and identification of

vulnerable carotid plaques are of importance, especially for post-radiotherapy head and neck patients.

Medical imaging is a useful tool to assist clinicians in detecting carotid atherosclerosis and monitoring its progression, by imaging examination of patient's anatomical structures. Ultrasound, magnetic resonance imaging and positron emission tomography are common noninvasive imaging modalities for the assessment of carotid atherosclerosis. Among them, ultrasound is the most common imaging modalities used to evaluate carotid atherosclerosis because it is cost effective, does not involve ionizing radiation and easily accepted by patients. Although ultrasound assessment of carotid atherosclerosis is common, detailed investigation of the differences of radiation-induced and non-radiation-induced carotid atherosclerosis is lacking, especially for the different characteristics of carotid plaque in these two types of atherosclerosis. Interpretation of ultrasound images is subjective and dependent on the experience of reviewers. Computer-assisted ultrasound assessment has been established and applied in the assessment carotid plaque (Lal et al., 2002; Madycki et al., 2006). However, this assessment method is not common in routine examinations, and the difference in carotid plaque characteristics between radiation-induced and non-radiation-induced carotid atherosclerosis is not fully understood. Chapter 3 presented a research study that comprehensively investigated the differences in radiation-induced and non-radiation-induced carotid atherosclerosis. The study also used a computer method for analyzing ultrasound images to investigate and compare the carotid plaque characteristics of these two types of carotid atherosclerosis.

The development of radiation-induced atherosclerosis is a complicated process involving various cells and cytokines, and is considered to be initiated by endothelial

dysfunction induced by radiation. In carotid atherosclerosis, the injury of carotid artery wall increases the endothelial permeability. Monocytes are then recruited from blood stream at the injured site of arterial wall, adhere to the intima, transmigrate across the impaired endothelial barriers into the media, and differentiate into macrophages. Meanwhile, lipids transmigrate the endothelium from the circulation and form the lipoproteins by oxidative-modification. The injury of endothelium also induce the aggregation of platelets, and a release of several cytokines, which further promote the migration of smooth muscle cells (SMCs) from media to intima. Subsequently, SMCs proliferate in the intima and produce fibrous tissue that attribute to the formation of fibrous cap. (Doran et al., 2008). Macrophages play the role as scavengers to take up the lipoproteins and form foam cells which induces progressive damage of artery. The accumulation of foam cells, T-lymphocytes and SMCs form an early lesion, which is covered by deposition of extracellular matrix, and eventually causes the plaque formation and thickening of CIMT (Gujral et al., 2014). Though, the exact pathogenesis of radiation-induced carotid atherosclerosis is still unclear, but reported pathological processes involve cell apoptosis, inflammatory response, nitric oxide synthesis, and angiogenesis (Han et al., 2018; Hess et al., 2001; Leborgne et al., 2003; Leborgne et al., 2005; Paris et al., 2001)., Moreover, vulnerable carotid plaques are characterized with thin fibrous cap, lager amount of lipids and intra-plaque hemorrhage, and are reported to be more predispose to cerebrovascular diseases. (Hollander et al., 2002; Molloy & Markus, 1999). Therefore, it is valuable to compare radiation-induced and non-radiation-induced endothelial dysfunction in vitro, and explore the possible signaling pathways involved. The related research study is presented in Chapter 4.

Chapter Two

Literature Review

2.1 Nasopharyngeal Carcinoma

2.1.1 Epidemiology of NPC

Nasopharyngeal carcinoma (NPC) is a regionally related cancer, which mostly occurs in the Southern China. In 2018, 129,079 new NPC cases were reported globally, constituting 0.7% of all cancer cases in that year. However, about 77% new cases were from South-eastern and Eastern Asia. The age-standardized rates (ASR) of incidence and mortality are shown in **Figure 2.1** (Bray et al., 2018; Gujral et al., 2016). NPC is also known as "Guangdong Cancer". Although the incidence of NPC in Hong Kong demonstrated a steady decrease since 1980's (overall decrease of 30%), NPC is more common in such endemic areas compared to the other regions (Lee et al., 2003). In Hong Kong, the incident rates of NPC was 7.4/100,000 in 2016, while less than 1/100,000 populations in North America and Europe according to the data of Union of International Cancer Control in 2014. The incidence data showed a peak in middle-aged and senior population from 40 to 65 years and the incidence of male patients was almost 3 times than that in female patients according to the Hong Kong Registry in 2016.

A.

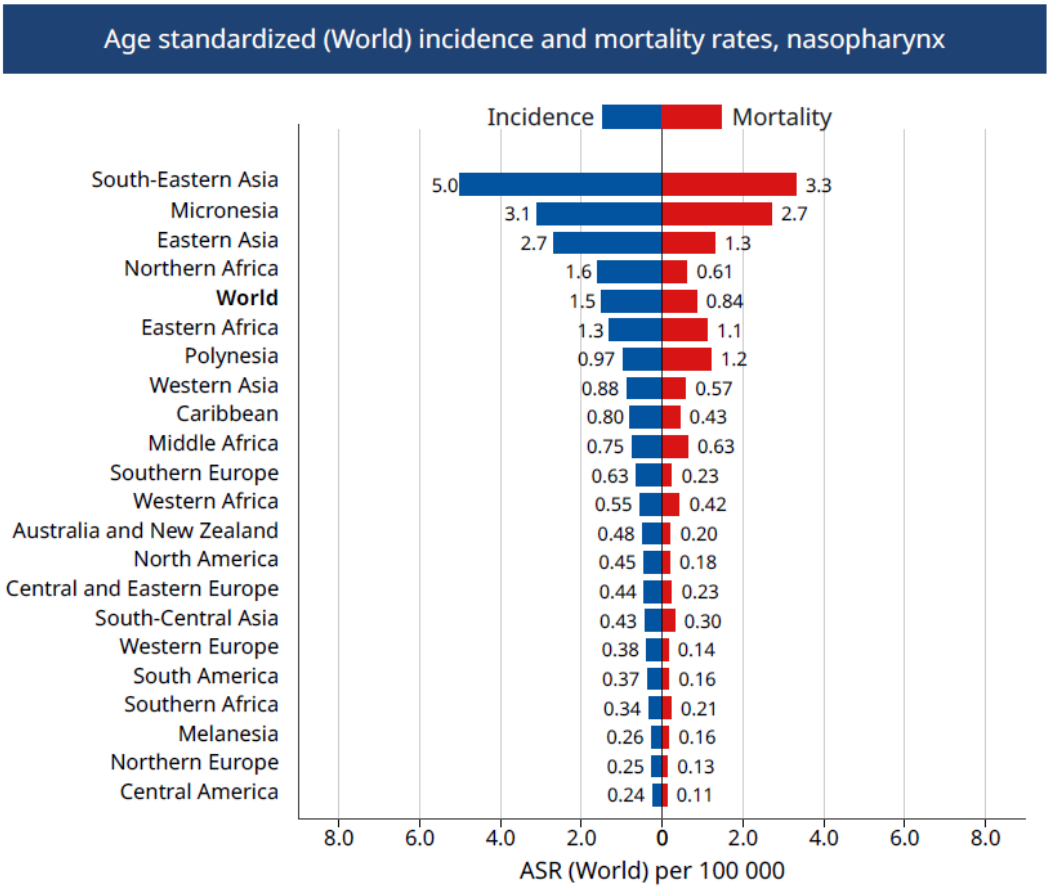
Age standardized (World) incidence and mortality rates, nasopharynx
Incidence
Mortality
South-Eastern Asia 5.0 3.3
Micronesia 3.1 2.7
Eastern Asia 2.7 1.3
Northern Africa 1.6 0.61
World 1.5 0.84
Eastern Africa 1.3 1.1
Polynesia 0.97 1.2
Western Asia 0.88 0.57
Caribbean 0.80 0.43
Middle Africa 0.75 0.63
Southern Europe 0.63 0.23
Western Africa 0.55 0.42
Australia and New Zealand 0.48 0.20
North America 0.45 0.18
Central and Eastern Europe 0.44 0.23
South-Central Asia 0.43 0.30
Western Europe 0.38 0.14
South America 0.37 0.16
Southern Africa 0.34 0.21
Melanesia 0.26 0.16
Northern Europe 0.25 0.13
Central America 0.24 0.11
8.0 6.0 4.0 2.0 0 2.0 4.0 6.0 8.0
ASR (World) per 100 000

B.

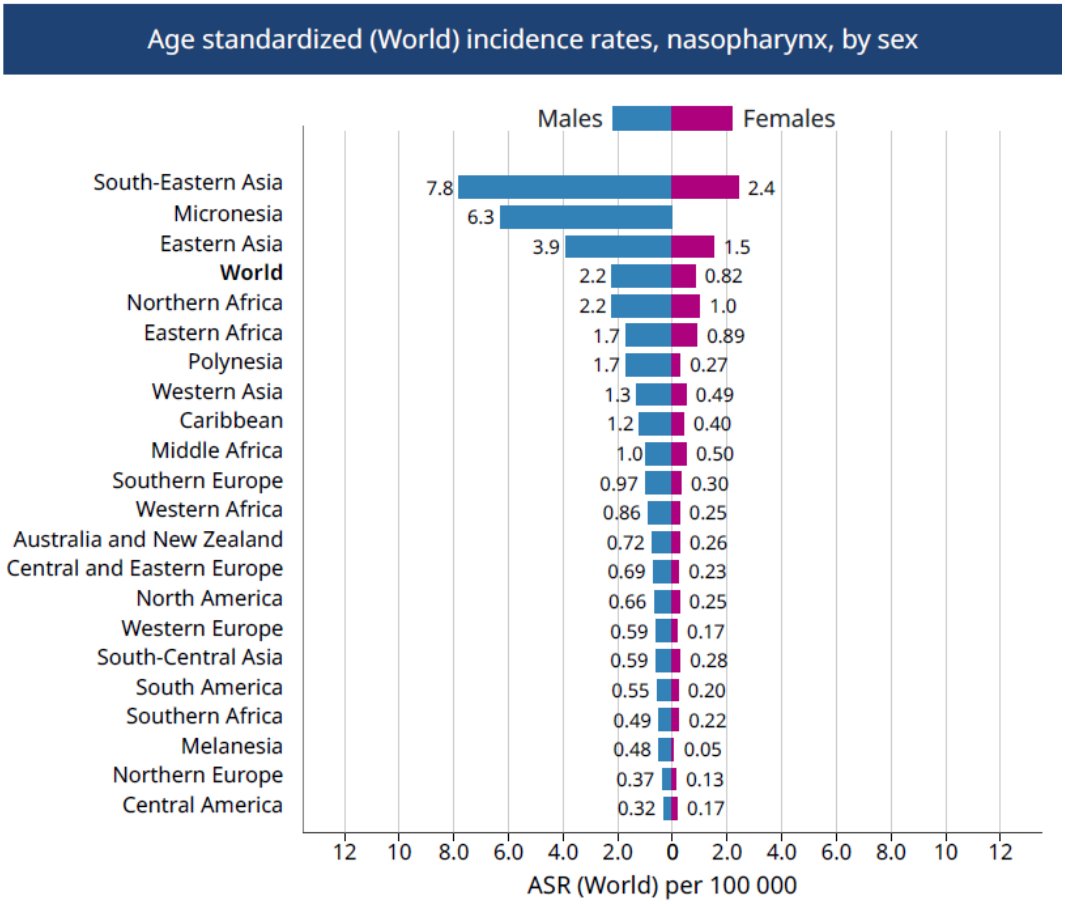

Figure 2.1 Epidemic data of NPC incidence in 2018 (A) Age-standardized and mortality rates of NPC cases in both genders worldwide are shown. **(B)** Age-standardized rates of NPC cases by male and female are shown. The figures and data are quoted from the webpage of the Global Cancer Observatory, possessed by the International Agency for Research on Cancer (IARC).

2.1.2 Etiology and Pathogenesis of NPC

The etiological factors leading to NPC include the lifestyle, gene, and Epstein-Barr virus (EBV).

Environmental carcinogens, such as lifestyle, may attribute to the dysplasia of nasopharynx. People living in the Southern China develop the diet habit of having preserved food (salted fishes and preserved vegetables), which contain carcinogenic nitrosamines and could give rise to the progression of NPC (Barrett et al., 2019; Tsao et al., 2014). Chinese living in the United States, with a diet of less preserved food, were less likely to develop NPC when compared to Chinese living in the Southern China, who frequently having the salted food (Buell, 1974; Dickson & Flores, 1985).

Genetic factor is also attributed to the development of NPC. It is more susceptible for Chinese to NPC than any other ethnicities (Buell, 1974; Dickson & Flores, 1985). People having familial history of NPC are more risky to the disease, especially for whom develops NPC at early age (≤20 years) (Chen Y.-P. et al., 2019; Ng et al., 2005; Zeng & Jia, 2002). It was reported that individuals with the genotypes of human leukocyte antigen (HLA) HLA-A2 are more vulnerable to NPC, including the HLA types of AW19, BW46, and B17 (Glastonbury, 2007; Liebowitz, 1994). In addition, the complex chromosome aberration is widely demonstrated in NPC patients, such as the depletion of chromosomes 3p (Deng et al., 1998; Lo et al., 2000; Tjia et al., 2005; Wu, 2006).

The endemic NPC is usually associated with EVB (Tsang et al., 2020). EBV-associated NPC is characterized by the persistence of an episomal EBV genome, with

the detection of EBV DNA or transcripts (such as latent membrane protein 1, latent membrane protein 2, and EBV-encoded small nuclear RNA) in tumor cells (Dawson et al., 2012; Yoshizaki, 2002; Yoshizaki et al., 2007). EBV-associated NPC is also characterized by the demands of multiple viral latent gene products to facilitate malignant transformation, with the presence of a clonal EBV genome in both NPC and precancerous lesions (Hau et al., 2020). Given to the above properties, EBV could be a predictor to identify the individuals who are at risk of early NPC (Chan et al., 2013; Ji et al., 2014). Besides, the levels of EBV could be the indicator of prognostic value of NPC patients (Du et al., 2019; Zhang et al., 2015). In addition, it could also be used as a therapeutic target in treatment (Hau et al., 2020).

2.1.3 Histological Classification of NPC

On the basis of the histopathological features, NPC is categorized into three subtypes according to the World Health Organization (WHO) criteria: keratinising squamous carcinoma, non-keratinising squamous carcinoma and undifferentiated non-keratinising carcinoma, named as Type I , Type II and Type III respectively (Chen Y.-P. et al., 2019; Shanmugaratnam, 1978).

Keratinising squamous carcinoma (Type I) is well differentiated carcinoma, with the presence of the intercellular bridges with/without keratinization in a large area. Non-keratinising squamous carcinoma (Type II) demonstrates the different levels of cell differentiation, containing matured and anaplastic at the same time. Undifferentiated non-keratinising carcinoma (Type III) does not contain keratin and has specific-growth-pattern cells (Shanmugaratnam, 1978; Zeng & Zeng, 2010).

As both Type II and Type III are non-keratinising, they are generally classified into the same category, and therefore NPC can be simplified as squamous cell carcinoma (SCC) and undifferentiated carcinomas of the nasopharyngeal type (UCNT) (Yoshizaki et al., 2012). In the globe, less than 20% of NPC cases were keratinising subtype (Type I). In endemic areas, such as the Southern China, the incidence of Type I NPC is even lower, while non-keratinising subtypes (Type II and Type III) account for more than 95% of NPC patients and notably associated with EBV infection (Chen Y.-P. et al., 2019; Pathmanathan et al., 1995; Wang et al., 2016; Young & Dawson, 2014).

2.1.4 Existing Treatments for NPC

The common therapeutic approaches for NPC include radiotherapy, chemotherapy, immunotherapy and molecular-target therapies. Because of the high sensitivity of the tumor to ionizing radiation and chemicals, radiotherapy is the primary therapeutic approach with or without chemotherapy.

2.1.4.1 Radiotherapy

Radiotherapy (RT) is the standard treatment for NPC patients, applied alone or in combination with chemotherapy depending on stages of the disease (Lee et al., 2012). RT treatments have developed from the conventional 2D RT to 3D conformal RT, and till the present intensity-modulated radiotherapy (IMRT).

IMRT is the mainstay modality for treating NPC by optimising the dosimetric planning, and performs higher locoregional control and survival, but lower toxicity. It was reported that IMRT can reduce the 5-year incidence of locoregional failure to 7.4%

in patients who have no metastasis and are newly diagnosed (Mao et al., 2016). Intensity-modulated proton therapy (IMPT) manifests the dosimetric advantages in treating NPC, minimizing the damage to normal tissues by delivering less radiation. A study of a small group of NPC patients found that IMPT could reduce the radiation dose to normal tissues, and increase the two-year locoregional control to as high as 100% and the two-year survival to 88.9% (Lewis et al., 2016).

Epidemic data showed that 92.2% of post-RT patients survived 3 years after the treatment. Besides, 67.1% to 81.6% of post-RT patients survived without distant metastases 5 years after the RT (Chen et al., 2013; Peng et al., 2012; Qi et al., 2011).

Metastases in neck lymph nodes are common in NPC patients because of the rich submucosal capillary lymphatic plexus of the nasopharynx. In a previous study with 2679 NPC patients, 86% of the cases had metastatic neck lymph nodes (Wang et al., 2015). Besides, up to half of the NPC patients were found to have bilateral cervical lymph nodes metastases because nasopharynx is on the body's central axis (Sham et al., 1990; Tang et al., 2008).

RT is also commonly used for treating lymph nodes metastasis in NPC patients. A retrospective study reported that up to 40% of patients without the prophylactic irradiation had subsequent nodal metastasis (Lee et al., 1992). These patients were more likely to develop distant metastases than those without nodal metastases (Lee et al., 1992). Therefore, prophylactic irradiation of cervical region is recommended for NPC patients (Biau et al., 2019; Wang et al., 2012).

2.1.4.2 Chemotherapy

Chemotherapy is commonly used for treating locoregional advanced NPC and usually applied in combined with RT (called chemoradiotherapy). There are different kinds of concurrent chemotherapy regiments, varying in chemical agents and intake dosage. Cisplatin is the most common agents, whereas others including nedaplatin, uracil plus tegafur and oxaliplatin (Kwong et al., 2004; Tang et al., 2018; Wu et al., 2013).

For an optimal efficacy, the threshold of Cisplatin dosing schedule may be 200 mg/m^2 and 160 mg/m^2 cumulatively without/with the further induction chemotherapy, respectively (Lee et al., 2011; Loong et al., 2012; Lv et al., 2018; Peng et al., 2016).

Several trials have reported that concurrent chemoradiotherapy improved the outcomes in stage III-IV NPC patients, when compared to RT alone (Chen et al., 2013; Lee et al., 2011; Lee et al., 2010; Wee et al., 2005). In stage II NPC patients, chemoradiotherapy improved overall survival, while outcomes (such as loco-regional relapse-free survival and distant metastasis-free survival) were inconclusive in various studies. A recent phase III randomized trials demonstrated that chemoradiotherapy improved 5-year overall survival rate (HR of death=0.30, 95% CI: 0.12 to 0.76, P=0.007), progression-free survival (HR of progression=0.45, 95% CI: 0.23 to 0.88, P=0.017) and distant metastasis-free survival (HR of distant relapse=0.27, 95% CI: 0.10 to 0.74, P=0.007). However, no statistical difference was found in 5-year loco-regional relapse-free survival rate (HR of locoregional relapse=0.6, 95% CI: 0.25 to 1.51, P=0.29) (Chen et al., 2011). Another meta-analysis (include 11 studies and 2138 patients) reported that chemoradiotherapy benefited the clinical outcomes with a higher overall survival (HR=0.67, 95% CI: 0.45-0.98, P=0.04) and loco-regional

relapse-free survival (HR=0.61, 95% CI: 0.46-0.80, P=0.0003) than RT alone, while no significant difference in distant metastasis-free survival (HR=0.83, 95% CI: 0.52-1.31, P=0.41) (Xu et al., 2017). Therefore, the improvement of overall survival rate was found in NPC patients who received chemoradiotherapy, when compared to RT alone.

2.1.4.3 Immunotherapy

Immunotherapy and molecular-target therapies are the treatment options for metastasis. Immunotherapy contains the strategies of EBV-targeted vaccination, adoptive T-cell treatment and immune checkpoints blockades.

Most of endemic NPC are infected by EBV and have consistent presence of the virus, which offer the possibility of targeting these cells in immune T-cell system through recognizing the specific viral antigens. Such expressed viral antigen targets include EBNA1, latent membrane protein 1 (LMP1), and LMP2 (Chen Y.-P. et al., 2019). Clinically, adoptive transfer of LMP2-specific cytotoxic T lymphocytes and dendritic cell-based vaccines targeting LMP2 epitopes have demonstrated the curative efficacy in NPC of advanced stage (Chia et al., 2012; Kong et al., 2018; Louis et al., 2010). In addition, modified vaccinia ankara (MVA-EL) could amplify EBV nuclear antigen 1 (EBNA1)-specific or LMP2-specific T lymphocytes in patients who retain EBV DNA load after traditional treatments (Taylor et al., 2004).

Recent trials of immune checkpoint blockade treatments also showed a prosperctive progress in NPC therapy. NPC tumors are widely known with high expressions of programme death ligand 1 (PD-L1) (Ma et al., 2018), and anti-PD1 antibodies therapies have a promising therapeutic efficacy on tumors. Thus, there are on-going

clinical trials testing the efficacy of anti-PD1 antibodies. The study results of these trials could offer the valuable cues in NPC treatment strategies by immunotherapy (Chen Y. P. et al., 2019).

2.1.4.4 Molecular-target therapies

Apart from the antigens and checkpoints, certain molecules could also be used as the therapeutic targets, such as epidermal growth factor receptor (EGFR) and vascular endothelial growth factor (VEGF). Such biomarkers are related to the development of NPC. Therefore, several antibodies against the above targets, including cetximab (Chan et al., 2005), sunitinib (Hui et al., 2011; Hui et al., 2011), famitinib, axitinib and pazopanib (Huang Y. et al., 2013; Hui et al., 2012; Lim et al., 2011) could be used to treat NPC, and there are ongoing clinical trials to evaluate their treatment efficiacy (Chen Y.-P. et al., 2019).The results of these studies and trils may provide more evidence in molecular-target therapies of treating NPC.

2.2 Carotid Atherosclerosis

Atherosclerosis is a chronic, systemic and inflammatory disease involved in complicated aetiology and pathology, which is characterized by the presence of soft-content and fibrous-cap atheroma. Atheroma formation primarily originates from the endothelial dysfunction occurred on the innermost of blood vessel wall (Lusis, 2000).

Carotid atherosclerosis is a manifestation of vascular damage when patients have one or more cardiovascular risk factors such diabetes, hypertension, etc. In addition,

carotid atherosclerosis is a late post-RT complication in patients who have received external irradiation to the head and neck regions. As a chronic inflammatory disease, subclinical carotid atherosclerosis is identified by the increased carotid intima-media thickness (CIMT) and the formation of carotid atherosclerotic plaque (Naqvi & Lee, 2014; Touboul et al., 2007). The development of carotid atherosclerosis is progressive, and therefore different characteristics of carotid plaques represent different stages of atherosclerotic development. It is generally believed that atherosclerosis is initiated by endothelial dysfunction lining on the surface of blood vessel wall. The injured endothelium elicits the sub-endothelial accumulation of cholesterol, namely oxidized low-density lipoprotein (LDL). Monocyte-derived macrophages and lymphocytes are then recruited at the intima, causing the formation of foam cells. Meanwhile, smooth muscle cells (SMC) migrate from the media and are recruited at the lesion site. The accumulation of cells thickens the CIMT and alternates the endothelium to a pro-inflammation, pro-thrombosis, pro-coagulation, fibrosis and vasoconstriction, resulting in more severe damage of the homeostasis on blood-tissue interface and eventually forming the plaque (Lusis, 2000; Ross, 1999; Sumpio et al., 2002).

2.2.1 Anatomy of Carotid Artery

Carotid artery is a large artery which supplies oxygenated blood to the brain and other organs in the head and neck. The carotid artery wall contains three layers. From the innermost to outmost, they are tunica intima, tunica media and tunica external (also called adventitia), respectively. The intima is structured as a monolayer of endothelial cells lined on the internal elastic lamia. The media is composed of smooth muscle cells supported by external elastic lamia, and the adventitia is composed of various types of

cell, including resident progenitor cells, fibroblasts and vasa vasorum endothelial cells (Stenmark et al., 2013). **(Figure 2.2A)**

Carotid arteries situated on both sides of the neck, dividing into four segments, which are internal carotid artery (ICA), carotid bulb (also known as carotid bifurcation), external carotid artery (ECA) and common carotid artery (CCA) **(Figure 2.2B).** The CCA branches into ICA and ECA at the carotid bulb, supplying oxygenated blood to the head and neck regions. The ECA supplies blood to numerous structures in the face, lower jaw, neck, esophagus, and larynx. The ICA is one of the primary supplies of blood to the human brain.

A. **B.**

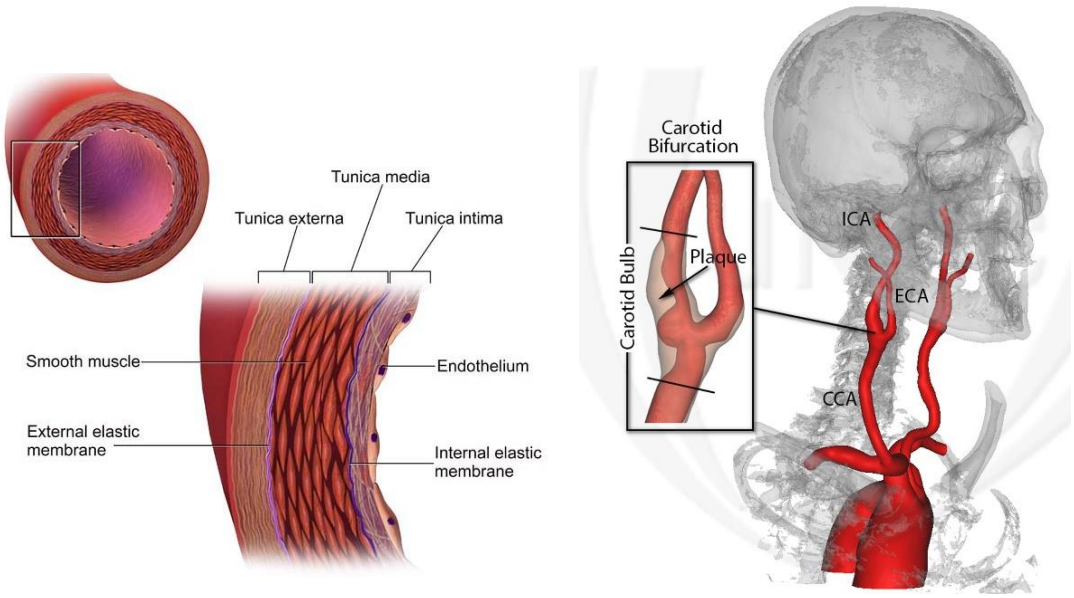

Figure 2.2 The structure of artery wall and anatomy of carotid artery. Carotid artery wall is structured by three layers: the intima (a single layer of endothelium lined on the internal elastic lamina), the media (smooth muscle cells and external elastic membrane) and the adventitia (connective tissues). The carotid arteries are on both sides of the neck. The common carotid artery branches into the internal and external carotid artery, supplying blood to the head and neck. (Rogers & Lowe, 2017 and Kamenskiy et al., 2015)

2.2.2 Risk Factors of Carotid Atherosclerosis

A variety of factors are considered to play role in initiating and progressing the development of atherosclerosis. Based on the difference of these factors, carotid atherosclerosis can be classified into two categories, namely cardiovascular risk factors (CVRFs)-induced carotid atherosclerosis and radiation-induced carotid atherosclerosis.

Cardiovascular risk factors (CVRFs) refer to traditional risk factors leading to the development of cardiovascular diseases, such as diabetes mellitus, hypertension, hypercholesterolemia, heart disease, and smoking. Meanwhile, radiation is another independent risk factor for the development of carotid atherosclerosis.

2.2.2.1 Cardiovascular Risk Factors (CVRFs)

2.2.2.1.1 Diabetes mellitus

Diabetes mellitus (DM), as a main risk factor inducing carotid atherosclerosis, is defined when the fasting plasma glucose level is than 7.0 mmol/L or the blood glucose level higher than 6.1 mmol/L (Alberti K. G. & Zimmet P. Z., 1998).

Inflammation, dyslipidemia and obesity are the risk factors of diabetes, which are the overlap-primary factors inducing carotid atherosclerosis. The underlying mechanisms of diabetes include upregulation of inflammatory, oxidative stress and activation the immune system, which are highly related to the pathophysiological processes of carotid atherosclerosis and exacerbates the progession of carotid atherosclerosis (Low Wang et al., 2016; Petrie et al., 2018). Hence, type 2 diabetes patients have a severer atherosclerotic burden in terms of the larger carotid artery wall thickness and higher

stiffness, and higher carotid artery stenosis, and the patients are more easily to have cerebrovascular events (Giannarelli et al., 2012; Matsumoto et al., 2002; Yuan et al., 2017).

2.2.2.1.2 Hypertension

Hypertension is defined when either the diastolic blood pressure higher than 90 mmHg or the systolic blood pressure is higher than 140 mmHg (Carretero O. A. & Oparil S., 2000).

Atherosclerosis can be prevalently found in patients with hypertention (Ambale Venkatesh et al., 2014; Cochain & Zernecke, 2015; Doyle, 1991). Several pathophysiological responses are involved in hypertention patients, including cell proliferation, endothelial dysfunction, fibrosis, immune regulatory T cells, oxidative stress and vascular remodeling (Ambale Venkatesh et al., 2014; Cochain & Zernecke, 2015; Libby, 2012). Consequently, patients having hypertension are more susceptible to atherosclerosis and suffer from cerebrovascular diseases (Ghiadoni et al., 1998; Hurtubise et al., 2016; Su et al., 2001).

2.2.2.1.3 Hypercholesterolemia

Hypercholesterolemia is an undisputed risk factor to cardiovascular diseases, which is defined as fasting total cholesterol concentration is higher than 6.22 mmol/L (240 mg/dL) (Song et al., 2017). Since atherosclerosis is affected by oxidized-LDL, cholesterol plays a dominant role in the development and progression of atherosclerosis. The accumulation of lipids at atherosclerotic lesion is related to the presence of concentrated serum cholesterol which causes thickening and stiffening of artery wall (Baldassarre et al., 2000). LDL-induced inflammatory responses can be appeared as early as childhood in patients with familial hypercholesterolemia

(Bernelot Moens et al., 2017; Christensen et al., 2017; Holven et al., 2017). Besides, patients with familial hypercholesterolemia are found to have higher circulating pro-inflammotary monocytes which facilitates the migration of monocytes to arterial wall (Holven et al., 2017).

Hypercholesterolemia is common in populations with changes of dietary. The latest survey reported that the weighted prevalence of hypercholesterolemia elevated from 1.6% (2.1% urban, 1.0% rural) in 2002 to 6.0% (6.4% urban, 5.1% rural) in 2012 (Song et al., 2017). The increase in the prevalence of hypercholesterolemia is due to the decrease in plant food intake, while increase in fatty food intake over the past 10 years.

2.2.2.1.4 Heart disease

Heart disease (mainly refers to coronary heart disease (CHD)) is an outcome of inflammatoty disease resulted from genetic, lifesyle and biochemical factors. CHD can be predicted by measuring CIMT, as CIMT is highly associated with the progression of atherosclerosis (Chambless et al., 1997; Polak & O'leary, 2015; Salonen & Salonen, 1991). Researchers found that CHD patients tend to have narrowed carotid arteries and greater CIMT (Chambless et al., 1997; Salonen & Salonen, 1991). Therefore, CHD is highly associated with carotid atherosclerosis, and increased CIMT is a predictor of CHD.

2.2.2.1.5 Smoking

Smoking, as an extensively-accepted risk factor of atherosclerosis, induces atherosclerosis by promoting inflammation, oxidative stress, autophagy and endothelial dysfunction (Babic et al., 2019; Prochaska & Benowitz, 2015). Nicotine is the main compound of cigarette, which could increase the expressions of several

inflammatory factors, such as C-reactive protein (CRP), nuclear factor-κB (NF-κB), interleukin-1β (IL-1β) and necrosis factor-α (TNF-α) (Lau et al., 2006; Wang et al., 2004; Wang et al., 2019). Recent study also suggested that nAChRs/reactive oxygen species (ROS)/NF-κB pathway may be the potential underlying mechanism of inducing autophage and phenotype changes of vascular smooth muscle cells, which promote the progression of atherosclerosis(Wang et al., 2019). It was reported that the baseline value of CIMT of smokers was 1185 μm (95% confidence interval [CI]: 1082-1287), and increased by 93 μm (95% CI: 25-161) and 108 μm (95% CI: 33-183) after 1 and 3 years of cigarette consumption, respectively (Zingg et al., 2016). Therefore, prevention and early cessation of smoking can help to prevent atherosclerotic diseases (Ding et al., 2019; Zingg et al., 2016).

2.2.2.2 Cumulative Effects of CVRFs on Carotid Atherosclerosis

The above-mentioned CVRFs could promote the atherosclerosis by interplaying each other and exert the complex effects on atherosclerosis (Doyle, 1991).

Previous studies demonstrated the association between carotid atherosclerosis and cumulative effect of CVRFs (Omisore et al., 2018; Takahashi et al., 2007). An Italian research group recruited 630 male and 718 female subjects (aged 18 to 99 years) from the local population and examined their carotid artery by ultrasound. They found that the worldwide incidence of carotid atherosclerosis is 25.4% for males and 26.4% for females. Besides, in middle-aged and elderly subjects, age ($p < 0.001$), systolic blood pressure ($p<0.01$), the protection of high density lipoprotein cholesterol ($p<0.037$) and smoking ($p<0.0001$) had significantly positive association with the severity of carotid atherosclerosis in terms of the presence of carotid plaque and degree of carotid artery stenosis (Prati et al., 1992).

Similar situation is occurred in Asian population. A previous Korean study of 20,712 subjects showed that the degree of carotid artery stenosis higher than 50% was significantly associated with the male (OR, 3.46; 95% CI, 2.12-5.66), advancing age (OR, 1.11; 95% CI, 1.1-1.13), hypertension (OR, 1.69; 95% CI, 1.25-2.28), DM (OR, 1.41; 95% CI, 1-1.99), and ischemic heart disease (OR, 1.93; 95% CI, 1.29-2.87) (Roh et al., 2011). Recently, another Korean study with 3030 subjects showed that the incidence of carotid artery stenosis was 1.1% and carotid plaque formation was 5.7%. Moreover, age (OR, 1.07; 95% CI, 1.03-1.12), hypertension (OR, 3.16; 95% CI, 1.34-7.46), smoking history (OR, 6.81; 95% CI, 1.66-27.93) and present smoker (OR, 6.97; 95% CI, 1.78-27.31) are the risk factors for carotid artery stenosis. Older than 80 years (OR, 8.11; 95% CI, 3.45-18.93), male gender (OR, 2.16; 95% CI, 1.29-3.61) , hypertension (OR, 1.72; 95% CI, 1.21-2.45), and hyperlipidemia (OR, 1.84; 95% CI, 1.30-2.62) are associated with the presence of carotid plaques (Woo et al., 2017). In China, a previous study also indicated that subjects with more CVRFs tended to have more severe carotid atherosclerosis (i.e. presence of carotid plaque and higher plaque score) (Yuan et al., 2014).

2.2.2.3 Radiation

Apart from traditional CVRFs, radiation is regarded as an independent factor inducing and aggravating carotid atherosclerosis, especially for head and neck cancer patients with previous radiotherapy (Yuan et al., 2017).

Although radiotherapy is an established strategy for treating NPC patients, it causes various radiation-induced complications. Neck lymph node metastases are often found in NPC patients, and RT is commonly used to treat metastatic neck lymph nodes. Since neck lymph nodes are situated closely to the extracranial carotid arteries, they are

unavoidably irradiated during RT of neck lymph nodes. Ionizing radiation can produce free radicals, which are the primary causes of endothelial dysfunction (Borghini et al., 2013; Jin et al., 2010). Endothelial dysfunction can result in downstream biological processes, which are different forms of compensatory effects for maintaining a stable homeostasis. These effects include elevated adhesiveness to leukocytes or platelets (Ross, 1999); activation of the property of pro-coagulant; down-regulation of the nitric oxidative synthesis and promotion of vasovascular molecule production (Upchurch et al., 1997). If these responses continue, without reverting to the basic homeostasis, the artery wall would be thickened.

It was widely reported that radiation is a risk factor of carotid atherosclerosis and associated with increased carotid arterial stiffness, CIMT, carotid artery stenosis and plaque burden (Chang et al., 2009; Cheng et al., 1999; Gujral et al., 2016; Yuan et al., 2017; Zaletel et al., 2018).

In a study of post-RT patients suffering from childhood cancers, the patients' arterial stiffness is significantly higher than non-irradiated age-matched controls (Zaletel et al., 2018). In a study of 290 head and neck cancer patients (192 post-RT patients; 98 no RT controls), post-RT patients had a significantly higher carotid plaque score than the non-irradiated patients (Chang et al., 2009). RT was one of the risk factors for high carotid plaque score, which was negatively correlated with age in post-RT patients >50 years, but positively correlated with age in post-RT patients ≤41 years (Chang et al., 2009). Moreover, previous studies documented the close relationship of radiation and higher CIMT and more severe carotid plaque burden, suggesting that CIMT could be a surrogate marker of cerebrovascular diseases in post-RT patients (Gujral et al., 2016; Yuan et al., 2017).

Post-RT duration is associated with the severity of radiation-induced carotid atherosclerosis. As carotid atherosclerosis is a chronic inflammatory disease, it is asymptomatic for most post-RT patients at the early stage of post-RT period. Therefore, the long-term effect of radiation is particularly important for post-RT patients. It was found that post-RT duration > 5 years could predict the severe stenosis (≥70%) of ICA/CCA (Cheng et al., 1999). Another study reported that a post-RT duration of ≥ 9 years is more susceptible to carotid atherosclerosis (Yuan et al., 2014).

2.3 Medical Imaging of Carotid Atherosclerosis

Clinically, medical imaging is commonly used for screening of patients who are of high risk of carotid atherosclerosis. It can also help in diagnosis of the disease, and monitoring disease progress and treatment responses. This section introduces the common medical imaging modalities that are used in evaluation of carotid atherosclerosis with an emphasis on the ultrasound assessment and its common assessment parameters.

2.3.1 Ultrasound (US)

Ultrasonography is easily available, low cost, non-invasive and does not involve ionizing radiation. Therefore, it is commonly used for screening purposes such as screening of individuals who are of high risk of carotid atherosclerosis. It also helps in treatment planning of patients with carotid atherosclerosis to reduce the risk of stroke (Brinjikji et al., 2015).

2.3.1.1 Carotid Artery Stenosis

Carotid artery stenosis serves as a critical parameter to evaluate the severity of carotid atherosclerosis, and is the assessment of arterial lumen diameters of stenotic and normal segments of artery (**Figure 2.3**). Thus, the severity of carotid atherosclerosis can be quantified by evaluating the degree of stenosis.

Three methods are mainly used to quantify the changes of arterial lumen diameter, namely European Carotid Surgery Trial (ECST), North American Symptomatic Carotid Endarterectomy Trial (NASCET) and common carotid (CC) (Group, 1991). The ECST measured the degree of stenosis by the percentage of reduction relative to the diameter of the artery at the stenotic site (**Figure 2.4A**) (Group, 1991; Rothwell et al., 1994). Similarly, the stenosis is quantified as the percentage of reduction in the stenotic lumen diameter in NASCET, but the baseline diameter of NASCET was the arterial lumen diameter distal to the stenosis (**Figure 2.4B**) (North American Symptomatic Carotid Endarterectomy Trial et al., 1991). Without substantial difference, the CC method used the diameter of CCA (proximal to carotid bulb) as the baseline lumen diameter (**Figure 2.4C**) (Williams & Nicolaides, 1987).

All the mentioned methods share the same rationale, which is employing the percentage of lumen reduction to estimate the degree of stenosis. The percentage of arterial lumen reduction is calculated as the luminal diameter of the artery at the stenotic site relative to the normal luminal diameter of the artery. However, measurement discrepancies exist amongst different techniques. Despite the NASCET and ECST methods are the most commonly adopted in the clinical practice and researches, obvious variations in the measurement of carotid artery stenosis are found

between the two techniques (Rothwell et al., 1994). Therefore, interpretation of results in previous studies that used different techniques should be in caution.

Following these method, patients could be stratified based on the different degrees of carotid artery stenosis: normal, mild-stenosis (1-29%), moderate-stenosis (30-69%), severe-stenosis (70-99%), or occluded (Cumming & Morrow, 1994).

A.

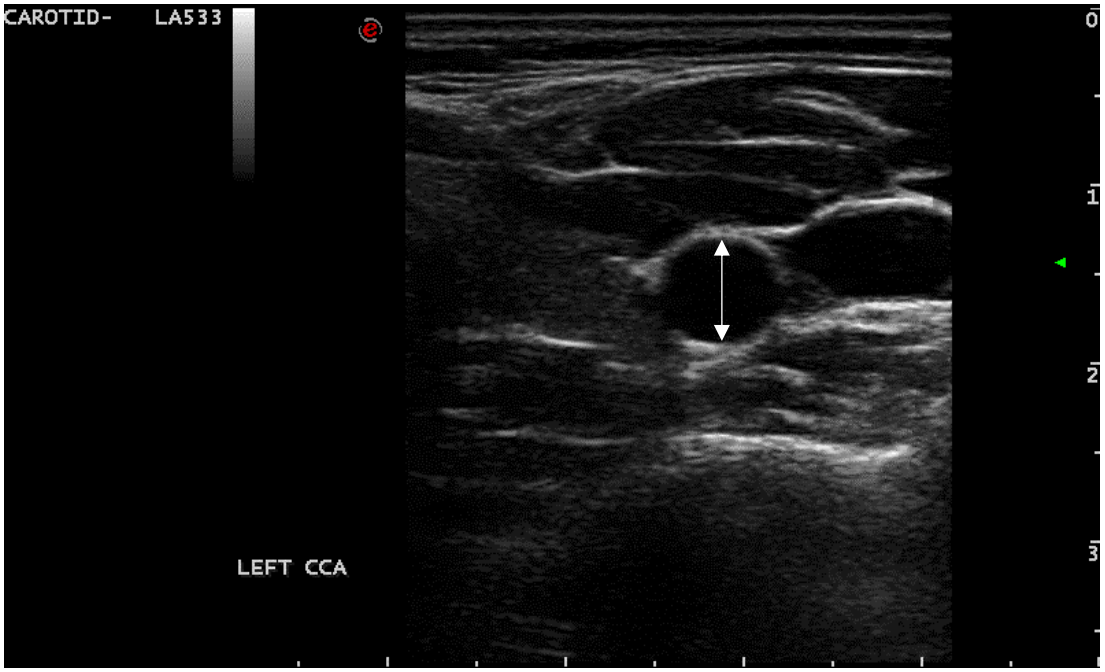

B.

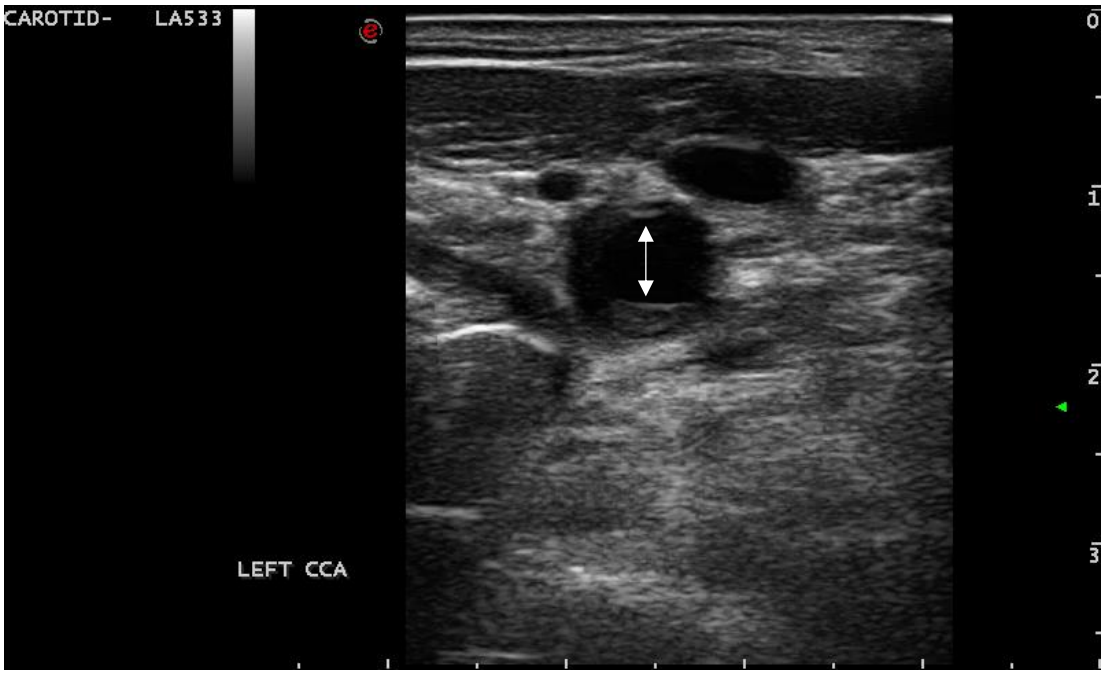

Figure 2.3 Ultrasonography imaging of carotid stenosis Image **A** shows a grey scale ultrasound image of normal carotid artery (white double-arrow) in transverse cross-section, while image **B** shows a narrowed carotid arterial lumen (yellow double-arrow) in transverse view.

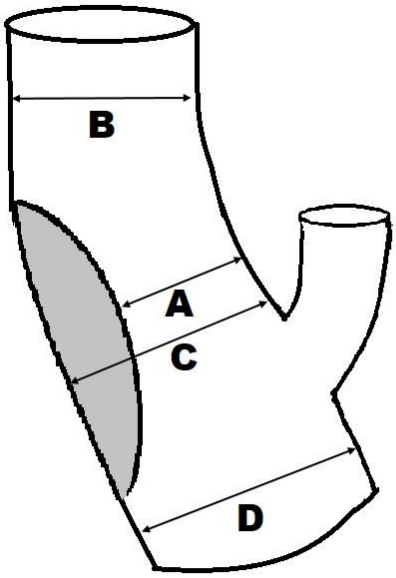

Stenosis by ECST: $\frac{C-A}{C} \times 100\%$

Stenosis by NASCET: $\frac{B-A}{B} \times 100\%$

Stenosis by CC: $\frac{D-A}{D} \times 100\%$

Figure 2.4 Different methods to determine the degree of carotid stenosis Different measurements of carotid stenosis are indicated by images **A**, **B** and **C**, representing the ECST, NASCET and CC, respectively. Measurement **A** indicates the narrowed diameter of the arterial lumen in the stenosis region, measurement **B** indicates the diameter of the arterial lumen distal to the stenosis, measurement **C** indicates the diameter of the artery at the stenotic site, and **D** indicates the normal diameter of lumen proximal to the stenosis.

2.3.1.2 Carotid Artery Stiffness

Carotid artery stiffness is widely used as a marker of carotid atherosclerosis (Blacher et al., 1998; Dijk et al., 2005; Gujral et al., 2016).

Atherosclerosis is an inflammatory disease which causes elastin disturbance through upregulating several elastolytic enzymes by inflammatory cytokines (Ben David et al., 2008; Shah, 1997).

CRP is an important inflammatory factor which promotes the atherosclerosis in various aspects. During atherosclerosis, CRP is upregulated, and inhibits the expression levels and bioactivity of endothelial nitric oxide synthase (NOS) which stiffen the artery vessel wall (Kinlay et al., 2001). Besides, CRP is found to be positively associated with carotid-femoral pulse wave velocity (cf-PWV) (Mattace-Raso et al., 2004; Yasmin et al., 2004) and the formation of atherosclerotic plaque (Makita et al., 2005). Additionally, CRP is associated with monocytes recruitment at the early stage of atherosclerosis. The diffuse deposition of CRP could be found in the regions of fibroelastic layer and the fibromuscular layer of the intima. The double staining results demonstrated that monocytes infiltrated the arterial wall with the deposition of CRP. Therefore, CRP deposits could induce the monocyte recruitment at the edematous and gelatinous lesion. (Torzewski et al., 2000). These demonstrate that the presence of CRP is highly associated with carotid atherosclerosis and increased carotid artery stiffness.

2.3.1.3 Carotid Intima-media Thickness

Carotid intima-media thickness (CIMT) refers to the carotid artery wall thickness measuring from the media-adventitia interface to the lumen-intima interface of carotid artery (Touboul et al., 2012) .Ultrasound is a common imaging tool to measure CIMT for the assessment of carotid atherosclerosis. Standard scanning protocol and measurement guidelines are well established (Kim et al., 2017; Marini et al., 2017; Stein et al., 2008; Yuan et al., 2015) (**Figure 2.5**)

CIMT serves as an early indicator for subclinical carotid atherosclerosis. (Touboul et al., 2012). It was reported that CIMT is a surrogate endpoint to evaluate the therapeutic efficacy of pharmacological interventions. 3-hydroxy-3-methylglutaryl–coenzyme A (HMG-CoA) reductase inhibitors (statins) were widely used in the treatment of hypercholesterolemia, because they could effectively reduce the serum cholesterol levels (Istvan & Deisenhofer, 2001). A meta-analysis of the published results demonstrated that CIMT, meeting clinical-based criteria, could serve as a surrogate endpoint for cardiovascular events in statin trials, based on relative efficiency, linkage to endpoints, and congruency of effects (Espeland et al., 2005). In addition, CIMT can be a marker of radiation-induced carotid atherosclerosis. Compared to the non-irradiated carotid artery, the CIMT of the carotid artery on the irradiated side was significantly larger (Gujral et al., 2016) . Therefore, the increase in CIMT is associated with the progression of radiation-induced carotid atherosclerosis, and thus it could be a potential marker for monitoring disease progression (Gujral et al., 2016).

CIMT can be measured by ultrasound using different methods (Chambless et al., 1997; Kastelein et al., 2007; Naqvi et al., 2010; Peters et al., 2012). CIMT can be measured

at different segments of carotid artery (CCA, ICA or/and carotid bulb), as well as at different measurement angles (perpendicular/oblique) (Cao et al., 2007; Howard et al., 1994; Price et al., 2007; Van Der Meer et al., 2004). The value of CIMT adopted could be a single measurement, or the mean/maximum value of multiple measurements. The measurement area could be plaque-included or plaque-free area. (Folsom et al., 2008; Naqvi & Lee, 2014) The standardized segment of CCA is usually measured along 1 cm length of the artery, proximal to the inferior end of carotid bulb (Frost et al., 1998). As previous studies used different techniques in ultrasound measurement of CIMT, interpretation and comparison of their results should be in cautious.

The reverberation artifacts from the artery wall lead to inaccurate measurement of CIMT of near wall, and thus CIMT measurements are usually performed in the far wall of artery (Pignoli et al., 1986; Wendelhag et al., 1991; Wikstrand, 2007). Moreover, ultrasound measurement of CIMT is of high reliability (coefficient of reliability, R, was 0.859) (Tang et al., 2000), in terms of high reproducibility and repeatability. The intra- and inter-reader reliability were 0.915 and 0.872 respectively. The intra- and inter-operator reliability was 0.866 and 0.972 respectively (Tang et al., 2000; Velazquez et al., 2008). In addition, ultrasound measurement of CIMT has high correlation with histological findings. According to Pignoli et al. (1986), evaluations of intimal medial thickness by B mode ultrasound and gross pathologic examination were not significantly different in both CCA segments with/without plaque (mean±SD, CCA with plaque: B mode vs histology = 2.06 ±1.02 vs 1.93 ± 0.84 respectively; CCA without plaque: B mode vs histology = 1.22 ± 0.37 vs 1.13 ±0.26respectively) (Pignoli et al., 1986).

A.

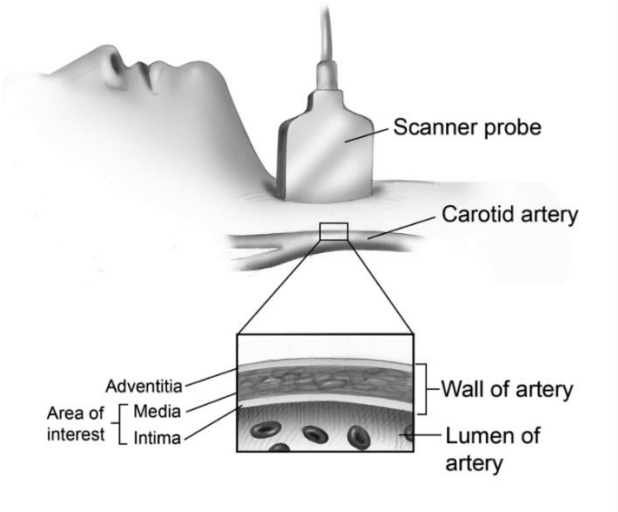

B.

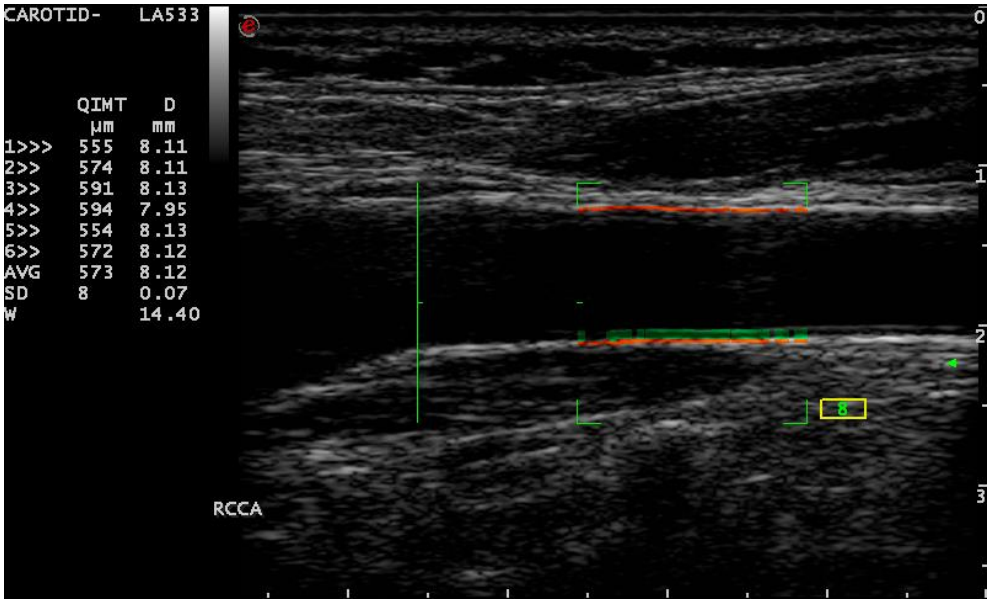

Figure 2.5 The Structure and US Imaging of Carotid intima-media thickness

Image **A** shows the longitudinal view of carotid arterial anatomy and image (Parcell, 2013). Image **B** is a longitudinal ultrasound image of common carotid artery for a 59-year-old man with hypercholesterol. The red line indicates the adventitia of carotid artery and the green transverse line indicates the carotid intima-media thickness.

2.3.1.4 Carotid Plaque

Carotid plaque is the carotid atherosclerotic lesion on the carotid arterial wall, which is commonly considered as the consequence of endothelial dysfunction in atherosclerosis (Libby, 2012; Mayer et al., 2013). Most carotid plaques are formed at the bifurcation of the carotid artery (Spanos et al., 2017). It is generally believed that the presence of carotid plaques, especially the unstable plaques, is related to a higher risk of cerebrovascular diseases (Hollander et al., 2002; Molloy & Markus, 1999).

Although histopathology is widely-accepted as the gold standard for the assessment of carotid plaque composition, it has drawbacks of destroying the integrity of plaques, and the technique is limited to in vitro assessment and retrospective studies. In addition, the procedures of collecting tissue samples for histopathology are invasive. Therefore, medical imaging is useful for in vivo assessment of carotid plaques that helps in predicting future cerebrovascular events (Jm et al., 2010; Park, 2016).

2.3.1.4.1 Carotid Plaque Formation and Development

The formation of carotid plaque is a continuous and complex process involving lipid accumulation, oxidation and modification, which lead to varied histological patterns representing different stages of atherosclerosis (**Figure 2.6**) (Insull, 2009).

Early fatty streak is present at the initial stage of atherosclerosis. LDL transports from blood stream to the intima, and is oxidized and modified by enzymes turning into oxidized-LDL. Oxidized-LDL, as a pro-inflammatory particle, provokes the inflammatory initiation innately.

It is well-known that endothelial dysfunction is highly related to the progression of atherosclerosis. In endothelium dysfunction, the endothelial cells are activated and release several adhesion molecules. Meanwhile, the smooth muscle cells (SMCs), with the accumulation of lipid-drop, release the chemoattractants and chemokines. Under the combined action of these biochemical factors, several immune cells (mast cells, monocytes, lymphocytes and neutrophils) are recruited at the arterial intima. Monocytes transform into macrophages in the sub-endothelial space and form the foam cells by taking up lipids. The degree of lipid-accumulation plays the vital role in determining the severity of early atherosclerosis. Additionally, SMCs migrate from media into intima within the matrix of proteoglycans, producing fibrous elements that are the source of fibrous cap. (Insull, 2009; Lusis, 2000; Ross, 1999).

After the formation of early atherosclerotic lesion, extracellular proteoglycan combines with lipid in an amplified way, leading to the formation of lipid pool and inducing cell necrosis. Besides, macrophages and SMCs are dead and the necrotic debris exacerbates the inflammation and development of atherosclerosis.

The necrosis and the excessive accumulation of lipids disturb the original structure of arterial wall through taking up the intima area by lipid-rich necrosis. In addition, fibrosis-cap covers the lipid-rich necrosis at the blood interface, forming a lipid-rich necrosis atherosclerotic lesion with fibrous cap.

The advanced atheroma is further developed when fibrosis are dissolved by excessive proteolytic enzymes, and characterized by the thin-cap fibroatheroma (TCFA). TCFA is usually considered as vulnerable plaque, because it is more likely to rupture and

produce the life-threatening thrombosis (Cheruvu et al., 2007; Moreno et al., 2006; Virmani et al., 2000).

Complex atherosclerotic lesion could be developed on the basis of the advanced atheroma involving the cycle of rupture, thrombosis and healing. Although TCFA has high tendency of rupture, a lot of these ruptures are clinically silent. The rupture may induce the formation of fibrous tissue matrix (collagen fibers, cells, and extracellular space) and is subsequently healed. However, the healed sites are easy to rupture again leading to the formation of thrombosis. Such dynamic cycle could be happened for up to four times at the same focal lesion, and finally results in a complex lesion with multiple stratifications. This cyclic process offers the possibility of the lesion to interact with the molecules in the blood stream which provoke the thrombosis in the artery. Subsequent rupture of the thrombus in the artery may cause the ischemic stroke and lead to mortality (Insull, 2009).

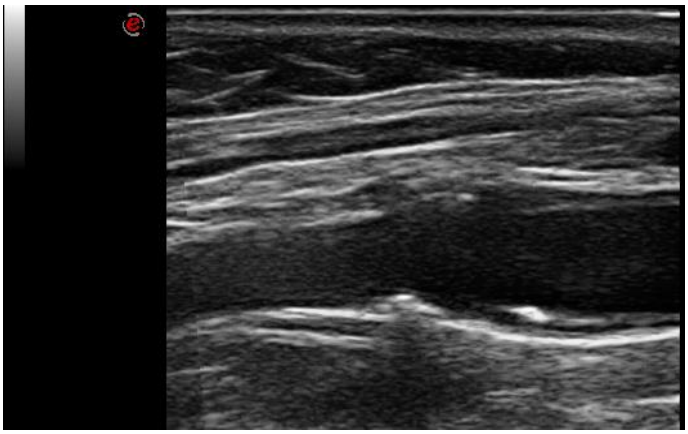

A. Left bulb

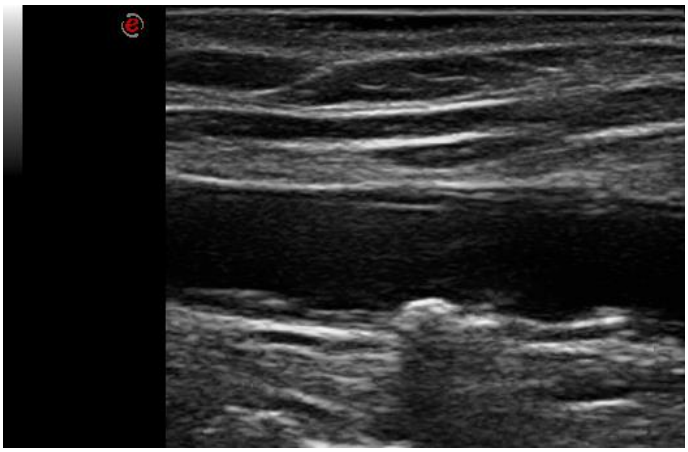

B. Left mid-CCA

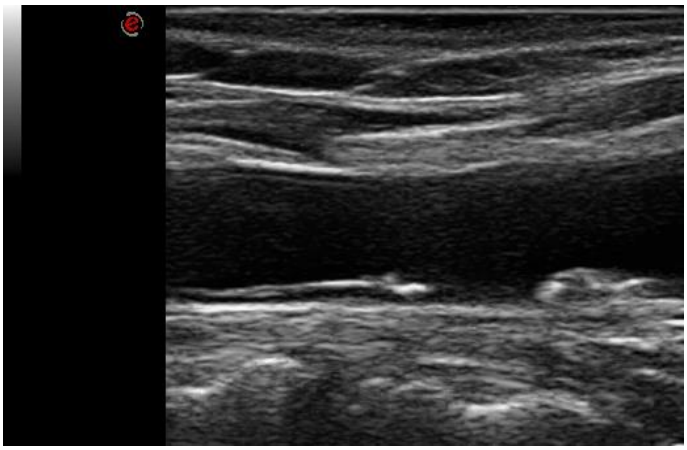

C. Left pro-CCA

Figure 2.6 Carotid plaque formation in ultrasound image. The ultrasound image of a post-RT NPC patient showed several carotid plaque formations with multiple locations, from left carotid bulb (**A**), left mid-CCA (**B**) to proximal CCA (**C**).

2.3.1.4.2 Plaque Composition and Vulnerability

Despite the process of carotid plaque formation is complicated with multiple cells involved (**Figure 2.7**), the main components that are frequently found in carotid plaques include lipids, vascular SMCs, macrophages, foam cells, extracellular matrix, collagen, elastin, necrotic cell debris, neovascularization, intra-plaque haemorrhage (IPH) and calcium (Peeters et al., 2009).

Carotid plaques could be classified into stable and unstable plaques. It was reported that unstable plaques are highly associated with cerebrovascular diseases, possibly leading to mortality (Dunmore et al., 2007; Hellings et al., 2010; Huibers et al., 2015; Iannuzzi et al., 1995; Marnane et al., 2014).

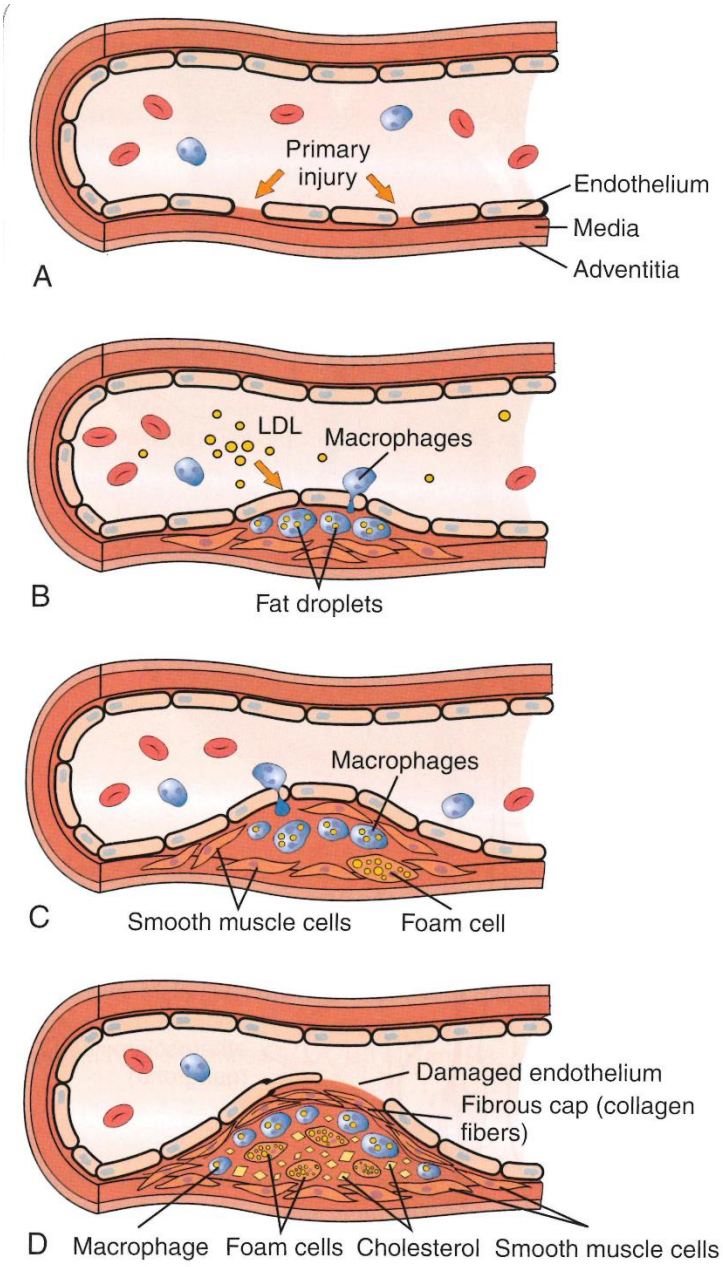

Figure 2.7 The formation and development of carotid plaque. When the vessels expose to risk factors, they are injured (**A**). The impaired endothelium induces the influx of lipids and monocytes-derived macrophages (**B**), and macrophages take up fat droplets to form the foam cells. SMCs migrate from media to the lesion and become the source of necrotic debris and promote the inflammation by increasing the lipids, SMCs, macrophages deposit in the vessel wall (**C**). Eventually, the complex and continuous process result in an atheroma, which is covered by a fibrous cap with soft lipid-contents (**D**). (Damjanov, 2011)

Since the development of atherosclerosis involves a series of complex biochemical factors and various cell types, the exact underlying mechanism for the development of vulnerable plaque is not fully revealed (Golledge et al., 2000).

A previous meta-analysis reviewed 1,031 articles and reported that subjects with acute ischemic stroke or transient ischemic attack (TIA) were highly associated with complex plaque (OR=5.12, 95% CI=3.42–7.67), plaque echolucency (OR=3.99, 95% CI=3.06–5.19), plaque ulceration (OR=3.58, 95% CI=1.66–7.71), plaque neo-vascularity (OR=19.68, 95%CI=3.14–123.16) and intra-plaque motion (OR=1.57, 95% CI=1.02–2.41) (Brinjikji et al., 2015). Complex plaque is also regarded as advanced plaque, which is characterized by fissuring of luminal surface, IPH and thrombotic deposits. The pathologic manifestations of plaque echolucency are lipid-rich necrotic core and IPH. Both of them are well-recognized risk factors for symptomatic transformation of carotid plaques (Kolodgie et al., 2017). Plaque ulceration in ultrasound images is the representation of plaque disruption (Glagov et al., 1987; Steinberg & Witztum, 1990). Such ulceration and fissuring can lead to the loss of normal endothelial cells and the exposure of necrotic core, and thus the luminal arterial wall is prone to thrombosis. Plaque neo-vascularity referred to the abnormal immature microvessels, which induce plaque instability by the recruitment of inflammatory cells and being a potential site of vascular leakage (Dunmore et al., 2007). Intraplaque motion referred to the longitudinal movement on the plaque surface or within the plaque (Iannuzzi et al., 1995), which cause IPH and plaque instability due to the rupture of vasa vasorum resulted from the luminal shear stress physically. The results of above studies are consistent with the widely-accepted characteristics of vulnerable plaques. This kind of plaques has increased inflammatory response and demonstrates

signs of instability which include plaque rupture, IPH and neovascularization (Golledge et al., 2000; Ijas et al., 2013; Marnane et al., 2014; Nighoghossian et al., 2005; Saam et al., 2013).

In a prospective study of 44 pre-carotid endarterectomy (CEA) patients with history of stroke, the study found that plaque inflammation was the sole independent predictor of recurrent stroke (adjusted hazard ratio: 9, CI: 1.1-70.6, p=0.04) (Marnane et al., 2014). The carotid plaques that were associated with higher risk of stroke recurrence demonstrated large area of dense macrophage infiltration, severe fibrous cap rupture, presence of neovascularization and low fibrous tissue content (Marnane et al., 2014).

Neovascularization and haemorrhage also play a crucial role in the progression of atherosclerosis and instability of carotid plaques (Dunmore et al., 2007; Hellings et al., 2012; Hellings et al., 2010). It was reported that neovascularization in carotid plaque tended to be immature, enlarged and dysmorphic, lacking of the adjacent cells (SMCs and macrophages), and it is commonly found in the area with haemorrhage and inflammatory responses (Dunmore et al., 2007).

In addition, the plaque vulnerability is affected by the physical forces, such as the shear stress (Rothwell et al., 2000) and mechanical forces between the arterial wall and motion of plaque caused by the flow of blood within the vessel (Heiland et al., 2013; Iannuzzi et al., 1995; Woodcock, 1989).

2.3.1.4.3 Plaque Echogenicity, Heterogeneity and Greyscale Median (GSM)

Plaque morphology could reflect the degree of carotid atherosclerosis, and help to identify vulnerable plaques (Kingstone et al., 2012). Ultrasound has been used to assess carotid plaque morphology and evaluate plaque vulnerability (Kingstone et al.,

2012). On ultrasound, carotid plaques can be classified as hypoechoic (echolucent) or hyperechoic (echogenic), and heterogeneous (non-uniform echogenicity) or homogeneous (uniform echogenicity). Based on the difference in plaque echogenicity and homogeneity, carotid plaques can be categorized into five types (Gray-Weale et al., 1988):

Type I: uniformly hypoechoic (< 25% of pixels within the plaque area have grey scale values > 40)

Type II: predominantly hypoechoic (25-50% of pixels within the plaque area have grey scale values > 40)

Type III: predominantly hyperechoic (50-75% of pixels within the plaque area have grey scale values > 40)

Type IV: uniformly hyperechoic (> 75% of pixels within the plaque area have grey scale values > 40)

Type V: plaque cannot be classified because of dense calcification causing acoustic shadowing.

The first report of ultrasound evaluation of carotid plaque texture was found in 1980's (Reilly et al., 1983). The study applied ultrasonography to investigate the carotid plaque echogenicity, as well as the association of carotid plaque echogenicity and the incidence of stroke or TIA. Carotid plaques were defined as heterogeneous or homogeneous through visual assessment of reviewers, who were blind to the results of gross and microscopic plaque analysis. The results showed that in symptomatic

patients (with stroke or TIA), 73% of carotid plaques were heterogeneous, while in asymptomatic patients (without stroke or TIA), 47% of carotid plaques were homogeneous. Therefore, the characterization of echogenicity could be the predictor to the future cerebrovascular diseases. However, the echogenicity of carotid plaques was assessed by visual judgment of reviewers, which is subjective and inaccurate. Therefore, it is necessary to have an objective method for accurate assessment of carotid plaque texture. Grey Scale Median (GSM) is the median of greyscale optical intensity of the pixels of ultrasound image. By outlining the carotid plaque on an ultrasound image and analyzing the image, the GSM of carotid plaque can be measured (**Figure 2.8**). GSM is commonly used to quantify the carotid plaque characteristics, and could be used to evaluate carotid plaque vulnerability (Mayer et al., 2013). It was found that carotid plaques with low GSM are associated with cerebrovascular diseases and plaque inflammation (Goncalves et al., 2003; Nicolaides et al., 2010).

When GSM measurement was initially used to assess carotid plaques in early studies, the study results were controversial because different ultrasound gain settings were used in the studies leading to substantial variability of GSM value. To reduce the discrepancy, Elatrozy et al. (1998) normalized the ultrasound image before the evaluation of the GSM of carotid plaque. They applied the linear scaling of image pixels to normalize ultrasonic images using the blood and adventitia of carotid artery as the two references, the lowest and highest pixel values respectively. In the normalization, the GSM value of blood is usually set at 0-5 pixel value, while that of adventitia is standardized at 185-195 pixel value (Elatrozy et al., 1998). Their study found that more reliable and accurate results were obtained after image normalization.

The evaluation of carotid plaque characteristic by GSM value is reproducible, and the lower value of GSM (hypoechoic) was found to be associated with vulnerable plaques. Elatrozy's group reported that after image normalization the coefficient of variation in the evaluation of GSM of adventitia, blood and carotid plaque amongst four observers was 0.7%, 0% and 4.7% respectively. The results also showed that symptomatic patients had a lower GSM (21±14.8 and 38±26 respectively, p=0.02) and higher percentage of echolucent pixels (70%±20% and 55%±25% respectively, p=0.01), when compared to asymptomatic patients (Elatrozy et al., 1998). It was showed that mean GSM of carotid plaques in patients with TIA (14.9±15.3) and stroke (15.8±18.0) were significantly lower than that of asymptomatic patients (30.5±26.2) ($p<0.05$) (Sabetai et al., 2000). Similar finding was also reported in another study in which the carotid plaques in symptomatic patients had lower GSM and were more hypoechoic when compared to those in asymptomatic patients (GSM: 10.5 and 28 respectively, p=0.001) (Tegos et al., 2001).

Results of previous studies revealed that hypoechoic plaques are more commonly found in symptomatic patients than hyperechoic plaques, indicating hypoechoic plaques are more vulnerable to cerebrovascular diseases (Elatrozy et al., 1998; Iannuzzi et al., 1995; Sabetai et al., 2000). Histologically, hypoechoic plaques have more lipids, necrotic areas or haemorrhage, whereas hyperechoic plaques have more calcification or fibrous tissues (El-Barghouty et al., 1996; Tegos et al., 2001); (Kardoulas et al., 1996; Mitchell et al., 2017). Therefore, hypoechoic plaques tend to be softer and their components are more easily to be detached leading to cerebrovascular diseases.

The results of previous studies on carotid plaque heterogeneity were controversial. Some studies reported that carotid plaques which are predominantly heterogeneous were more likely to cause cerebrovascular symptoms (Aburahma et al., 2002; Elatrozy et al., 1998), and associated with higher degree of carotid artery stenosis (Holdsworth et al., 1995). Another study also showed that higher carotid artery stenosis was significantly correlated with decreasing homogeneous pattern (from 16.7% to 5.6%, $p<0.0001$), and increasing heterogeneous pattern of carotid plaque (from 83.8% to 94.5%, $p<0.0001$) (Polak et al., 1993). Holdsworth's group also found that at carotid artery stenosis ≤20%, only 4.4% of carotid plaques were heterogeneous, whereas at 80-90% carotid artery stenosis, 84.5% of carotid plaques were heterogeneous (Holdsworth et al., 1995). Moreover, regardless of the degree of carotid artery stenosis, heterogeneous carotid plaques were more commonly found in symptomatic patients (Aburahma et al., 2002). In contrast, Tegos and his co-workers reported that higher prevalence of homogeneous carotid plaques (88%) was found in symptomatic patients than asymptomatic patients (65%, $p=0.003$) (Tegos et al., 2001). Another study also reported that the carotid plaques in symptomatic patients were less heterogeneous than those in asymptomatic patients (El-Barghouty et al., 1996).

The controversial findings of the association between carotid plaque heterogeneity and incidence of patient symptoms in the previous studies may be due to the different carotid plaque heterogeneity measurement methods used in the studies. In AbuRahma's and Polak's studies, carotid plaques were considered to be homogeneous when they demonstrated either hypoechoic, hyperechoic, isoechoic or calcified-pattern, whereas plaques were regarded as heterogeneous when they had a mixture of these echo-patterns (Aburahma et al., 2002; Polak et al., 1993). Holdsworth et al. (Holdsworth et al., 1995) classified carotid plaques as homogeneous when they were

fibrous and predominantly echogenic, and heterogeneous when they were haemorrhagic and predominantly echolucent. Elatrozy et al. (Elatrozy et al., 1998) used computer-aided assessment and defined homogeneity when all the pixels of the region of interest were similar. However, Tegos et al. and El-Barghouty at al. adopted the quantitative GSM measurement method and used heterogeneity index (HI) to evaluate the carotid plaque heterogeneity. HI is the calculated difference of $GSM_{\text{hyperechoic region}}$ and $GSM_{\text{hypoechoic region}}$. When HI is higher than GSM_{plaque}, the plaque is regarded as heterogeneous plaque. The greater the HI, the higher degree of heterogeneity is the carotid plaque (El-Barghouty et al., 1996; Tegos et al., 2001).

A.

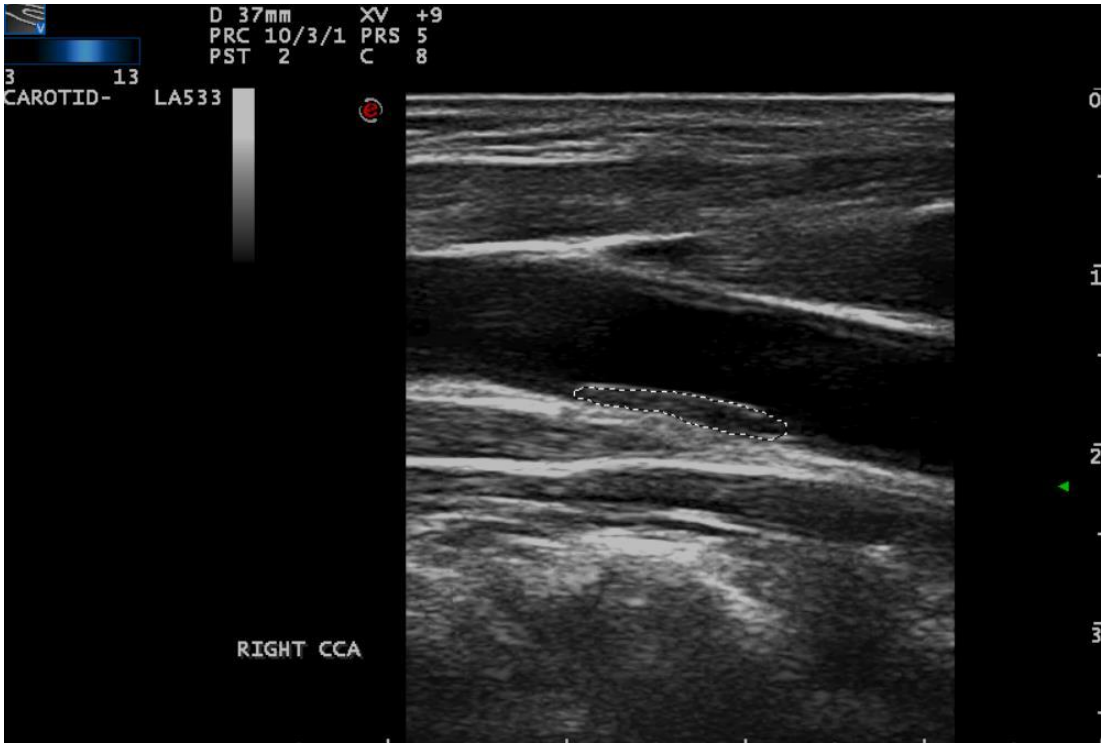

B.

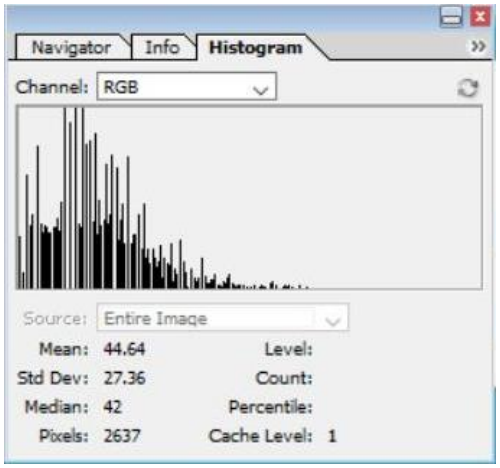

Figure 2.8 GSM evaluation of carotid plaque echogenicity. Carotid plaque (**A**) with GSM of 42 analyzed by computer using software Adobe Photoshop CS, v.8.0 (**B**).

2.3.1.4.4 Plaque Texture Assessment

Though GSM is a useful quantitative parameter for evaluating carotid plaques, it can only give an overview of the echogenicity and heterogeneity of carotid plaques, lacking of the detailed assessment of plaque composition. Thus, other approaches for detailed assessment of carotid plaque texture are needed. Lai et al. (2002) (Lal et al., 2002) used computer software to analyze B-mode ultrasound images and assessed the plaque constituents by computing the image pixel distribution of carotid plaque. They found that the pixel distribution of carotid plaques in ultrasound image was highly correlation with the histology results. The pixel distribution of carotid plaques was expressed as five ranges (0 to 4, 8 to 26, 41 to 76, 112 to 196, and 211 to 255), which are correlated with the histology results in which carotid plaques were classified as blood ($p=0.012$), lipid ($p<0.001$), muscle ($p=0.035$), fibrous tissue ($p=0.035$) and calcium ($p<0.001$), respectively.

In Lai et al. (Lal et al., 2002), they first examined the following anatomical structures in 10 healthy controls: abdomen, biceps, iliotibial tract, tibia and skull, which represented the tissues of subcutaneous fat, muscle, fibrous tissue, and calcified structure. GSM analysis was performed to obtain the pixels distribution pattern of different tissues. They then assigned different colors to the corresponding grey scale ranges determined within a plaque based on the results of the healthy controls. This carotid plaque assessment method was named detailed plaque texture analysis (DPTA). The area occupied by each grey scale range was then calculated as a percent of the total area of the plaque. They also evaluated the correlation of the percentage of different tissues calculated by DPTA and histologic results. Subsequently, a Polish research group adopted DPTA to evaluate correlation of carotid plaque texture and the

occurrence of silent brain infarcts (Madycki et al., 2006). They optimized the GSM ranges of different tissues as below:

Partition 1:	Blood	GSM: 0-9
Partition 2:	Lipid	GSM: 10-31
Partition 3:	Muscle	GSM: 32-74
Partition 4:	Fibrosis	GSM: 75-111
Partition 5:	Calcification	GSM: 112-255

According to the multivariate logistic model in Madycki's study , carotid plaques with the total areas of partition 1, 2 and 3 (represented blood, lipid and muscle respectively) greater than 72% were defined as predominantly hypoechoic, and had a high risk of silent brain infarcts. Besides, their study results showed that DPTA can help in the prediction of TIA or stroke (Madycki et al., 2006).

According to Madycki's study, DPTA was more effective in predicting neurological complications than traditional GSM analysis (Madycki et al., 2006). The reasons can be explained as below: first and the most importantly, DPTA was able to discriminate the tissue compositions in detail, such as blood, lipid, muscle and calcium. Therefore, instead of simply classifying carotid plaques into two categories (predominantly hypoechoic or predominantly hyperechoic), DPTA provided more details in carotid plaque composition which helps in identifying vulnerable plaques. Intra-plaque hemorrhage is a well-established marker of unstable plaque (Liu et al., 2019; Lusby et al., 1982; Rots et al., 2019). However, both blood and lipid were hypoechoic in

ultrasound, and it was difficult to differentiate these two types of tissue in GSM analysis. On contrary, DPTA can help in distinguishing these two intra-plaque components. Therefore, DPTA could be an efficient method to assess plaque vulnerability. Based on this, DPTA was adopted to compare the carotid plaque composition characteristics between radiation-induced and non-radiation-induced atherosclerosis in the present study.

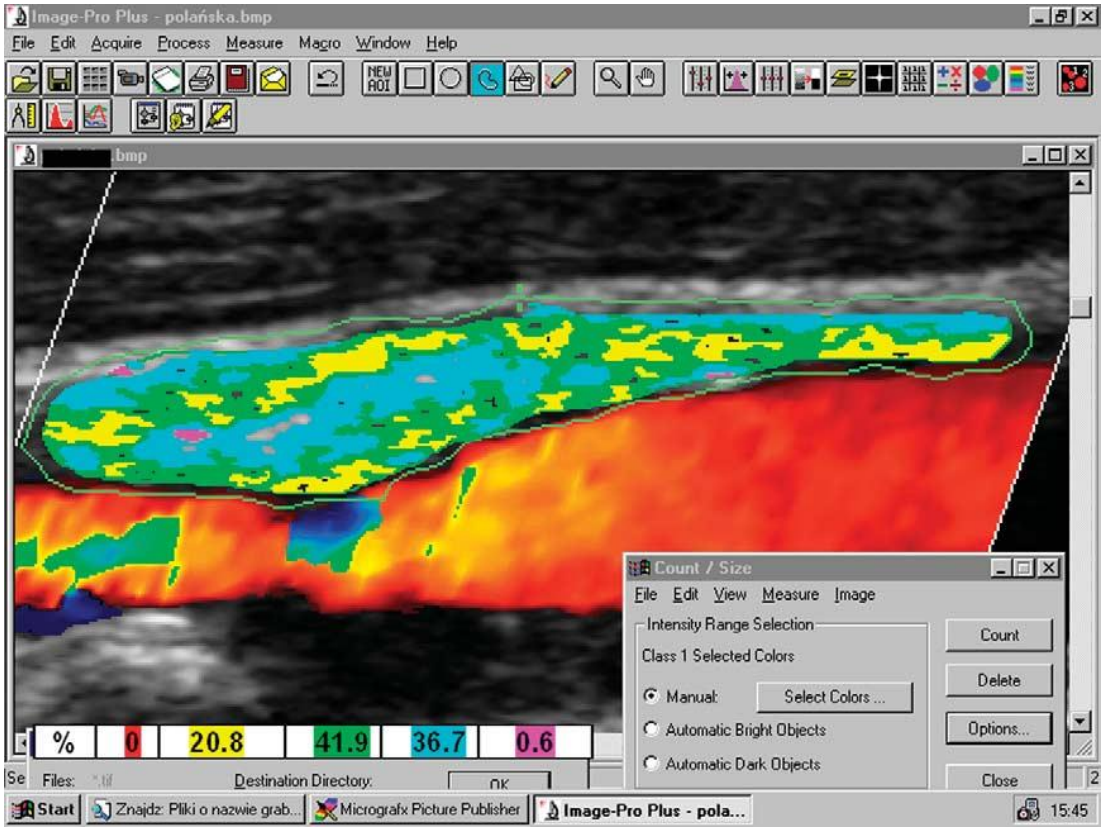

Figure 2.9 Detail Plaque Texture Analysis (DPTA) of carotid plaque morphology. longitudinal image of carotid plaque by ultrasonography, the bar at the bottom indicates different proportions of five tissues (blood in red, lipid in yellow, muscle in green, fibrosis in blue, and calcification in purple) accounting for the entire plaque. (Madycki et al., 2006)

2.3.2 Magnetic resonance imaging (MRI)

In the assessment of carotid atherosclerosis, magnetic resonance imaging (MRI) can be used to assess the component of carotid plaque (Chu et al., 2004; Fayad & Fuster, 2000; Sanz & Fayad, 2008). The various contents of carotid atherosclerotic plaque (lipids, fibrous cap, calcium deposit, and blood clots) indicate the different stages of atherosclerosis. On MRI, lipids are demonstrated as hyperintense regions on T1-weighted (T1W) and proton-density weighted (PDW) images; fibrous tissues are hyperintense on T1W, T2-wighted (T2W) and PDW images; thrombotic plaques also appear as hyperintense areas in T1W, T2W and PDW images with appearance of irregularities on the plaque surface. In contrast, calcifications are demonstrated as hypointense in these three image sequences (Fayad & Fuster, 2000).

By characterizing the carotid plaque component, MRI can monitor the changes of atherosclerosis so that timely treatment can be given to patients (Pletsch-Borba et al., 2018; Sanz & Fayad, 2008). MRI characterization of carotid plaque is prominently beneficial for atherosclerosis patients because ischemic stroke is highly associated to the unstable plaque (Wasay et al., 2007). IPH is a widely-accepted marker of plaque instability. In order to evaluate the plaque stability, Chu et al. (2004) developed a criteria to detect and identify the different stages of IPH by MRI (Chu et al., 2004). They classified the IPH into three categories: fresh hemorrhage (<1 week), recent hemorrhage (1 to 6 weeks) and old hemorrhage (> 6 weeks). Fresh hemorrhage are demonstrated as hyperintensity on T1W/time of flight (TOF) images and isointense or hypointense regions on T2W/PD images. Recent hemorrhage are demonstrated as hyperintense regions, while old hemorrhage is demonstrated as hypointense regions on these four contrast weightings (Chu et al., 2004). According to a meta-analysis

study in MRI assessment of carotid plaques, subjects with detectable IPH have about 6 times higher risk for cerebrovascular disease (hazard ratio: 5.69; 95% CI: 2.98 to 10.87) (Saam et al., 2013), which suggested that IPH could be a parameter for evaluating carotid plaque vulnerability. Besides, MRI can classify the plaques (Type I-VIII) and identify the advanced lesions (Type IV-V, VI,VII or VIII) from the early (Type I-II) and intermediate stage lesions (Type III), through comparing the MRI results with histology staining (Cai et al., 2002). The classification methods and histological features of each plaque type are summarized in **Table 2.1**. Cai and the co-workers modified the American Heart Association (AHA) classification by combining Type I and Type II into Type I-II, and Types IV and V into Type IV-V. One reason for this modification was that discrete foam cells in Type I and the multiple foam cell layers of the fatty streak in Type II were indistinguishable. Another reason was that the application of MRI in distinguishing the proteoglycan composition of the Type IV cap versus the dense collagen of the type V cap were undemonstrated. Moreover, some researchers applied an innovative strategy (namely two-step method) to solve the misalignment of MRI of different image sequences, and improved the accuracy of image registration of multi-contrast MRI in detecting carotid wall boundaries and evaluation of plaque components (Wu et al., 2017). The method included two steps: the rigid-step and non-rigid step. The rigid-step used iterative closest point to register the centerlines of carotid artery longitudinally taken from different MRI image sequences. Afterwards, the non-rigid step used thin plate spline to register the boundaries of lumen by identifying the corresponding points of similar boundaries. After image registration, the overlap of two boundaries from different sequences can be as high as 95% (Wu et al., 2017).

Conventional AHA Classification	Modified AHA Classification for MRI
Type I: initial lesion with foam cells	Type I–II: near-normal wall thickness, no calcification
Type II: fatty streak with multiple foam cell layers	
Type III: preatheroma with extracellular lipid pools	Type III: diffuse intimal thickening or small eccentric plaque with no calcification
Type IV: atheroma with a confluent extracellular lipid core	Type IV–V: plaque with a lipid or necrotic core surrounded by fibrous tissue with possible calcification
Type V: fibroatheroma	
Type VI: complex plaque with possible surface defect, hemorrhage, or thrombus	Type VI: complex plaque with possible surface defect, hemorrhage, or thrombus
Type VII: calcified plaque	Type VII: calcified plaque
Type VIII: fibrotic plaque without lipid core	Type VIII: fibrotic plaque without lipid core and with possible small calcifications

Table 2.1 Conventional and modified AHA classification of atherosclerotic plaque (Cai et al., 2002).

Magnetic resonance angiography (MRA) is a MRI technique that focuses on the assessment of blood vessels and their morphological abnormalities. A thinning fibrous cap is less likely to withstand the pulsatile mechanical force, so that it is more likely to cause plaque fissuring and ulceration. Thus, assessment of carotid plaque surface morphology is a sensitive biomarker for the evaluation of plaque stability. It was reported that time-of-flight MR angiography (TOF-MRA) can accurately evaluate carotid plaque surface morphology, and has high sensitivity in identifying the fibrous cap of carotid plaque 90% (95% CI = 81–98) (Watanabe et al., 2014). However, TOF-MRA is not accurate in distinguishing carotid plaques with lipid core and/or IPH from the vessel lumen because both of them appear hyperintense. For this kind of carotid plaques, black-blood T1 and T2-weighted imaging could be used to identify carotid plaque and determine the presence / absence of plaque ulceration (**Figure 2.10**) (Watanabe et al., 2014). Therefore, multiple MRI image sequences should be used for identifying carotid plaque and comprehensive assessment of plaque surface morphology.

In summary, MRI is useful in examining the morphology of carotid plaque for risk assessment of cerebrovascular diseases. However, MRI is relatively expensive and thus is not available in all centers. Moreover, patients with metal implants or pacemakers, and patients suffer from claustrophobia are not suitable for MRI examination. These make MRI is largely used in symptomatic patients and not commonly used in screening of patients.

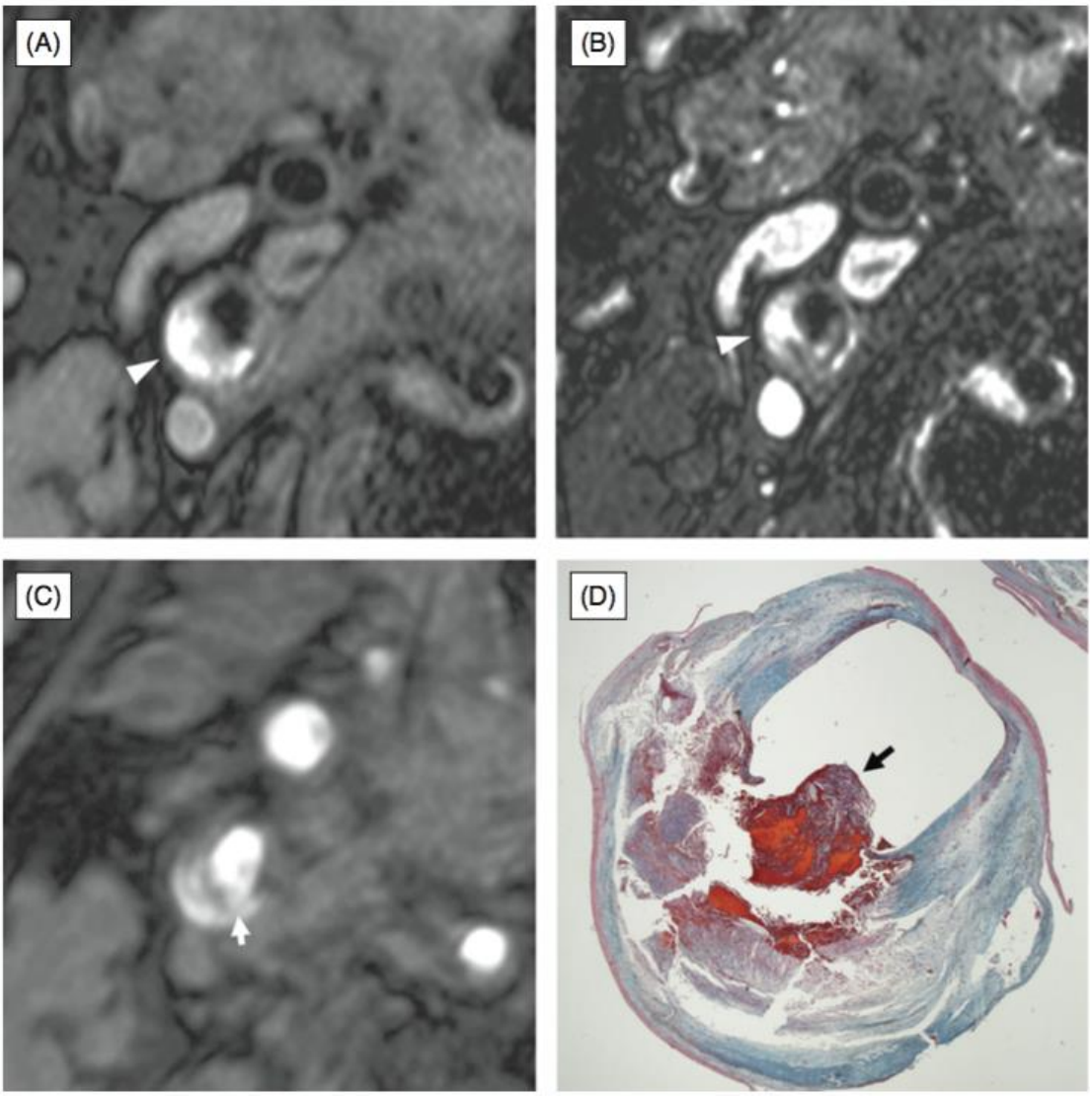

Figure 2.10 Plaque formation imaging of MR angiography. Plaque rupture and intraplaque hemorrhage detected by black-blood T1 weighted image (**A**), black-blood T2 weighted image (**B**), TOR-MR angiography (**C**) and immunohistological section with Masson-Trichrome staining (**D**). Arrows reveal the fibrous (Watanabe et al., 2014).

2.3.3 Positron emission tomography (PET) and computed tomography (CT)

In the recent years, radionuclide imaging has been increasingly used to investigate carotid plaques characteristics. Different labeled radiotracers can be applied to detect various types of cells through binding the specific ligands. Annexin A5 is a plasma protein and can bind to apoptotic cells. Technetium-99m-labeled annexin A5 can be used to identify carotid plaque vulnerability and assess the risk of cerebrovascular disease caused by carotid plaque rupture (Kietselaer et al., 2004).

^{18}F-fluorodeoxyglucose (^{18}F-FDG) positron emission tomography (PET) is a noninvasive medical image method, which can detect the cell activity with different ^{18}F-FDG uptakes. FDG is an analogue of glucose, and living cells uptake the FDG through the glucose gate on the cell membrane via glucose transporters. Combined PET with computed tomography (CT) can display the biological information with anatomical imaging. Therefore, PET/CT is becoming popular in the assessment of carotid atherosclerosis (Miyagawa et al., 2014). There are two major radiopharmaceuticals for PET imaging, namely ^{18}F-fluorocholine ^{18}F-FCH and ^{18}F-Galacto-RGD. 18F-fluorocholine (^{18}F-FCH)/PET can be used to evaluate the proliferation of cancer cells as well as active and proliferating macrophages. A study evaluated the use of ^{18}F-FCH in assessing the vulnerable plaques with macrophages infiltration in pre-endarterectomy atherosclerosis patients. The results showed that the uptake of ^{18}F-FCH in carotid plaques in vivo was significantly correlated with the staining with $CD68^{+}$ (marker of macrophages) within the carotid plaque in surgical specimens in vitro (Spearman's ρ=0.648, P=0.04). Therefore, the use of ^{18}F-FCH can

indicate the amount of macrophages and ^{18}F-FCH PET/CT could be a novel image fusion technology for examining carotid plaque vulnerability (Voo et al., 2016) (**Figure 2.11**). Besides, αvβ3 is a type of integrin in plaque formation with the expression existed in angiogenic endothelial cells and macrophages, which could be specifically bound by ^{18}F-Galacto-RGD (PET tracer). The in vitro results of Beer's group showed that, the accumulation of ^{18}F-Galacto-RGD PET/CT of thromboendarterectomy specimen was significantly correlated with the αvβ3 expression (R=0.787, p=0.026) (Beer et al., 2014). The results of these previous studies demonstrated the value of using ^{18}F-Galacto-RGD PET/CT with αvβ3 in the assessment of carotid plaques.

In summary, ^{18}F-FDG PET combination with CT can improve the efficiency in detecting carotid plaque. It helps monitoring the progression of atherosclerotic plaques, identifying vulnerable plaques and evaluating treatment effect. PET/CT imaging can manifest the inflammatory-related cells proliferation, such as macrophages and endothelial cells, which indicates the degree of inflammatory, and the various cells distribution within the carotid plaque in vivo.

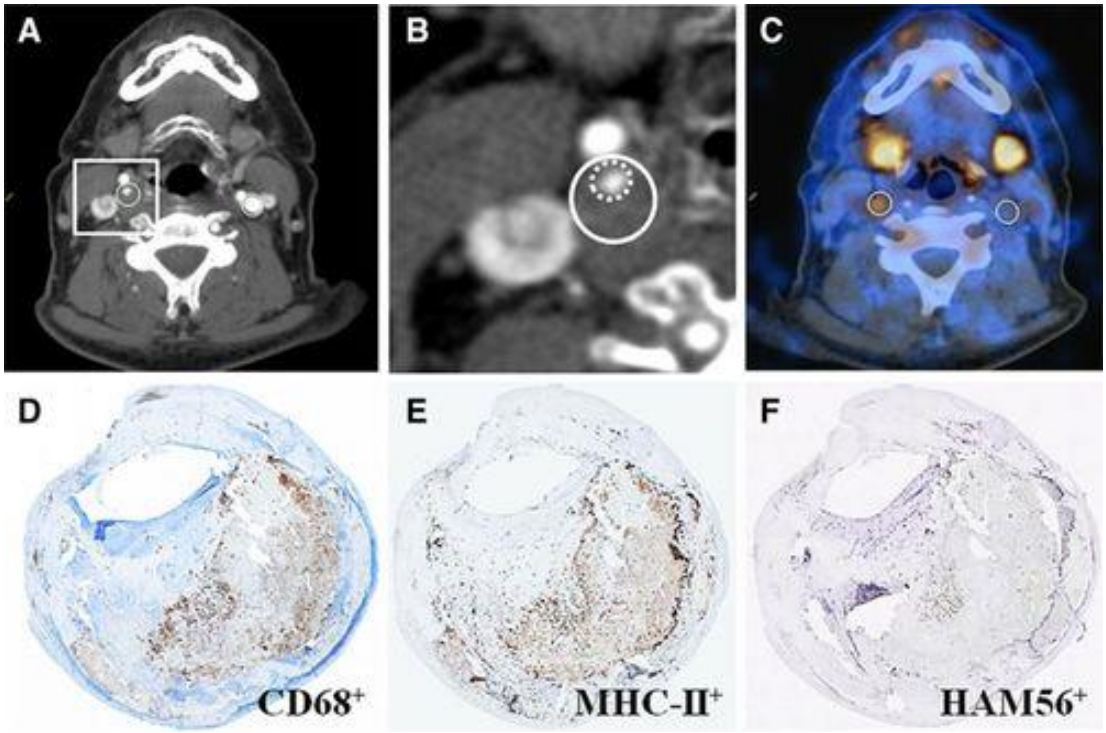

Figure 2.11 ^{18}F-FCH PET-CT demonstrative image and its corresponding histology of a symptomatic and contralateral asymptomatic carotid plaque of a 67-year-old patient in previous study. The patient experienced right-sided stroke 12 days before PET-CT imaging. **A**, Contrast-enhanced CT shows a significant stenosis in the right ICA. Area within white outlining indicated the outer border of the vessel walls placed along the right carotid stenosis and along the contralateral carotid artery, respectively. **B**, CT, inset on the symptomatic plaque. **C**, The fused PET-CT image shows a focal area of high ^{18}F-FCH uptake in the ROI drawn onto the right symptomatic carotid plaque, whereas there is no visible ^{18}F-FCH uptake in the left asymptomatic carotid plaque. Corresponding immunohistochemistry sections indicating CD68^{+} (**D**), MHC-II^{+} (**E**), and HAM56^{+} (**F**) cells (all in brown). MHC-II indicates major histopathology complex class-II; HAM56, human alveolar macrophage marker-56. (Voo et al., 2016)

2.4 Endothelial Dysfunction in Radiation-induced Carotid Atherosclerosis

Endothelial cells lined the inner surface of blood vessels (including arteries and veins) and lymphatic vessels. As a major component of vascular intima layer, endothelium is a thrombo-resistant and semi-permeable barrier, and involves in maintaining the anti-inflammatory circumstances through the interactions to the circulating immune cells. When the blood vessels exposed to the pulsating flow and pressure, endothelium is also involved in maintaining the hemodynamic homeostasis through machinery transmitting the hemodynamic forces (Leopold, 2013).

When exposed to various stimuli, such as ionizing irradiation, the endothelium would be trigged into an activated status (Sumpio et al., 2002). If the activation is not reversed, it will eventually result in endothelial dysfunction (Mudau et al., 2012). The consistent and accumulative damages of endothelium cause different tissue injuries such as chronic inflammatory diseases leading to the development of atherosclerosis. This section reviews the effect of ionizing radiation on the major biological processes of arterial endothelial cells. This section provides an insight into the underlying mechanisms and potential protections for radiation-induced impairment of vascular endothelial cells.

2.4.1 Carotid artery microstructure

Endothelial cells originate from the splanchnopleuric mesoderm and are vital components in the vascular system. Approximately 1 to 6×10^{13} endothelial cells comprise the endothelium, accounting for about 1 kg of the total body weight in an

adult (Sumpio et al., 2002). Blood vessel wall consists of three layers. From the internal vessel wall to the outermost layer, they are tunica intima, tunica media and tunica adventitia, respectively. In both artery and vein, endothelial cells line at the inner surface of tunica intima, and serve as a semi-permeable barrier between circulating blood and the tissues.

2.4.2 Endothelial cell's responses after irradiation

Among the three layers of vessel wall, the tunica intima is the most radiosensitive due to the presence of the monolayer of endothelium (Dimitrievich et al., 1984). Therefore, radiation-induced endothelial dysfunction is common in patients with previous irradiation.

The reactions of endothelial cells to radiation are varied, depending on the dosage of radiation and the specific sites where they are taken from. The post-irradiated effects of vascular include acute and chronic effects. Acute effect could take place within a few weeks after irradiation, while the chronic effect could occur after several years. The different responses of endothelial cells to radiation are the manifestation of different biological effects. Acute responses are commonly triggered by cell apoptosis, whereas chronic responses are more related to the senescence of endothelial cells (Venkatesulu et al., 2018). Moreover, the extent of differentiation of endothelial cells could affect the responses of vessel wall to radiation.

The elevated apoptosis of vascular endothelial cells could provoke the atherogenesis through the proliferation and migration of smooth muscle cells, and the alteration of the homeostasis into pro-coagulated condition (Choy et al., 2001).

2.4.2.1 Apoptosis

Apoptosis, also known as programmed cell death, is a biological process of natural cell mortality and a significant feature for cell injury. It is commonly observed in aging cells. Apoptosis is also the main mechanism of inducing cell death in response to radiation, especially in lymphoid and myeloid cell lineages (Dewey et al., 1995; Radford et al., 1994; Verheij & Bartelink, 2000). Cells are characterized by several morphological changes when undergoing apoptosis, such as cytoplasma and nucleus condensation, cell shrinkage, internucleosomal cleavage of chromatin, blebbing of the plasma membrane. The debris of cellular organelles with or without nuclear fragment are packaged into a tiny membrane-structure vesicle with cytoplasm, which is termed "apoptotic body". These apoptotic bodies are engulfed and digested by macrophages, and this triggers the inflammatory responses (Winn & Harlan, 2005).

It is generally noticed that apoptosis is mediated by various signaling pathways (extrinsic and intrinsic). However, radiation-induced apoptosis is mainly regulated by P53-mediated and sphingomyelin ceramide pathways (Venkatesulu et al., 2018).

Cysteinyl aspartate-specific proteases (Caspases), a family of cysteine proteases, are regulated by the P53-mediated pathway as downstream targets (Fridman & Lowe, 2003). Caspases family is divided into the initiator caspases (caspase-9 in mammals) and effector caspases (caspase-3 and caspase-7 in mammals). Under the apoptotic conditions, caspases are activated from the inactive zymogens. The initiator caspase (Caspase-9) is activated automatically with the assistance of multicomponent complexes. The effector caspase, such as caspase-3, is activated by the initiator

caspase and cleaved into two subunits (a large one and a small one) (Adams & Cory, 2002; Shi, 2002).

Clinically, previous studies focused on the protective factors against the radiation-induced inflammatory disease (such as atherosclerosis) for cancer patients (Eriksson & Stigbrand, 2010; Fuks et al., 1994; Igney & Krammer, 2002; Kolesnick & Fuks, 2003; Li et al., 2003; Wu et al., 2019). As ionizing radiation induces cell apoptosis by causing DNA double-strand breaks (DSB), DNA-dependent protein kinase (DNA-PK) is a potentially protective factor against ionizing radiation. Ku86, as an 86-kDa proteins of Ku family, is a composite submit of DNA-PK end-binding complex. It was recently reported that Ku86 can inhibit the apoptosis induced by low doses of ionizing radiation, because overexpression of Ku86 significantly decreased the levels of caspase-3, -8 and -9,but increased the expressions of Bcl-2 ($p<0.01$). As the cleavage of caspase-3, -8 and activation of caspase -9 are pro-apoptosis proteins, whereas Bcl-2 protein is anti-apoptosis protein, the above findings demonstrated that Ku-86 can suppress the radiation-induced apoptosis in cells (Wu et al., 2019).

Radiation-induced inflammatory diseases are commonly found in post-RT patients (Eriksson & Stigbrand, 2010). Basic fibroblast growth factor (bFGF) can protect endothelial cells from radiation-induced apoptosis in an animal study. In a previous study, when mice received the 320KV, 10mA dosage of irradiation in the lung, endothelial cells apoptosis could be found in the pulmonary vessels of the mice in 6 to 8 hours after the radiation exposure. With the injection of bFGF to the mice, radiation-induced endothelial cells apoptosis in the pulmonary vessels was ameliorated. This proved that bFGF could protect the mice lung from pneumonitis

(Fuks et al., 1994). Moreover, bFGF could also exert a protective effect on the irradiated intestinal damage of mice that may lead to gastrointestinal syndrome.

Another effective Angiopoitin-1 variant, COMP-Ang1, has been tested on the lung, intestine and liver of irradiated mice. COMP-Ang1 can protect the endothelial cells of the vasculature in lung and intestinal villi from radiation-induced apoptosis. However, its protection against the radiation injury of hepatic microvasculature is limited (Cho et al., 2004).

Radiation therapy is a common treatment for cancer patients. However, radiation-induced apoptosis of endothelia cells adversely affects the function of vasculature. Different radiation therapy techniques such as intensity-modulated radiation therapy and use of shielding should be used in order to spare the normal tissues from radiation and minimize the radiation dose in normal cells.

2.4.2.2 Senescence

Senescence is a cellular response that causes the loss of proliferation in aged or damaged cells. It is another common response to the radiation in endothelial cells. Senescent endothelial cells possess specific characteristics, such as down-regulating the levels of released thrombomodulin and nitric oxide, releasing elevated inflammatory cytokines and inhibiting the proliferation and formation of capillary-like structures (Campisi, 2013; Childs et al., 2015). They play a vital role in dysregulating homeostasis by promoting inflammation and preventing angiogenesis, which result in chronic inflammation of vascular endothelium and cause carotid atherosclerosis eventually. Heart is composed of different kinds of cell, and endothelial cells account for 24% of adult ventricles. Therefore, endothelial cells senescence may result in

cardiovascular diseases (CVDs) (Bergmann et al., 2015). At present, the best way to avoid endothelial cell senescence is to reduce the radiation dose of heart, when patient receiving radiation therapy. Although the contemporary medical technology applies the optimized treatment plan and software tool to minimize radiation dose in normal tissues during radiotherapy, it is inevitable to irradiate the normal cells or tissues in some patients, such as head and neck cancer patients.

Senescent endothelial cells manifest into various unique phenotypes. They expressed with increasing p16 and p21, which are markers of senescence by mediating G1 arrest of cell cycle in p53-mediated pathway. Moreover, it also caused overexpression of senescence-associated β-galactosidase staining. They commonly arrest in cell cycle and morphological changes are observed as well. These cells fail to form capillary-like structures due to the inability of sprout and migration (Dong et al., 2014). The accumulation of senescent cells impede the self-renewal, proliferation and differentiation of cells, rendering them incapable of tissue maintenance, regeneration and repair and resulting in the primary lesion of vascular.

In addition, microRNAs are found to be relevant to endothelial cell senescence. Senescent endothelium is under the control of miR-34a and miR-127 (Ito et al., 2010; Menghini et al., 2009; Tazawa et al., 2007). miR-34a exhibits a higher expression in atherosclerotic arteries (Ito et al., 2010). It induces the endothelial cells senescence by interacting with SIRT1 (Raitoharju et al., 2011). SIRT1 belongs to class III histone deacetylase, which deacetylase a variety of proteins such as necrosis factor kappa b (NF- Kb) (Haigis & Guarente, 2006). miR-127 also exhibits an expression in human atherosclerotic lesions, and the levels of miR-127 is inversely related to the levels of SIRT1 and acetylation status of FoxO1 (forkhead box protein O1, transcription factor

negatively regulating angiogenesis and vascular growth). This indicates the role of miR-127 in promoting endothelial cell senescence in vascular diseases, such as atherosclerosis (Menghini et al., 2009).

2.4.3 Post-irradiated biological effects

Endothelial dysfunction can result in various forms of compensatory effects to alter the stable homeostasis. These effects may include elevated adhesiveness to leukocytes or platelets (Ross, 1999); activation of the property of pro-coagulant; down-regulation of the nitric oxidative synthesis, and promotion of vasovascular molecules production (Upchurch et al., 1997). If these responses continue, without reverting to the basic homeostasis, the artery wall would be thickened leading to atherosclerosis.

2.4.3.1 Platelet aggregation

To maintain the anti-platelet healthy status in arterial lumen, vascular endothelial cells release anti-platelet factors into circulating blood. Among these anti-platelet factors, prostacyclin (PGI_2) and nitric oxide (NO) are highly associated with platelet aggregation (Cines et al., 1998). PGI_2 and NO inhibit the platelets aggregation by elevating the amount of cAMP (Cyclic adenosine 3, 5'-monophosphate) in platelets corporately. Besides, PGI2 and NO levels are increased in response to a range of agonist, such as bradykinine, thrombin and ATP. Therefore, PGI_2 and NO assist in keeping the blood fluidity in the blood vessel by inhibiting the platelets aggregation. Once the endothelial cells are activated in response to the stimuli, the non-activated anti-thrombogenic endothelium will shift to pro-thrombogenic status, and platelet-activating factor (PAF) and von Willebrand factor (vWF) are secreted into blood stream by the activated endothelial cells (Verheij et al., 1994). vWF is released from

endothelial cells and blood platelets, in which endothelial cells are the primary source (Sumpio et al., 2002). Whereas PAF is released from endothelial cells in response to a range of agonists, including histamine, thrombin and cytokines (Zimmerman et al., 1996). The non-activated vascular endothelial is anti-thrombogenic, besides, the platelets are non-activated in the blood stream. vWF and PAF are two mediators that favor the activation of platelets (when platelets roll and adhere to any surfaces, it is activated), and thus promote the activated platelets adhesion to both vWF and circulating leukocytes. Consequently, the leukocytes are recruited at the injury site, and form a leukocyte microparticle, which is an indicator of subclinical atherosclerosis (Lindemann et al., 2007; Santoso et al., 2002).

2.4.3.2 Coagulation

In non-activated endothelial cells, the inhibition of coagulation pathway is characteristic by the complex protein C/protein S. Thrombomodulin is anchoring on the endothelial cells as receptors. It can bind to the thrombin and then assist protein C activation. The activated protein C would inhibit the expression of factors VIIIa and Va. These two factors are associated with endothelial cells coagulation. Protein C exerts the inhibition on coagulation factors VIIIa and Va when combined with protein S (Sadler, 1997). The combination of circulating thrombin with thrombomodulin can impede the thrombin to form clot, as well as prevent stimulating the platelets. However, radiation stimulation can injure the endothelial cells through inducing the production of thrombin-antithrombin III complex, which promotes clot formation and increases the circulating nucleosome/histone (cNH) levels. cNH levels can be detected in patients' blood sample (Kennedy et al., 2016). Besides, thrombomodulin could also be a biomarker for radiation-induced injury of endothelial cells. It has been detected

in supernatants, on the surface of cells and within the cells. Up-regulation of thrombomodulin level , more thrombomodulin molecules and higher activity of thrombomodulin have been observed in the human umbilical vein endothelial cells after radiation (Zhou et al., 1992).

2.4.3.3 Fibrinolysis

To maintain intravascular fluidity, endothelial cells play an important role in reducing thrombi by plasmin. Endothelial cells could release tissue-type plasminogen activator (t-PA) by constitute secretory pathway. Urokinase is synthesized when endothelial cells are activated. Both t-PA and urokinase facilitate the plasminogen transforming to plasmin (Michiels, 2003). By this way, t-PA and urokinase increase the level of plasmin and clear the fibrin network. Stimuli, such as radiation, can activate the resting endothelial cells. The activated endothelium becomes fibrous and pro-coagulant. Recent studies reported different biomarkers and inhibitors of fibrosis that are resulted from radiation exposure. DNA methyltransferase gene polymorphrisms, such as DNMT1 rs2228611, was reported to be an indicator for radiation-induced fibrosis in breast cancer (Terrazzino et al., 2016). Other inhibitors have been studied and were found to have protective effect in minimizing radiation-induced endothelial dysfunction and tissue fibrosis. Angiotensin converting enzyme inhibitor CL242817 is one of these inhibitors (Ward et al., 1989). In the study, result showed that CL242817 could prevent radiation-induced fibrosis and endothelial dysfunction in lung endothelial cells. Besides, α-lipoic acid was found to have protective effect in radiation-induced fibrosis in a mice model by impeding the necrosis factor kappa B (NF- Kb) activity (Ryu et al., 2016). Thus, α-lipoic acid could be a novel approach to treat the radiation-induced injury. (Summary in **Figure 2.12**)

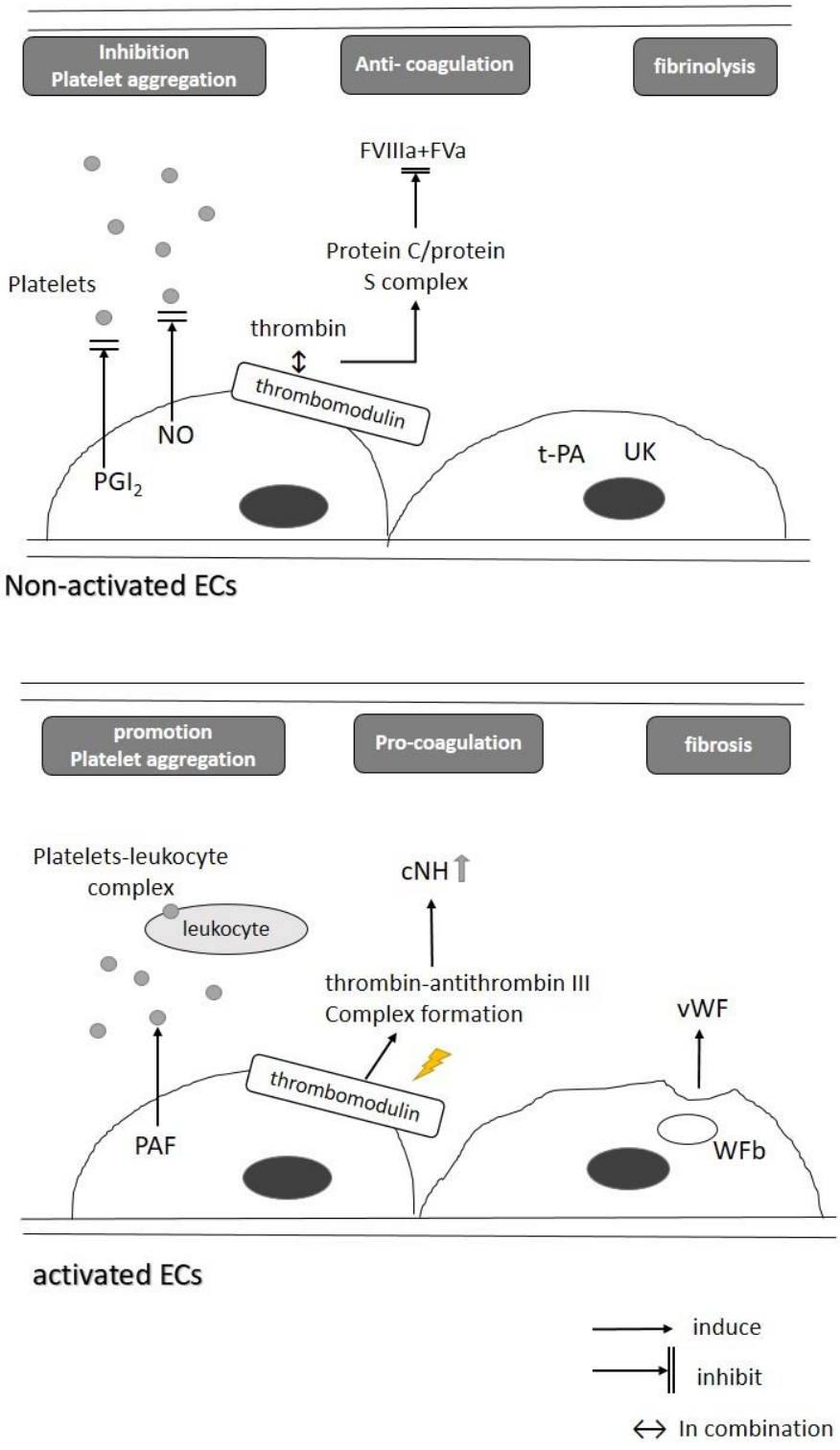

Figure 2.12 Biological responses of endothelial cells after radiation. PGI_2: prostacyclin; NO: nitric oxide; FVIIIa: factors VIIIa; FVa: factors Va; UK: urokinase; WFb: Willebrand factor body.

2.4.4 Related signaling pathways in vascular regulations

2.4.4.1 Vascular endothelial growth factor (VEGF)

VEGF is a mitogen for vascular endothelial cells with five isoforms that could bind to two tyrosine-kinase receptors, i.e. VEGFR1 and VEGFR2 (Neufeld et al., 1999). VEGF is a well-known pro-angiogenic factor in the pathological processes, which involve in angiogenesis and increased vascular permeability (Hanahan & Folkman, 1996). Combined with other factors, VEGF play the roles in endothelial cells differentiation, proliferation, migration and modulation of cell-cell interactions in the vasculature (Ferrara & Davis-Smyth, 1997; Larrivee & Karsan, 2000).

According to a previous study performed by Davis et al. (1996), VEGF regulates angiogenesis through αvβ5-mediated integrin pathway (Davis et al., 1996). The combined effect of Angiotensin I (Ang I) and Angiotensin II (Ang II) play the crucial role in VEGF-mediated angiogenesis. Ang I, as a selective ligand for Tie-2 (EC-specific tyrosine kinase), is responsible for assembling the vascular wall (Suri et al., 1996), whereas Ang II could disturb the formation of vascular network by blocking Tie-2 receptor (Maisonpierre et al., 1997).

VEGF receptor is a common therapeutic target in neovascularization related diseases. through the neutralization and combination with dominant negative soluble receptors to inhibit the growth of tumors and metastasis (Gorski et al., 1999; Hess et al., 2001; Ng et al., 2006). Therefore, anti-VEGF antibodies, such as mAb, can protect the impaired cells from radiation-induced hypoxia (Lee et al., 2000). Besides, blockage of Ang II receptor decreases the radiation-induced renal tubular proliferation, and reduces its magnitude, leading to the delay of radiation-induced nephropathy.

(Moulder et al., 2002). Therefore, the inhibition of Ang II could a treatment strategy for angiogenesis involved diseases. Moreover, VEGF could exert the influence in tumor radioresistence, as the presence of VEGF induced a higher survival, but eliminated the activation of mitogen-activated protein kinase (MAPK) and MAPK kinase (MEK1/MEK2) (Gupta Vinay K. et al., 2002).

2.4.4.2 Focal adhesion kinase (FAK)

Focal adhesion kinase (FAK) is a non-receptor tyrosine kinase, and it regulates the cellular biological processes such as survival, migration, proliferation and growth. FAK controls these cellular processes through mediating the biological signals that are simulated by integrins or growth factor receptors to intracellular cytoskeletal and signaling proteins (Parsons, 2003; Schlaepfer & Mitra, 2004).

FAK is phosphorylated at Tyr^{397} promptly once the cell adhesion or growth factor receptor are activated, and thus offers a highly affinitive binding sites for Src homology 2 (SH2) domains-carried molecules (such as Src family kinases). Subsequently, the corresponding SH2 activates other phosphorylated sites of FAK and the residuals of Tyr^{576} and Tyr^{577} are included to amplify the cascade of FAK-mediated signaling (Calalb et al., 1995; Owen et al., 1999).

FAK is also an important scaffold protein that can mediate the signaling of Scr family kinase phosphorylation to synthesize various proteins by scaffold portion (long N- and C-terminal segments), such as endophilin A2 (Wu et al., 2005), p130Cas (Ruest et al., 2001; Vuori et al., 1996) and paxillin (Burridge et al., 1992; Schaller & Parsons, 1995), which are subsequently bound to FAK at carboxyl terminal.

The amplified phosphorylated cascade process and interactions between proteins are widely reported in multiple cellular functions which modulate a variety of biological regulations. In a recent animal study, Sun at al. found that VEGFE2 expression was regulated by FAK due to its kinase activity and its translocation into the nucleus. They also found that FAK was involved in the regulating VEGFR2, because of the detection of nuclear FAK in RNA polymerase II complex (Sun et al., 2018).

Previous studies of VEGF involved FAK signaling pathways revealed some novel modulators, and they may be the potential therapeutic targets in inflammatory and cardiovascular diseases. An animal study found that overexpression of Semaphorin 7A (Sema7A) could increase VEGFA/VEGFR2-inducing cell migration and angiogenesis, and such upregulating of VEGFA/VEGFR2 was vanished when Sema7A receptor and β1 integrin were blocked. Besides, cell migration and angiogenesis were found to be significantly inhibited by the inhibition of FAK or ERK1/2 downstream of β1 integrin signaling pathway through Rho-associated coiled forming protein kinase and myosin phosphatase targeting subunit (Hu et al., 2018). Another study using knock-out mice and endothelial cells found that apolipoprotein L3 (APOL3) played the role in angiogenesis and was involved in MAPK and FAK signaling. This finding was proven by experimental results in which the absence of APOL3 enhanced the permeability of endothelial cells, while decrease the ability of wound repairmen and forming tubules. Consistently, some of the pro-angiogenic signaling pathways (ERK1/2 and FAK) and expressions of the relevant genes were downregulated in the cells with the absence of APOL3 (Khalil et al., 2018). Moreover, thrombospondin type I domain 1 was found to be a protective angiopotent factor in severe atherosclerotic plaques by preventing intraplaque microvessels from hemorrhage (Haasdijk et al., 2016).2.4.4.3 Nitric oxide pathway

Nitric oxide (NO) is produced from oxidation of amino acid L-arginine at the terminal guanidine nitrogen atom, through an enzyme called nitric oxide synthase (NOS). NOS is composed of constitutive NOS (cNOS) and inducible NOS (iNOS). Furthermore, the presence of isoforms of cNOS in endothelial cells (eNOS), as well as in some neuronal cells (nNOS) have been reported (Bult, 1996).

The major effect of NO is to coordinate the vasomotion between vasodilation and vasoconstriction. In healthy conditions, the physical (e.g. pressure, shear stress) and chemical [5-hydroxytryptamine (5-HT), bradykinin, acetylcholine] stimulations upregulate the levels of cytoplasmic Ca2+ in endothelial cells. The Ca2+-calmodulin-dependent eNOS is therefore activated, and leads to the formation of NO (**Figure 2.13**).

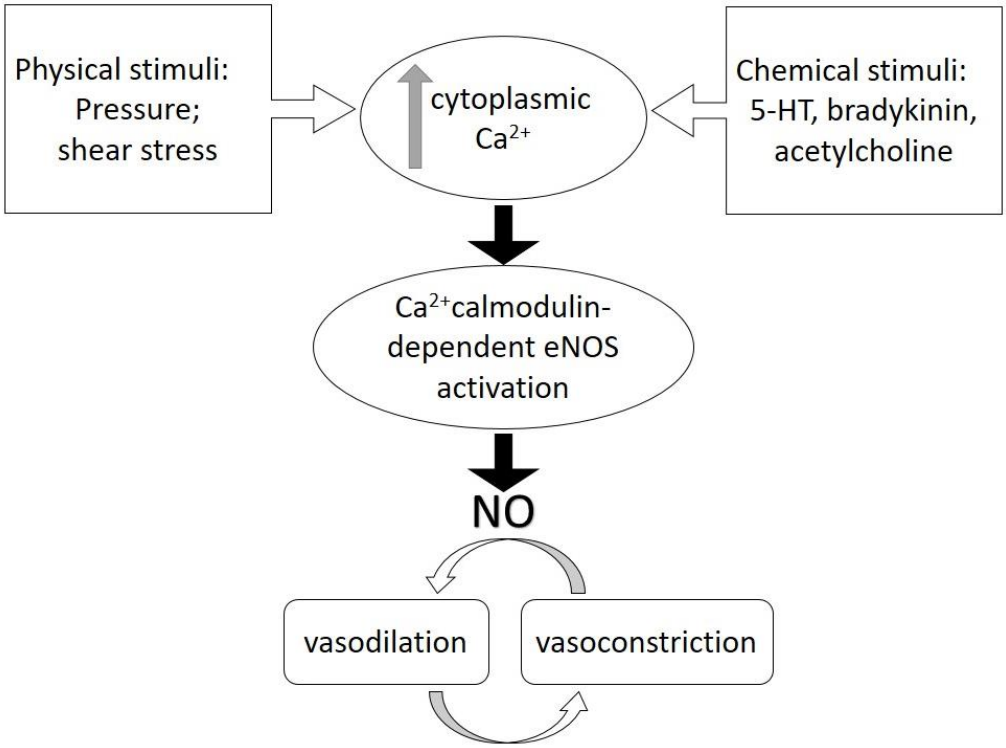

Figure 2.13 NO production in endothelial cells.

As a small diatomic molecule, NO could diffuse into the underlying smooth muscle cells, which involves cytoplasmic guanylate cyclase and forms cyclic GMP (cGMP), and eventually result in vascular dilation and smooth muscle relaxation (Gross & Wolin, 1995). In the contrary, under the same physical and chemical stimulation, an impaired eNOS pathway would result in vascular contraction instead of vascular dilation. Particularly, with the stimulation of catecholamines and 5-HT, the impaired eNOS induces further vasoconstriction. The abnormal vasoconstriction narrows vessel lumen and reduces the oxygen supply to cells leading ischaemia (Meredith et al., 1993).

In addition, NO is found to restrain the early development of atherosclerosis. As introduced in Section 2.2, the development of atherosclerosis involves the invasion of oxLDL from blood to vessel wall, recruitment of monocyte-derived macrophages and lymphocytes, formation of foam cells, and the migration and accumulation of SMCs. It was reported that NO inhibits the adhesion of monocytes (Mehta et al., 1995; Tsao et al., 1994), decreases the release of chemotactic molecule and monocyte chemotactic protein 1 (MCP-1, which could induce migration and differentiation of monocytes to macrophages) (Zeiher et al., 1995), inhibits oxidation of LDL (Witztum, 1993), and suppresses the migration and proliferation of SMCs (De Meyer et al., 1995; Marks et al., 1995). At the same time, NO could expedite the formation of necrotic core (Kockx et al., 1996), and promote the plaque vulnerability (Davies & Woolf, 1993). Therefore, NO plays an important role in the development of atherosclerosis, by suppressing its initiation, but increasing the instability of advanced plaques.

In 2015, Sakata et al. examined the post-radiation effect (≤20 Gy) on human umbilical vein endothelial cells (HUVECs) through eNOS signaling. The results showed that radiation-induced defective eNOS signaling caused activation of eNOS in HUVECs,

and this was probably due to the upregulation of reactive oxygen species (ROS) production and upregulation of protein kinase C- βII (PKC-βII) (Sakata et al., 2015).

2.5 Basis of this study

NPC is an endemic head and neck carcinoma and is prevalent in Hong Kong and South-eastern Asia. Metastasis of neck lymph nodes is common in NPC patients. Clinically, RT is an effective and common therapeutic method to treat both NPC and nodal metastasis. As carotid arteries are in close proximity to the neck lymph nodes, they are unavoidably exposed to radiation during neck RT. As a result, carotid atherosclerosis is commonly found in post-RT NPC patients as a long-term complication (i.e. radiation-induced carotid atherosclerosis).

Besides of radiation, the presence of one or more CVRFs can also cause carotid atherosclerosis (i.e. non-radiation-induced carotid atherosclerosis). Carotid atherosclerosis is characterized of increased CIMT, presence of plaque and arterial stenosis. Carotid plaques are atherosclerotic lesions, which are composed of different types of cell, such as SMCs, lipid-rich foam cells and macrophages. The carotid plaque composition affects the stability of plaque. Rupture of an unstable plaque could result in cerebrovascular diseases, such as strokes, which could be fatal.

Ultrasound is a non-invasive medical imaging modality and frequently used to evaluate and monitor carotid atherosclerosis. However, few studies investigated the difference between non-radiation-induced and radiation-induced carotid atherosclerosis, especially with respect to the characteristics of carotid plaque. To fill

this research gap, the present PhD project recruited post-RT NPC patients with/without CVRFs and subjects with CVRFs, and comprehensively investigated the differences of ultrasound features of carotid atherosclerosis among post-RT patients and subjects with CVRFs. Ultrasound can be used to evaluate carotid plaque components and estimate plaque stability. However, previous studies used either subjective visual assessment or GSM analysis which are inaccurate and not comprehensive. The present project used a detailed computer image analysis method, the DPTA, to investigate and compare the carotid plaque components in non-radiation-induced and radiation-induced carotid atherosclerosis.

More evidence suggested that endothelial dysfunction is an early marker for atherosclerosis. Exposure of endothelial cells to CVRF such as high glucose environment can cause endothelial dysfunction. Radiation causes cell damage and is an independent risk factor of atherosclerosis. However, there is limited information in the literature about the combined effect of radiation and exposure to high glucose environment on endothelial cells. In the present PhD project, an in vitro study was performed to investigate the effect of high-glucose and radiation on human vascular endothelial cells through FAK-mediated signaling pathway in regulation of angiogenesis. The result of this study contributes to a further understanding of radiation-induced carotid atherosclerosis. The study result also provides an insight of the risk of carotid atherosclerosis in post-RT NPC patients with diabetes.

Chapter Three

Computer-assisted Ultrasound Assessment of Plaque Characteristics in Radiation-induced and Non-radiation-induced Carotid Atherosclerosis

3.1 Introduction

Nasopharyngeal carcinoma (NPC) is a common head and neck cancer in Southeast Asia. The top nine countries in the world with the highest incidence of new NPC cases are all in Southeast Asia. In 2018, there were 129,079 new NPC cases globally (Bray et al., 2018). Nodal metastasis is common in NPC patients, and about 60% to 85% of the patients have neck lymph node metastasis (Chong & Ong, 2008). For NPC, radiotherapy (RT) is the common treatment method for both the primary tumour and metastatic neck lymph nodes, and chemotherapy may be used in conjunction with RT for patients in advanced stages of the disease (Lee et al., 2015). Since extracranial carotid arteries are in close proximity to neck lymph nodes, they are unavoidably irradiated during the RT of neck lymph nodes (Glastonbury, 2007; Leung et al., 2005).

Carotid atherosclerosis is a late post-RT complication in patients who have received external irradiation to the head and neck. As a chronic inflammatory disease, subclinical atherosclerosis is identified by the increased carotid intima-media thickness (CIMT) and the formation of carotid atherosclerotic plaque (Naqvi & Lee,

2014; Touboul et al., 2007). The development of carotid atherosclerosis is a progressive process, and therefore different characteristics of carotid plaques represent different stages of atherosclerotic development. It is generally believed that atherosclerosis is initiated by endothelial dysfunction on the inner surface of artery wall. The injured endothelium elicits the sub-endothelial accumulation of cholesterol, namely oxidized low-density lipoprotein (LDL). Monocyte-derived macrophages and lymphocytes are then recruited at the intima, causing the formation of foam cells. Meanwhile, smooth muscle cells (SMC) migrate from the media and are localized at the atherosclerotic lesion. The accumulation of cells thickens the CIMT and alternates the endothelium to pro-inflammation, pro-thrombosis, pro-coagulation, fibrosis and vasoconstriction, resulting in more severe damage of the homeostasis on blood-tissue interface and eventually forming a plaque (Lusis, 2000; Ross, 1999; Sumpio et al., 2002).

The composition of carotid plaque is largely associated with the risk of stroke of patients. Advanced atherosclerotic lesion forms a thrombus, which can occlude the blood vessel. Rupture and erosion of carotid plaque may form emboli in the circulation which lead to stroke and cerebrovascular events. Therefore, carotid atherosclerosis and the presence of carotid plaque increase the risk of cerebrovascular diseases (Lam et al., 2001; Lusis, 2000; Stein et al., 2008; Yuan et al., 2017).

Clinically, ultrasound is a non-invasive imaging tool and is commonly used to evaluate carotid atherosclerosis by examining various atherosclerotic parameters including CIMT, carotid arterial stiffness (CAS) and carotid plaque score. Nevertheless, the difference of radiation-induced and non-radiation-induced carotid atherosclerosis was not comprehensively investigated. Computer-aided assessment of carotid plaque

characteristics on ultrasound images is recently available (Lal et al., 2002; Madycki et al., 2006). However, there is no previous studies used this method to assess radiation-induced and non-radiation-induced carotid plaques, and compare their differences. Therefore, in the present study, we aimed to evaluate the degree of carotid atherosclerosis of NPC patients with previous RT and subjects with cardiovascular risk factor (CVRF) by evaluating their CIMT and incidence of carotid plaque using ultrasonography. This study also investigated the differences in carotid plaque characteristics in radiation-induced and non-radiation-induced carotid atherosclerosis by using a computer-assisted ultrasound assessment method.

3.2 Materials and methods

3.2.1 Subject recruitment

Post-radiotherapy (RT) NPC patients treated with intensity-modulated radiation therapy (IMRT) were recruited from the Department of Clinical Oncology of Queen Mary Hospital. The inclusion criteria of post-RT NPC patients were Chinese NPC patients, 18 years old or above, a single completed RT course, and a post-RT duration of 4 years or more (according to the results of previous study, radiation-induced carotid atherosclerosis could be assessed when the post-RT duration was greater than 4 years) (Yuan et al., 2014); while the exclusion criteria were a known history of leukopenia, thrombocytopenia, severe hepatic or renal dysfunction, an evidence for inflammatory or other malignant diseases, a known history of carotid atherosclerosis prior to RT, previous carotid endarterectomy or stenting.

Subjects with cardiovascular risk factor (CVRF) were also recruited for the study. They were recruited by poster advertisement in the campus of the Hong Kong Polytechnic University. The inclusion criteria of CVRF subjects were Chinese, older than 40 years, and at least having one CVRF, including smoking (current smoker), diabetes mellitus (DM), hypertension, hypercholesterolemia or coronary heart disease (CHD). The exclusion criteria for the subject recruitment were previous RT, carotid endarterectomy or stenting.

For each CVRF subject, the presence of CVRF was identified by the following methods:

(1) DM, diagnosed with DM clinically, under medications to lower the glycaemic level and/or fasting plasma glucose≥ 7.0 (6.1) mmol/L (Alberti K. G. M. M. & Zimmet P. F., 1998);

(2) hypertension, diagnosed with hypertension clinically, under anti-hypertensive medications and/or the measured blood pressure≥ 140/90 mmHg (Carretero Oscar A & Oparil Suzanne, 2000);

(3) hypercholesterolemia, diagnosed with hypercholesterolemia clinically, enduring medications to lower the cholesterolemia level and/or fasting total cholesterol value≥ 5.2 mmol/L (Chang et al., 2009; Ford et al., 2010);

(4) CHD, diagnosed with coronary vascular disease clinically and/or noticed with coronary stenting;

(5) smoker, habitually smoking with 10 cigarettes a single day lasting for at least half a year.

3.2.2 Study design and ultrasound examination

The Human Subject Ethics Subcommittee of the Hong Kong Polytechnic University (HSEARS20160930001) and the Institutional Review Board of the University of Hong Kong/Hospital Authority Hong Kong West Cluster approved this study (HA RE001F3). All participants (recruited post-RT NPC patients and CVRF subjects) were provided an information sheet with detailed information of the study and the rights of participants. Informed written consent was obtained from all participants before the commencement of the examinations.

Medical history of the post-RT NPC patients including post-RT duration, history of chemotherapy and atherosclerotic diseases was obtained from archived clinical records of the patients.

Individual face-to-face interview was conducted with post-RT NPC patients and CVRF subjects to obtain the demographical information and history of CVRF.

All participants had a carotid ultrasound examination. All ultrasound examinations were performed by a single dedicated ultrasound researcher with five years of carotid ultrasound experience using the Esaote MyLab™ Twice eHD CrystaLine ultrasound unit in conjunction with a 3-13 MHz linear transducer (SL1543) (Esaote, Genoa, Italy). In order to ensure the measurements were obtained with the subjects at resting state, all subjects were allowed to rest for at least 10 minutes before the ultrasound examination. In the carotid ultrasound examination, the subject lay supine on the

examination couch with the shoulders and neck supported by a pillow so that the neck was slightly extended and the head turned away from the side under examination. On each side of the neck, the CIMT was evaluated using the automated quantification programs of the ultrasound unit: radiofrequency-based quality intima-media thickness (RF-QIMT) (**Figure 3.1B**).

For each subject, the presence or absence of carotid plaque in the internal, external and common carotid arteries was assessed. Carotid plaque was identified as focal arterial wall thickening >50% of the adjacent intima-media layer (Touboul et al., 2012). In any cases that the carotid plaque was not clearly demonstrated on grey scale ultrasound such as hypoechoic plaque, colour Doppler ultrasound was used to demonstrate the vessel lumen at the stenosis for identify the carotid plaque.

A.

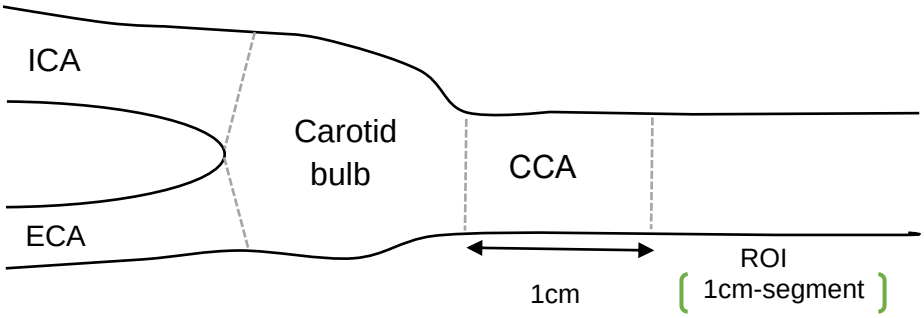
ICA
Carotid
bulb
CCA
ECA
1cm
ROI
1cm-segment

B.

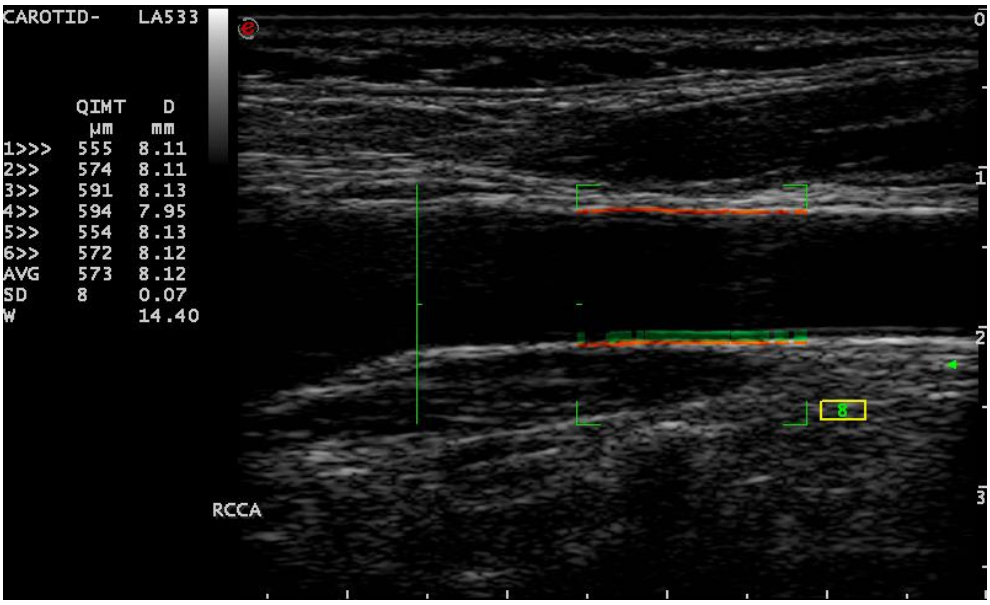
CAROTID- LA533
QIMT D
µm mm
1>>> 555 8.11
2>> 574 8.11
3>> 591 8.13
4>> 594 7.95
5>> 554 8.13
6>> 572 8.12
AVG 573 8.12
SD 8 0.07
W 14.40
RCCA

C.

D.

Figure 3.1 Ultrasound measurement of carotid intima-media thickness (CIMT) and detection of carotid plaque. Carotid artery is examined by ultrasound from CCA (common carotid artery) to ECA (external carotid artery) and ICA (internal carotid artery). **Image A** shows a schematic diagram of carotid artery. The CIMT (i.e. ROI) is measured over a 1-cm segment of the CCA that is 1 cm proximal to the inferior end

of the carotid bulb. **Image B** is a longitudinal grey scale sonogram that shows the measurement of CIMT using the radiofrequency-based quality intima-media thickness function (Esaote, Genoa, Italy). The green square brackets indicate the region of interest (ROI, 1-cm segment of CCA that is 1cm proximal to the inferior end of carotid bulb). The red lines indicates the tracking of the interfaces between the media and adventitial layer in both the near and far walls of the carotid artery. In the ROI, the thickness of the green line means the thickness of the intima-media layer in the far wall of the carotid artery. **Image C** is a longitudinal grey scale sonogram that shows a carotid artery without carotid plaques. **Image D** is a longitudinal grey scale sonogram that shows a carotid artery with a carotid plaque at the carotid bifurcation (arrow).

All identified carotid plaque of each subject were included in the study, and the characteristics of each carotid plaque were evaluated for:

1. grey-scale median (GSM);

2. detailed plaque texture analysis (DPTA):

   (1)average pixel density, referring to area pixel density for each component;

   (2)area percentage, referring to area percentage for each component relative to the entire plaque;

   (3)integrated of density (IOD), referring to the product of average pixel density and area percentage for the certain component.

In the evaluation of GSM and DPTA, archived digital images were reviewed and analysed using the image-processing software Adobe Photoshop CS, v.8.0 (Adobe, San Jose, CA, United States) and Image Pro Plus, v.6.0 (Media Cybernetics, Rockville, MD, United States) respectively. For each carotid plaque, five longitudinal grey scale sonograms which clearly demonstrating the borders and internal echotexture of the plaque were selected to evaluate the GSM and plaque characteristic analysis. Image normalization was performed before the evaluation. With the use of the histogram facility of the software, the grey scale value of two reference areas (blood and adventitia) in the image were adjusted to standardise the grey scale value of blood as 0 and adventitia as 190. All the pixels of the image were shifted accordingly based on the standard linear scale, and a normalized image was produced (Gronholdt et al., 2002; Pedro et al., 2000; Tegos et al., 2000).

For the evaluation of GSM, the carotid plaque was outlined manually on the normalized grey scale ultrasound image using software Adobe Photoshop CS, v.8.0 (Adobe, San Jose, CA, United States) using the function “Lasso Tool”. The software then calculated the median of the grey scale value of pixels (i.e. GSM) within the region of interest (ROI) and the GSM value was displayed in the Histogram window.

For the DPTA, the software Image Pro Plus v.6.0 (Media Cybernetics, Rockville, MD, United States) was used to analyse the normalized grey scale ultrasound images. In the image analysis, the different components of carotid plaque were color-coded by the software based on the different grey scale ranges as suggested by a previous literature (Lal et al., 2002; Madycki et al., 2006): yellow for blood (grey scale ranges 0-9), orange for lipid (10-31), red for muscle (32-74), light blue for fibrous tissue (75-111) and dark blue for calcium (112-255) (**Figure 3.2**). On ultrasound, the blood, lipid and muscle appeared hypoechoic, while fibrous tissue and calcification were hyperechoic (75-255) (Madycki et al., 2006). Each carotid plaque component was evaluated by three parameters, namely average pixel density, area percentage and integrated optical density (IOD). Average pixel density (or intensity) indicated the mean value of pixel densities of each component. Area percentage indicated the percentage that the area of each component relative to the area of the entire plaque. IOD indicated integration of pixel density of each component, which was also equal to area × average pixel density. Thus, it was an accumulative factor account for both pixel density and area percentage of each component.

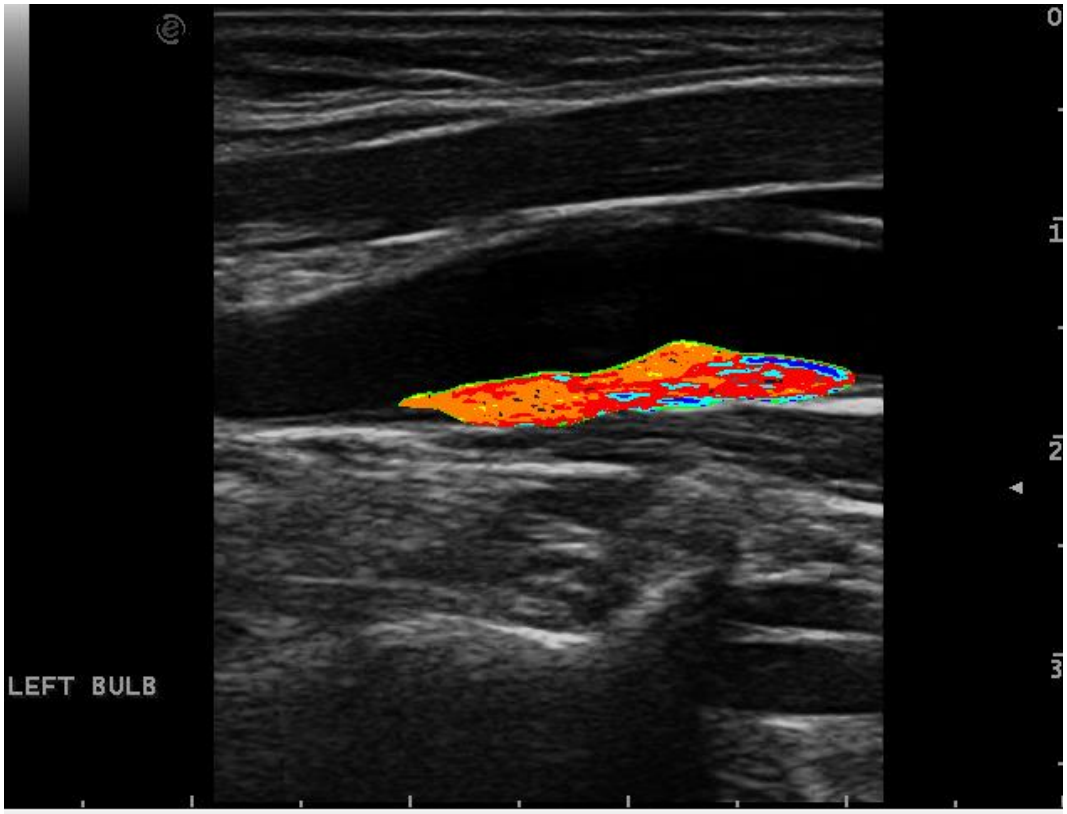

Figure 3.2 Carotid plaque coded by different colours indicates different tissues within the plaque. Different tissues within a plaque is indicated as followed: yellow for blood (grey scale ranges: 0-9), orange for lipid (10-31), red for muscle (32-74), light blue for fibrous tissue (75-111) and dark blue for calcium (112-255)**.**

3.2.3 Statistical analysis

Basic information of the subjects and plaque characteristics were expressed as mean ± SD or SEM for the continuous data; counts and percentage were presented for categorical data. Normal distribution of the data was evaluated by Shapiro-Wilk test. The difference between post-RT NPC group and CVRF group were evaluated using Mann Whitney U test and Chi-square test for nonparametric variables (number of CVRFs, plaque number per subject, plaque presence, CIMT and GSM), and unpaired Student t-test for parametric variables (age). Comparisons among groups were evaluated by one-way ANOVA. The effects of age, gender, number of CVRFs and exposure to radiation on carotid plaque characteristics were analysed by multiple linear regression models. The risk factors regarded as candidate variables were age, gender, number of CVRFs and radiation. We used multivariable model to analyse the effects of different risk factors on plaque characteristics (CIMT, plaque presence, number of plaques per subject, plaque components). All statistical analyses were performed using SPSS 22 (IBM Corporation, Armonk, NY, United States) and Prism 7.0 (GraphPad Software, San Diego, CA, United States). P value<0.05 was considered to be significant.

3.3 Results

3.3.1 Demographical information

From April 2017 to May 2018, a total of 111 post-RT NPC patients and 110 CVRF subjects were recruited. Four post-RT patients were excluded from the study because

two of them did not have comprehensive clinical information, and two were unsatisfied to the inclusion criteria, because the post-RT duration of one patients was less than four years, and another patient was treated with stenting without informing the researcher during the face-to-face interview. Finally, 107 post-RT NPC patients and 110 CVRF subjects were included in the study. The demographic and clinical information of the post-RT NPC patients and CVRF subjects are summarized in **Table 3.1**. There was no significant difference in the age of the post-RT NPC patients and CVRF subjects (58.4 ± 1.1 vs. 60.7 ± 0.7 respectively, $p>0.05$). There were significantly more males among the post-RT NPC patients when compared to the CVRF group (68/107 vs. 44/110, $p<0.001$). Among the post-RT NPC patients, 57 of them (53.3%) had no CVRFs, 31 patients (28.9%) had one CVRF and 19 patients (17.8%) had more than one CVRFs.

In the CVRF group, 58 out of 110 subjects (52.7%) had only one CVRF and the remaining subjects had at least two CVRFs (47.3%). The most prevalent CVRF was hypertension (n=74, 67.3%), followed by hyperlipidaemia (n=69, 62.7%), diabetes (n=23, 20.9%) and smoking (n=9, 8.2%).

Table 3.1 Demographic information of subjects

	post-RT NPC (n=107)	**CVRF (n=110)**	**P Value**
Age, yrs	58.4 ± 1.1	60.7 ± 0.7	0.069
Gender(female/male), n	39/68	66/44	<0.001***
Chemotherapy, n (%)	59 (55.1)	-	-
Post-RT Duration	15 ± 8.9	-	-
Number of CVRF†			
0, n (%)	57 (53.3)	-	-
1, n (%)	31 (29.0)	58 (52.7)	<0.001***
≥2, n (%)	19 (17.7)	52 (47.3)	<0.001***
CVRF			
Hypertension, n (%)	40 (37.4)	74 (67.3)	<0.001***
Hyperlipidaemia, n (%)	17 (15.9)	69 (62.7)	<0.001***
Diabetes, n (%)	6 (5.6)	23 (20.9)	<0.001***
Current Smoking, n (%)	6 (5.6)	9 (8.2)	0.455
Heart disease, n (%)	4 (3.7)	-	0.041*

Values are expressed as mean ± SD;

†CVRF = cardiovascular risk factor; yrs = years

*p<0.05, ** p<0.01, ***p<0.001

3.3.2 Carotid plaque assessment

Table 3.2 shows the comparison of the characteristics of radiation-induced and non-radiation-induced carotid atherosclerosis. Results showed that post-RT NPC patients were more likely to have carotid plaques when compared to the CVRF subjects (80.4% vs. 38.2%, $p<0.001$). Regardless of the presence or absence of CVRF, the mean number of carotid plaques in post-RT NPC patients was significantly higher than that in CVRF subjects ($p<0.001$). There was no significant difference in the number of carotid plaques between post-RT NPC patients with or without CVRF ($p>0.05$).

Among the 247 carotid plaques in the post-RT NPC patients, 7 (2.8%) were located in internal carotid artery (ICA), 160 (64.8%) were in carotid bulb, and 80 (32.4%) were in common carotid artery (CCA). Among the 59 carotid plaques in the CVRF subjects, 3 (5.1%) were found in ICA, 2 (3.4%) were in external carotid artery, 45 (76.3%) were in carotid bulb, and 9 (15.2%) in CCA.

3.3.3 CIMT assessment

As shown in the **Figure 3.3** and **Table 3.2**, post-RT NPC patients had significantly larger CIMT (748 ± 15.1 μm) than CVRF subjects (680.4 ± 10 μm, $p=0.001$). Besides, both post-RT NPC patients with CVRF (740.4 ± 20 μm) and those without CVRF (756.7 ± 23 μm) had significantly larger CIMT than subjects in CVRF group (680.4 ± 10 μm, $p=0.004$). However, the difference in the CIMT between post-RT NPC patients with CVRF and those without CVRF was not statistically significant ($p>0.05$).

3.3.4 GSM assessment

Results showed that there was no significant difference in the GSM of carotid plaque in post-RT NPC patients and CVRF subjects (p=0.087), nor among post-RT NPC patients with or without CVRF and CVRF subjects (p=0.229) **(Table 3.2).**

A. CIMT in post-RT NPC subject

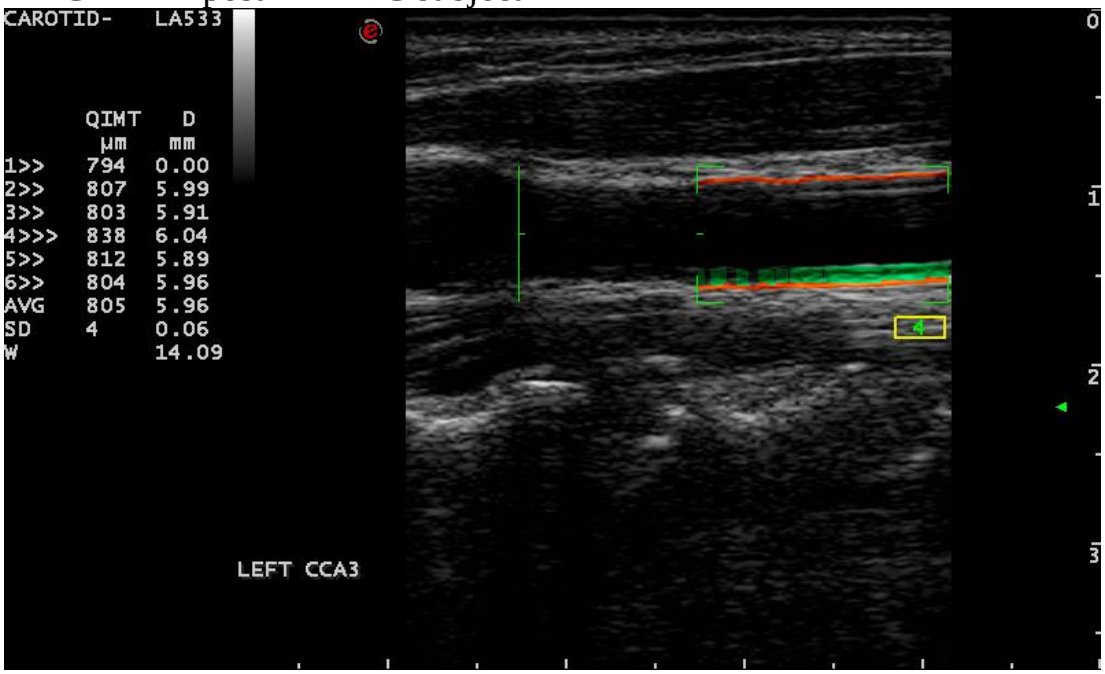

B. CIMT in CVRF subject

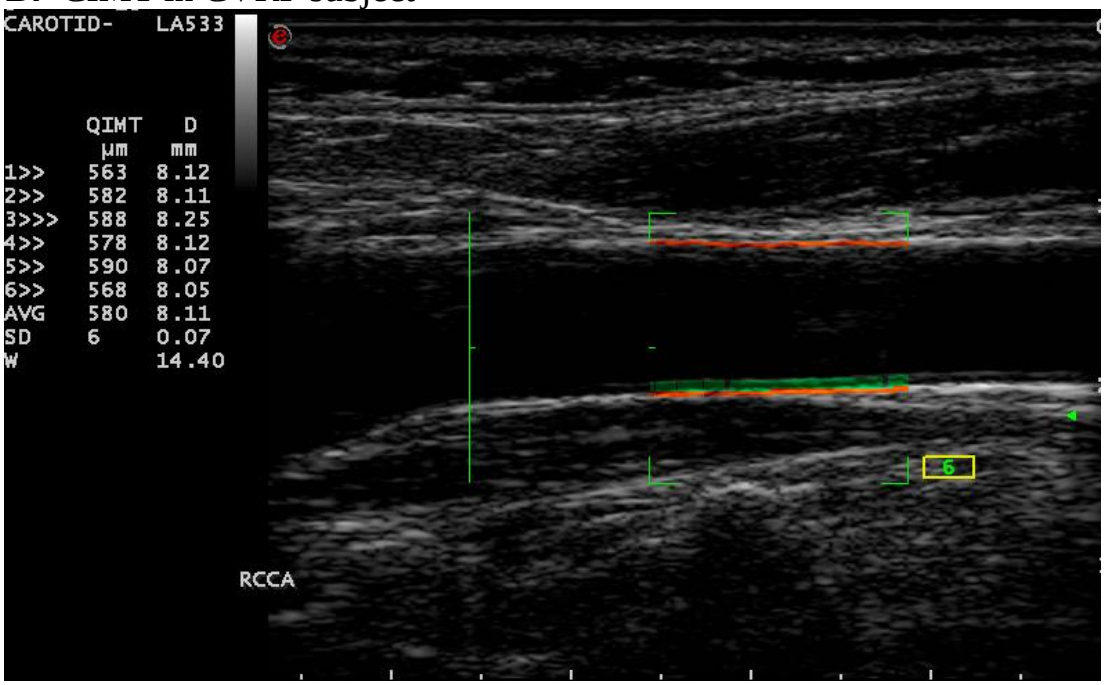

Figure 3.3 The comparison of carotid intima-media thickness between post-RT NPC and CVRF subjects. Longitudinal sonograms show carotid intima-media thickness of 1-cm segment in 1 cm proximal to the inferior end of the carotid bulb of a post-RT NPC patient **(A)** and of a CVRF subject **(B)**. Noted the radiation-induced carotid intima-media thickness is higher **(A)** than the non-radiation-induced one **(B)**.

Table 3.2 Comparison of the characteristics between radiation-induced and non-radiation-induced carotid atherosclerosis

	Post-RT NPC (Total) (N=107)	**(1) Post-RT NPC (with CVRF, N=50)**	**(2) Post-RT NPC (without CVRF, N=57)**	**(3) CVRF (N=110)**	**P^T**	**P^M**	**Dunnett Post-hoc**
Number of subjects with plaque (%), N[†]	86 (80.4), N=107	-	-	42 (38.2), N=110	<0.001***	-	-
Plaque numbers per subject, N	2.3 ± 0.2, N=107	2.6 ± 0.3, N=50	2.0 ± 0.2, N=57	0.5 ± 0.1, N=110	<0.001***	<0.001***	1 > 3*** 2 > 3***
CIMT (μm), N	748.0 ± 15.1, N=107	740.4 ± 20.0, N=50	756.7 ± 23.0, N=57	680.4 ± 10.0, N=110	0.001***	0.004**	1 > 3* 2 > 3*
GSM of plaque, n	29.1 ± 18.0, n=247	28.7 ± 16.7, n=131	29.6 ± 19.4, n=116	25.5 ± 15.0, n=59	0.087	0.229	-

Values are mean ± SEM

[†]N=total number of subject in the corresponding analysis; n=total number of carotid plaque in the corresponding analysis; GSM=grey-scale median

P^T=Comparison between total post-RT NPC patients and CVRF subjects.

P^M=Multiple comparison among post-RT NPC patients with CVRF, post-RT NPC patients without CVRF, and CVRF subjects.

*P<0.05, ** P<0.01, ***P<0.001

3.3.5 Carotid plaque component assessment

Table 3.3 and **Table 3.4** show the DPTA results in terms of the presence of different components within the carotid plaque of post-RT NPC patients and CVRF subjects. Results showed that carotid plaques in post-RT NPC patients, regardless the patients had CVRF or not, were more often to have calcification (total, 73.7%; with CVRF, 75.6%; without CVRF, 71.6%) when compared to carotid plaques in CVRF subjects (57.6%), and the differences were statistically significant ($p=0.015$, $p=0.041$, respectively). By contrast, no significant differences were observed in the other four plaque components (blood, lipid, muscle and fibrous tissue) among the study groups ($p>0.05$). (**Figure 3.4**)

Table 3.3 Comparison of the presence of different components within the carotid plaques in post-RT NPC patients and CVRF subjects

Components	Number of carotid plaques (%)		P Value[†]
	Post-RT NPC (n=247)	CVRF (n=59)	
Blood	229 (92.7%)	55 (93.2%)	0.885
Lipid	246 (99.6%)	59 (100.0%)	0.625
Muscle	247 (100.0%)	59 (100.0%)	>1.000
Fibrous tissue	231 (93.5%)	52 (88.1%)	0.159
Calcification	182 (73.7%)	34 (57.6%)	0.015[*]

[†]P value=Difference between post-RT NPC patients and CVRF subjects.[*]P<0.05

Table 3.4 Comparison of the presence of different components within the carotid plaques among post-RT NPC patients (with or without CVRF) and CVRF subjects

Component	Number of plaques (%)			P Value[†]
	Post-RT NPC with CVRF (n=131)	Post-RT NPC without CVRF (n=116)	CVRF (n=59)	
Blood	112 (93.1%)	107 (81.7%)	55 (93.2%)	0.955
Lipid	131 (100.0%)	115 (99.1%)	59 (100.0%)	0.379
Muscle	131 (100.0%)	116 (100.0%)	59 (100.0%)	-
Fibrous tissue	123 (93.9%)	108 (93.1%)	52 (88.1%)	0.360
Calcification	99 (75.6%)	83 (71.6%)	34 (57.6%)	0.041[*]

[†]P value= Difference in post-RT NPC patients (with/without CVRF) and CVRF subjects.[*]$p<0.05$.

Carotid plaque components were further evaluated for average pixel density, area percentage and IOD. **Table 3.5** shows the differences of these plaque component parameters between post-RT NPC patients and CVRF subjects. **Table 3.6** compares the plaque component parameters among the post-RT NPC patients with or without CVRF and CVRF subjects.

There was no significant difference in the average pixel density of the five plaque components between post-RT NPC and CVRF groups ($p>0.05$).

For the area percentage of different components within carotid plaque, CVRF subjects had significantly larger area of lipid (46.3 ± 17.9%) than all the post-RT NPC patients (42.1 ± 16.9%, $p=0.034$, **Table 3.5**) and post-RT NPC patients with CVRF (40.5 ± 16.1%; $p=0.020$, **Table 3.6**). Conversely, carotid plaques in CVRF subjects had significantly lesser calcification (3.0 ± 5.7%) than post-RT NPC patients (4.8 ± 7.7%, $p=0.012$, **Table 3.5**) and post-RT NPC patients with CVRF (4.4 ± 6.6%, $p=0.030$, **Table 3.6**). No significant differences were found between post-RT NPC patients and CVRF subjects in the area percentage of blood, muscle and fibrous tissue within carotid plaque ($p>0.05$).

For the IOD of carotid plaque components, the aggregate post-RT NPC patients had a significantly higher value than CVRF subjects in both muscle (3086.0 ± 3121.0 and 2392.0 ± 1911.0 respectively, $p=0.043$) and calcification (4073.0 ± 6667.0 and 2675.0 ± 6615.0 respectively, $p=0.007$) (**Table 3.5**). Carotid plaques in post-RT NPC patients with CVRF had significant higher IOD of muscle (3416.0 ± 3106.0) when compared to those in post-RT NPC patients without CVRF (2712 ± 3108) and CVRF subjects (2392.0 ± 1911.0) ($p=0.004$) (**Table 3.6**). Additionally, carotid plaques in post-RT

NPC patients with CVRF had significant higher IOD of calcification (3767.0 ± 5593.0) when compared to carotid plaques in CVRF subjects (2675.0 ± 6615.0) (p=0.018) (**Table 3.6**).

Table 3.5 Difference of carotid plaque component parameters between post-RT NPC patients and CVRF subjects

Parameters	Post-RT NPC (n=247)	CVRF (n=59)	P value[†]
Average pixel density			
blood	7.5 ± 2.9	7.3 ± 1.0	0.316
lipid	22.1 ± 3.7	21.4 ± 4.5	0.432
muscle	44.6 ± 6.4	43.2 ± 6.4	0.072
fibrous tissue	86.6 ± 4.1	86.5 ± 4.7	0.973
calcification	129.5 ± 11.8	130.2 ± 13.36	0.851
Area percentage (%)			
blood	14.8 ± 14.1	15.0 ± 13.4	0.720
lipid	42.1 ± 16. 9	46.3 ± 17.9	0.034[*]
muscle	31.0 ± 13.4	29.2 ± 15.3	0.249
fibrous tissue	7.4 ± 7.6	6.6 ± 8.3	0.176
calcification	4.8 ± 7.7	3.0 ± 5.7	0.012[*]
IOD			
blood	224.4 ± 938.0	143.3 ± 197.4	0.802
lipid	1986.0 ± 2157.0	2056.0 ± 1967.0	0.498
muscle	3086.0 ± 3121.0	2392.0 ± 1911.0	0.043[*]
fibrous tissue	1147.0 ± 1112.0	1090.0 ± 1181.0	0.278
calcification	4073.0 ± 6667.0	2675.0 ± 6615.0	0.007[**]

Values are presented as mean ± SD. [†]P value=Difference between total post-RT NPC patients and CVRF subjects. [*]P<0.05, [**] P<0.01.

Table 3.6 Differences of carotid plaque component parameters among post-RT NPC patients (with or without CVRF) and CVRF subjects

Parameters	Post-RT NPC		(3) CVRF	P value†	Dunnett Post-hoc
	(1) with CVRFs（n=131)	(2) without CVRFs（n=116）	(n=59)		
Average pixel density					
blood	7.8 ± 3.9	7.2 ± 0.8	7.3 ± 1.0	0.160	-
lipid	22.3 ± 4.0	21.9 ± 3.5	21.4 ± 4.5	0.259	-
muscle	44.8 ± 6.5	44.4 ± 6.4	43.2 ± 6.4	0.167	-
fibrous tissue	86.6 ± 3.8	86.5 ± 4.4	86.5 ± 4.7	0.994	-
calcification	128.3 ± 10.6	131.0 ± 13.0	130.2 ± 13.36	0.432	-
Area percentage (%)					
blood	15.9 ± 15.2	13.6 ± 12.8	15.0 ± 13.4	0.640	-
lipid	40.5 ± 16.1	43.8 ± 17.8	46.3 ± 17.9	0.020*	1<3*
muscle	31.3 ± 13.5	30.6 ± 13.4	29.2 ± 15.3	0.460	-
fibrous tissue	7.8 ± 8.1	6.9 ± 7.1	6.6 ± 8.3	0.220	-
calcification	4.4 ± 6.6	5.1 ± 8.8	3.0 ± 5.7	0.030*	1 > 3*
IOD					
blood	313.2 ± 1276.0	124.1 ± 148.1	143.3 ± 197.4	0.194	-
lipid	1503.0 ± 1097.0	1581.0 ± 1171.0	2056.0 ± 1967.0	0.966	-
muscle	3416.0 ± 3106.0	2712.0 ± 3108.0	2392.0 ± 1911.0	0.004**	1 > 2*; 1 > 3**
fibrous tissue	1299.0 ± 1334.0	975.3 ± 760.0	1090.0 ± 1181.0	0.065	-
calcification	3767.0 ± 5593.0	4419.0 ± 7714.0	2675.0 ± 6615.0	0.018*	1 > 3*

Values are presented as mean ± SD. P value=Difference among post-RT NPC patients with/without CVRF VS. CVRF subjects. *P<0.05, ** P<0.01.

A. **B.**

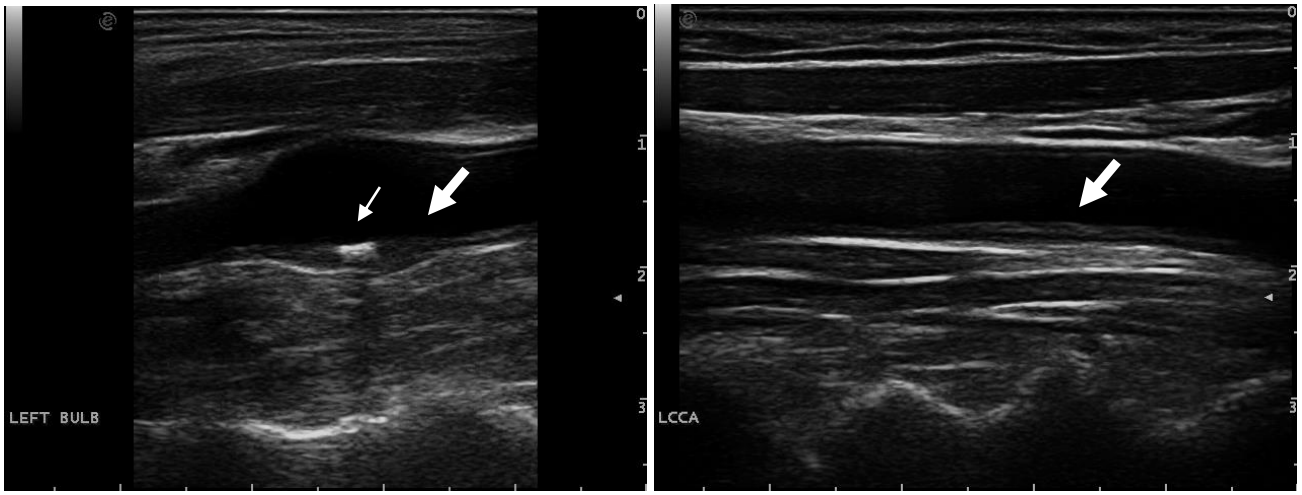

C. **D.**

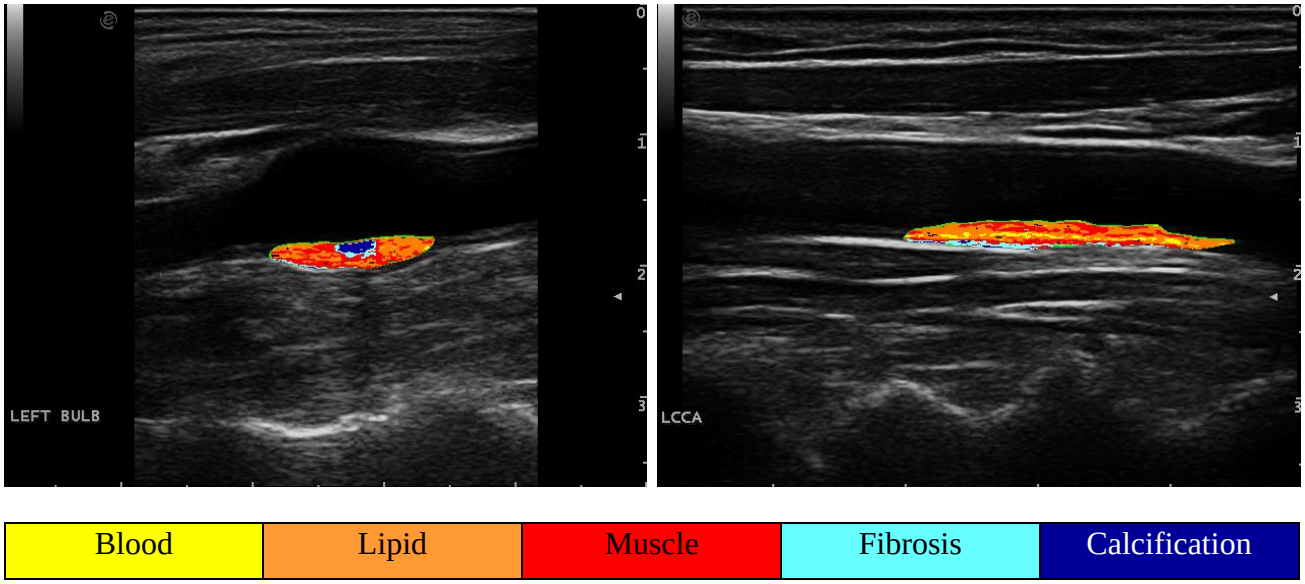

Figure 3.4 Grey scale ultrasound and DPTA of carotid plaque. Longitudinal sonograms show carotid plaques (large arrows) in the carotid bifurcation of a post-RT NPC patient **(A)** and in the common carotid artery of a CVRF subject **(B)**. In image **A**, note the intra-plaque calcification that appears hyperechoic (small arrow) with acoustic shadowing (arrowhead). Images **C** and **D** show the detailed plaque texture analysis of the two carotid plaques. Noted the radiation-induced carotid plaque has more calcification **(C)** than the non-radiation-induced carotid plaque **(D)**.

3.3.6 Association of carotid atherosclerosis parameters and various risk factors in post-RT NPC

Carotid atherosclerosis parameters that showed significant difference between post-RT NPC patients and CVRF subjects in the previous analyses were further evaluated for their associations with different risk factors. **Table 3.7** summarises the effects of various risk factors on atherosclerosis related parameters in post-RT NPC patients. The patients were divided into three subgroups: 1.) without CVRF, 2.) with one CVRF, and 3.) with more than one CVRFs. After adjustment of age and gender, results showed that age and radiation had significantly impact on the CIMT, the presence and number of carotid plaque ($p \leq 0.001$). The number of CVRF was significantly associated with CIMT and number of carotid plaque ($p < 0.05$). The elder subjects tended to have a higher CIMT (r=0.36; [95% CI: 0.23 to 0.47]) and larger number of plaques (r=0.25; [95% CI: 0.12 to 0.37]).

Among the risk factors studied, age played a significant role in the area percentage of lipid and calcification within a plaque ($p < 0.001$, **Table 3.8**). Results show that advancing age of patient decrease the area percentage of intra-plaque lipid (r= -0.27; 95% CI [-0.43 to -0.10]), but increases the area percentage of calcification within carotid plaque (r= -0.29; 95% CI [0.12 to 0.44]). Additionally, radiation has significant influence on the IOD of intra-plaque muscle component (p=0.046) in a positive correlation pattern (r=0.116). However, results indicated that none of the risk factors played statistically significant role on the IOD of calcification (**Table 3.8**).

Table 3.7 Effects of various risk factors on plaque characteristics by multivariate analysis, with the adjustment of age and gender

	CIMT			Presence of plaque			Number of plaque per subject			Overall p value
	Partial η^2 (df_1,df_2)	F	p	Partial η^2 (df_1,df_2)	F	p	Partial η^2 (df_1,df_2)	F	p	
Age	0.181(1,210)	46.510	<0.001***	0.136(1,210)	13.442	<0.001***	0.060(1,210)	33.090	<0.001***	<0.001***
Gender	0.008(1,210)	1.717	0.192	0.004(1,210)	0.935	0.335	0.006(1,210)	1.341	0.248	0.346
Number of CVRF	0.029(2,210)	3.018	0.048*	0.006(2,210)	0.638	0.529	0.024(2,210)	2.616	0.075	0.025*
Radiation	0.052(1,210)	11.423	0.001**	0.143(1,210)	35.055	<0.001***	0.260(1,210)	73.967	<0.001***	<0.001***

number of CVRFs were grouped by subjects without CVRF, with one CVRF or at least two CVRFs. *P<0.05, ** P<0.01, ***P<0.001

Table 3.8 Effects of various risk factors on plaque components characteristics by multivariate analysis

	Area percentage-lipid			Area percentage-calcification			IOD-muscle			IOD-calcification		
	Partial η^2	**F**	**P**	**Partial η^2**	**F**	**p**	**Partial η^2**	**F**	**p**	**Partial η^2**	**F**	**p**
Age	0.063	20.121	<0.001***	0.056	17.802	<0.001***	0.002	0.625	0.430	0.011	3.448	0.064
Gender	0.001	0.156	0.694	0.003	0.875	0.350	0.004	1.280	0.259	0.006	1.728	0.190
Number of CVRF	0.006	0.855	0.426	0.005	0.717	0.489	0.014	2.109	0.123	0.013	1.955	0.143
Radiation	0.012	3.699	0.055	0.002	0.750	0.387	0.013	4.012	0.046*	0.001	0.383	0.536

number of CVRFs were grouped by subjects without CVRF, with one CVRF or ≥ two CVRFs. *P<0.05, ** P<0.01, ***P<0.001

3.4 Discussion

In this study, we investigated the difference in CIMT and carotid plaque components of radiation-induced and non-radiation-induced atherosclerosis in post-RT NPC patients and CVRF subjects, respectively. For unveiling the plaque components characteristics, we used computer-assisted methods to evaluate the plaque GSM (Bassiouny et al., 1997) and perform DPTA (Lal et al., 2002) . Besides, we also investigated the effects of common risk factors on plaque constituents. The major findings of the present study are as follows:

(a) Radiation-induced carotid atherosclerosis leads to higher CIMT, and is more likely to develop carotid plaques than non-radiation-induced carotid atherosclerosis; (b) there is no significant difference in the GSM between radiation-induced and non-radiation-induced carotid plaques; (c) DPTA results indicated that radiation-induced carotid plaques tend to have more calcification, while non-radiation-induced carotid plaques have more lipid contents, and thus are more unstable; (d) the plaque components are affected by the age of patient and exposure to radiation.

3.4.1 Carotid Intima-media Thickness

CIMT is a parameter reflecting the degree of carotid atherosclerosis of the patients, even at the early stage of the disease. The more severe carotid atherosclerosis was commonly indicated by a higher CIMT. The measurements of CIMT vary in the assessment sites and definitions of CIMT. In this study, we examined CIMT at the far wall of CCA and with the ultrasound beam perpendicular to the CCA. This scanning

method allowed accurate measurement and had high measurement reliability (Pignoli et al., 1986; Wendelhag et al., 1991; Wikstrand, 2007).

The difference in radiation-induced atherosclerosis and spontaneous atherosclerosis was rarely studied. A previous study reported that there was no significantly difference in CIMT between radiation-induced carotid atherosclerosis in post-RT NPC patients and non-radiation-induced carotid atherosclerosis in diabetes patients (p_{cor}=0.732) (Yuan et al., 2017). The study also found that the males and elderly tended to have higher CIMT (Yuan et al., 2017). However, our study showed that patients with radiation-induced atherosclerosis, regardless of the presence of CVRF, had a higher CIMT than patients with non-radiation-induced atherosclerosis. This result was consistent with the existed studies that found the increased CIMT as an early alteration after irradiation, when compared to the carotid artery without irradiation (Fernandez-Alvarez et al., 2018; Toprak et al., 2012). However, with respect to the comparison of radiation-induced atherosclerosis and spontaneous atherosclerosis, this finding was inconsistent with the results of the previous study. The discrepancy of the two studies may mainly arise from different study subjects. Previous study demonstrated the comparison of CIMT between post-RT patients (≥4 yrs) and Type-2 diabetics, while our study compared CIMT value of post-RT patients (≥4 yrs) and subjects commonly with multiple CVRFs. More CVRFs exerted cumulative stress on vessel wall, and thus led to a more advanced atherosclerosis by manifesting in a greater CIMT.

Moreover, in post-RT patients, CIMT was noted to have significant association with previous history of radiation therapy, patient's age, and number of CVRF by present study. The CIMT increased with the previous irradiation, advancing age and more CVRFs. Result of the present study was consistent with previous studies which found

that radiation, patient's age and the presence of CVRF played an important role in carotid artery wall thickening (Bilora et al., 2006; Cheng et al., 2002; De Freitas et al., 2008; Gujral et al., 2016; Kruglikova et al., 2013).

The radiation-induced carotid artery wall thickening could be explained from two aspects. The first one is the direct injury to endothelium, resulting in a series of biological responses of endothelial cells to ionizing radiation. In radiation-induced atherosclerosis, CIMT was the manifestation of endothelial impairment caused by ionizing radiation. Exposure to the ionizing radiation caused double strands DNA damage of endothelial cells. When the rate of DNA repair was not high enough to suppress the damage, the accumulated injury induced the expression of adhesion molecules, and thereby promoted the atherosclerosis by facilitating the circulating immune cells anchoring on the endothelium. This eventually resulted in the advanced atherosclerosis through inflammation, cell apoptosis, proliferation and fibrosis in the artery wall (Gray & Bennett, 2011; Yuan et al., 2017). Subsequently, the intima was thickened because of the deposition of lipids, and the accumulation of macrophages, smooth muscle cells and extracellular matrix. The second one is the impairment of vasa vasorum caused by radiation. Vasa vasorum was microvascular network and vulnerable to radiation. The occlusion of vasa vasorum caused by radiation played a crucial role in the progression of vascular ischemic necrosis, leading to destruction of the inner elastic membrane, fibrosis of the adventitia and significant thickening of the endothelium. Thus, CIMT could be a comprehensive result of fibrin accumulation in both the intimal and media layer, and gradually being replaced by collagen (Xu & Cao, 2014) (Gujral et al., 2014). Therefore, the thickening of CIMT may be due to the direct injury of endothelial cells on intima and the indirect injury of vasa vasorum in both the intima and media.

Age was another risk factor of increased CIMT in our results, which was consistent with the existed studies that demonstrated the positive relation between aging and CIMT (De Freitas et al., 2008; Liu et al., 2017). Similarly, a recent systematic review found a strong positive linear association between age and CIMT in the healthy population, without differing between age decades and affecting by CVRF (Van Den Munckhof et al., 2018). CIMT was widely-known to increase by 0.01–0.03 mm with age each year. According to a Korean study, an increased CIMT by aging was mainly due to the increase in carotid media thickness rather than carotid intima thickness in asymptomatic adults (Bae et al., 2016). The role of SMC on the thickening of CIMT can explain the underlying causes (Doran et al., 2008; Stary et al., 1994). SMCs facilitated the lymphocytes and macrophages adhering and migrating from blood stream into intima, by expressing various adhesion molecules (such as vascular cell adhesion molecule-1 and intercellular adhesion molecule-1). Meanwhile, SMCs could also modify the external matrix into a readily adhering basement. In return, the modified matrix affected the proliferative index of the cells that adhered to, resulting in a proliferation of SMCs in media. Consequently, the recruitment of cells in intima and the proliferation of SMCs in media led to the thickening of CIMT.

Single or double CVRFs had positive association with an increased CIMT in several population-based studies on non-radiation-induced carotid atherosclerosis(Guan et al., 2017; Kasliwal et al., 2016; Liu et al., 2017; Owolabi et al., 2015), but the combined effects of multiple CVRFs on radiation-induced carotid atherosclerosis were rarely mentioned. Present study was the first one to demonstrate that CIMT was affected by the number of CVRF in post-RT patients. The underlying causes could be explained from two aspects. Firstly, since pathophysiological progressions were promoted by similar risk factors, such as obesity and insulin resistance, CVRFs were closely

interlinked, and exerted the cumulative stress to the vascular (Petrie et al., 2018). Thus, CVRFs were commonly co-existed in the same individual. According to a prevalence study in Chinese population, only 12.6% of them did not have any CVRFs, and the prevalence of subjects with 1, 2, 3, or ≥4 of CVD risk factors was 30.5%, 29.8%, 19.7%, and 7.4%, respectively (Yang et al., 2016). Secondly, CVRF caused vascular alterations through the similar biological processes. Elevated vascular oxidative stress due to diabetes and hypertension induced posttranslational oxidative modification of proteins, resulting cellular damage and vascular dysfunction, which initiated the early atherosclerosis. CVRF (such as hypertension) could also cause the hypertrophy and hyperplasia of SMC, as well as increase density of collagen and elastin in media of an artery (Michel et al., 1989). These events eventually resulted in a thickening of CIMT.

3.4.2 Presence of carotid plaque formation

Given that plaque formation is a consequence of carotid atherosclerosis, the presence of carotid plaque was a useful indicator to monitor the progression of carotid atherosclerosis and predict cerebrovascular disease. Some studies found post-RT head and neck cancer patients were more likely to suffer from stroke/TIA (Dorresteijn et al., 2002; Gujral et al., 2014; Huang et al., 2011). In a mean of 9.5 years follow-up study, with 6700 participates and >500 cardiovascular disease events, presence of carotid plaque was found to be a strong predictor of stroke/TIA in asymptomatic subjects ($p=0.045$), compared with coronary artery calcium ($p=0.438$) and high CIMT ($p=0.160$) (Gepner et al., 2015). Therefore, the combined assessments of CIMT and carotid plaque might provide more comprehensive assessment of radiation-induced carotid atherosclerosis for early detection of carotid atherosclerosis and better predicting the future cerebrovascular disease.

In this study, result showed that more carotid plaques were formed in radiation-induced carotid atherosclerosis when compared to non-radiation-induced carotid atherosclerosis, and the number of carotid plaques in post-RT NPC patients increased with advancing age. Besides, radiation-induced carotid atherosclerosis, regardless of the presence of CVRFs, had a higher presence of carotid plaque formation than non-radiation-induced carotid atherosclerosis. Our findings demonstrated that age and radiation were highly correlated with the formation of carotid plaque in radiation-induced carotid atherosclerosis. The finding was consistent with that of previous study, which found that post-RT NPC patients had more carotid plaques than the health, and higher plaque burden than DM patients (Yuan et al., 2017).

Although the pathogenesis of radiation-induced carotid plaque has not been fully revealed, the presence of carotid plaque caused by radiation was a consequence of the combination of direct vascular injury, inflammatory and accelerated atherosclerosis (Fernandez-Alvarez et al., 2018; Stewart et al., 2006; Tribble et al., 1999). Endothelial dysfunction was the primary response to radiation eliciting direct injury on vascular. Endothelium barrier was destructed and permitted oxidative-LDL accumulation in the sub-endothelial space, as well as migration of circulating lymphocytes and monocytes to intima. Monocytes derived to macrophages scavenging lipids and formed foam cells. Meanwhile, SMCs migrated to intima and proliferated in media, which caused by platelet-derived growth factor and basic fibroblast growth factor released by platelets. The accumulation of lymphocytes, macrophages, foam cells and SMCs formed an early lesion of carotid artery (Gujral et al., 2014).

Accelerated atherosclerosis was promoted by inflammation and endothelial-to-mesenchymal transition. The impaired endothelium was activated and shifted to a pro-

inflammatory state with elevated expression of. C-reactive protein (CRP) (Cleland et al., 2000) and nuclear factor-κB (NK- κB) (Dong et al., 2015), which accelerated atherosclerosis by a more severe inflammation due to radiation. Moreover, radiation induced the endothelial cells to implement phenotypic conversion to form fibroblast-like cells. This process was called the endothelial-to-mesenchymal transition (EndMT), which was amplified by oxidized-LDL (Kim et al., 2013). EndMT was found in radiation-induced atherosclerotic plaques of the aortic sinus, with expression of a fibroblast marker (α-SMA) and an endothelial cell marker (CD31) in the endothelium, which were found mainly in large and small arteries of the irradiated heart with fibrosis (Kim et al., 2013). (Zeisberg et al., 2007). Similar results were found in animal and human studies, and increased mesenchymal cells (include fibroblasts and smooth muscle cells) was trigerred by EndMT. Subsequently, these cells infiltrated the fatty streak and secreted extraculluar matrix components such as collagen and fibronectin, resulting in the formation of a fibrous cap. Therefore, EndMT probably involved in the increase presence of plaque in radiation-induced atherosclerosis(Chen et al., 2015).

3.4.3 Evaluation of carotid plaque components

The stability of carotid plaque could be evaluated by examining the plaque composition. Assessment of the sonographic features of carotid plaque was reported to be a method for evaluation of plaque composition and stability (Goncalves et al., 2003; Lal et al., 2002; Tegos et al., 2001). It was reported that hypoechoic plaques were more vulnerable and unstable, and had higher association with cerebrovascular events than hyperechoic plaques (Elatrozy et al., 1998; Pedro et al., 2000). The likelihood of carotid plaque rupture is highly associated with the components of the plaque. Vulnerable plaques are usually characterized by larger volume, having slim

cap with lipid-rich necrosis core inside and highly inflammatory (Bentzon et al., 2014; Carr et al., 1996; Naim et al., 2014). Therefore, assessing the plaque components could evaluate the plaque vulnerability and help treatment planning.

GSM analysis is a common method to evaluate the overall carotid plaque echogenicity for assessing plaque vulnerability. However, it has limited value in distinguishing different components within a carotid plaque (Elatrozy et al., 1998). Thus, to assess carotid plaque vulnerability, GSM is more commonly used in conjunction with other parameters such as degree of carotid artery stenosis and CIMT (Biasi et al., 1999; Cheng et al., 2002; Ibrahimi et al., 2015; Martinez-Sanchez et al., 2012). A previous study demonstrated that there was no significant difference in GSM between radiation-induced and non-radiation-induced carotid plaques (Cheng et al., 2002). Result of the present study was consistent with the previous study. We found that the GSM of radiation-induced and non-radiation-induced carotid plaques were not significantly different. To further evaluate the difference of these two types of carotid plaque in detail, a DPTA of carotid plaques was conducted in the present study.

Numerous studies have reported the application of different medical imaging techniques in carotid plaque component analysis. Magnetic resonance imaging (MRI) is a robust imaging tool for soft tissue examination and has been used for the evaluation of carotid plaque composition (Kerwin et al., 2006; Lin et al., 2017; Sun et al., 2016). Intravascular ultrasound (IVUS) elastography (De Korte et al., 2000; De Korte et al., 2000) and acoustic radiation force impulse (ARFI) elastography ultrasound (Allen et al., 2011; Czernuszewicz et al., 2015) can be used to estimate the carotid plaque stiffness and assess the plaque composition. Multi-detector computed tomography angiography (CTA) can assess carotid plaque complicated with

intraplaque haemorrhage with high sensitivity (100%) and inter-observer reliability (64.7%) (Ajduk et al., 2009). Meanwhile, some drawbacks should be aware when using these imaging modalities for carotid plaque assessment. MRI is not suitable for patients with metal implants or pacemakers. MRI examination is costly and time-consuming. IVUS is an invasive procedure and the clinical value of ARFI elastography for investigation of carotid plaque composition is uncertain due to the unavailability of comprehensive study. CTA cannot distinguish intra-plaque haemorrhage and lipids, and the examination involves ionizing radiation and administration of iodinated contrast agent which is not suitable for patients with deteriorated renal function (Naim et al., 2014).

The first application of ultrasound to investigate carotid plaque components preoperatively was reported in 1980's (Reilly et al., 1983). The study applied ultrasound to classify the carotid plaques as heterogeneous or homogeneous, and compared the ultrasound images with pathological findings. Lai et al. (Lal et al., 2002) assessed the carotid plaque components by analysing the pixel distribution of B-mode ultrasound images. They found that the pixel distribution of ultrasound image was highly correlation with the result of histological sections ($r= 0.53-0.86$, 95% CI [0.03-0.92], $p < 0.05$). They set different pixel ranges according to pathologic findings and applied the digital DPTA as an additional analysis combined with GSM. Subsequently, a Polish research group utilized the DPTA to assess carotid plaques and found that DPTA result was highly consistent with histologic findings, and was effective in predicting neurological complications through detecting microembolism (Madycki et al., 2006). Therefore, computer-aided DPTA could be an efficient method to assess carotid plaque vulnerability. Based on this rationale, computer-aided DPTA was

adopted in the present study to compare the carotid plaque composition characteristics between radiation-induced and non-radiation-induced atherosclerosis.

In the DPTA of carotid plaques in the present study, there were more radiation-induced plaques contained calcification than non-radiation-induced plaques. Radiation-induced carotid plaque tended to be more hyperechoic. The results are consistent with previous studies. Toprak et al. found that carotid plaques in head and neck cancer patients became calcified after the patients received radiotherapy (Toprak et al., 2012). Other studies also reported that microcalcification (Rebner et al., 1989), cardiovascular calcification (Apter et al., 2006), calcification in basal ganglia (Harwood-Nash & Reilly, 1970) and cerebral calcification (Suzuki et al., 2000) could be found in thoracic and cranial cancer patients after therapeutic radiation.

The causes of radiation-induced atherosclerosis with more calcification in carotid plaques may be resulted from the serial responses of mesenchymal stem cells (MSCs) after ionizing radiation. Radiation induced excessive oxidative stress in the microenvironment of carotid artery, and induced endothelial dysfunction, which could create the cross-talk with MSCs. When MSCs were exposed to oxidative environment, necrosis and apoptosis are induced. Besides, MCSs had extremely low survivability and this made them difficult to recover by their own stem cells. Subsequently, dead MSCs exerted the residual influence on vascular calcification to propel the progress constantly (Xie et al., 2019). Moreover, the differentiation of MSCs can be affected by the co-cultured differentiated cells through paracrine mechanism. Under the process of atherosclerosis, the existed osteo-like cells could induce MSC differentiation, and the MSCs would differentiate into calcified vascular smooth muscle cells, which facilitate the progress of vascular calcification (Xie et al., 2019).

Although the conditioned medium of MSCs (medium harvest from cultured MSCs) plays the protective role by anti-inflammation, anti-apoptosis, regulating the Wnt signal in a negative way and inhibiting the combination of BMP2 signal, the excessive oxidative stress could still trigger the amplified atherosclerosis responses. Massive pathological cells are recruited at a localized region of the vessel wall, and release various inflammatory factors to disturb the original chemical and biological equilibrium created by MSCs. These may be the potential biological mechanisms of radiation-induced carotid plaques showing more calcification when compared to non-radiation-induced carotid plaques.

Our results also showed that the combined effects of radiation and CVRF induced less lipid area than spontaneous carotid atherosclerosis caused by CVRF. The possible reason could be radiation-induced lipid peroxidation. Lipid peroxidation was a process that free radicals removed electrons from lipids, resulting in the production of reactive intermediates that could implement further reaction (Kiang. et al., 2012). Previous study found radiation induced both cell plasma and mitochondrial plasma lipid peroxidation(Choi et al., 2007). In addition, another study reported the results of increased production of lipid peroxidation (Malondialdehyde) and higher cell apoptosis in human T cells (Kiang. et al., 2012). Radiation-induced lipid peroxidation further evoked the caspase-mediated apoptotic cell death and light chain-3-mediated autophagic cell death in mice ileum (Kiang. et al., 2012). However, the above studies were not manipulated on endothelial cells or blood vessel wall. A study used pulmonary endothelial cells and mice lung found radiation-induced apoptosis in vivo and in vitro was accompanied by non-random oxidation of phospholipids (Tyurina et al., 2011). Phospholipids is well-known as substantial components of cell membrane (Gm., 2000), suggesting that lipid peroxidation was also occurred on

endothelial cells. Moreover, previous studies found the progression of radiation-induced carotid atherosclerosis was involved in caspase-mediated apoptosis (Tricot et al., 2000; Winn & Harlan, 2005) and excessive production of reactive oxidative species (ROS) (Azzam et al., 2012; Kim et al., 2019; Winn & Harlan, 2005). Results of these previous studies demonstrated that lipid peroxidation was more likely to be triggered in the radiation-induced atherosclerotic lesion with abundant of ROS. Therefore, lipids peroxidation may account for the lesser lipid deposition within the plaques in radiation-induced carotid atherosclerosis.

3.4.4 Limitations

This study was a cross-sectional study. Further follow-up studies should be conducted to investigate the value of the present DPTA method in predicting the stroke risk of the post-RT NPC patients and CVRF subjects. Secondly, based on the sample size of this study, the observed power of radiation (0.358) and gender (0.172) are less than 0.6 in multivariate models, which may influence the statistical results. Further studies with a larger sample size are suggested. Thirdly, as vulnerable plaques are related to the greater volume, the thin cap and the higher inflammatory content, so despite the plaque component, the plaque volume is another crucial factor to be considered in further studies. Moreover, to investigate the association between the ultrasound features of radiation induced atherosclerosis and radiotherapy, the following parameters could be considered in the further evaluation: <50% stenosis, total plaque area (plaque burden), carotid artery stiffness.

3.5 Conclusions

Radiation caused more severe carotid atherosclerosis than CVRF with larger CIMT and more prevalent of carotid plaque. The presence or absence of CVRF in post-RT NPC patients might not affect the degree of carotid atherosclerosis. Radiation-induced carotid plaques tended to have more intra-plaque calcifications, whereas non-radiation-induced carotid plaques seemed to have more lipids. Considering both carotid atherosclerosis burden and plaque component, both post-RT NPC patients and individuals with CVRF have a high risk of cerebrovascular diseases. Ultrasound aided by computer-assisted image analysis has potential for more accurate assessment of carotid atherosclerosis.

Chapter Four

An Investigation of the Effects of Radiation and High Glucose on Endothelial Dysfunction

4.1 Introduction

Carotid atherosclerosis could be caused by several risk factors, which can be divided into two categories: the conventional cardiovascular risk factors and radiation (Yuan et al., 2017). Endothelial cells (ECs), lining on the inner surface, are the major

components of vessel wall. Not only acting as a permeable barrier, endothelial cells also regulate the physiological and mechanical functions of vessel wall to maintain vascular homeostasis. When blood vessels are exposed to ionizing radiation, the endothelial cells are activated and shifted to a state of pro-thrombosis and pro-inflammation with the production of various growth factors and expression of adhesion molecules (Blann, 2000). Chronic activation results in endothelial dysfunction, manifesting as an irreversible loss of endothelial function, and is commonly associated with cell apoptosis and senescence as the consequences of the accumulative damage of double-strand DNA caused by radiation.

As reviewed in Section 2.4.4.1, vascular endothelial growth factor (VEGF) is involved in cells differentiation, proliferation, migration, by modulating cell-cell interactions in vessels, and thus it plays an important role in the progression of atherosclerosis (Ferrara & Davis-Smyth, 1997; Larrivee & Karsan, 2000). Focal adhesion kinase (FAK) is a non-tyrosine receptor kinase that can be stimulated by ligands. It is responsible for the biological signals through integrin or growth factor receptors to control the cellular processes of cytoskeleton and signalling transduction in the cell.(Parsons, 2003; Schlaepfer & Mitra, 2004). Nitric oxide synthase (NOS) is the catalytic enzyme for producing NO, which is responsible for maintaining the vasomotion tone. VEGF, FAK and NO were found to be associated with atherosclerosis (Gupta V. K. et al., 2002; Pipili-Synetos et al., 1993; Rizzo, 2004; Sun et al., 2018). Since the exact signaling pathway is unclear, the present in vitro study examined the individual and combined effects of radiation and high glucose on endothelial cells in vascular function, explored the possible mechanisms of radiation-induced and hyperglycaemia-induced endothelial dysfunction, which cause the primary injury to vascular wall, resulting in the carotid atherosclerosis.

4.2 Materials and methods

4.2.1 Cell culture

Human umbilical vein endothelial cells (HUVECs, Cat. #CRL-1730) were purchased from the American Type Culture Collection (ATCC, Manassas, VA, USA). The medium used for this study was endothelial cell medium (ECM, Cat. #1001), purchased from the ScienCell Research Laboratories (Carlsbad, CA, USA). The ECM kit consisted of 500 mL ECM basal medium, 25 mL of FBS (Cat. #0025), 5 mL Endothelial Cell Growth Supplement (ECGS, Cat. #1052) and 5 mL of penicillin/streptomycin solution (P/S, Cat. #0503). The completed medium contained 5% FBS, 1% ECGS, 100 units/mL penicillin and 100 μg/mL streptomycin solution.

HUVECs were seeded at least 3×10^5 cells/mL in T75 flask (SPL, Cat. #70075, Gyeonggi-do, Korea). Cells were maintained at 37℃ in a humiliated atmosphere containing 5% CO_2. Culture medium were refreshed every 48h. Cells were passaged at the ratio of 1:3 when cells reached 80% confluence. HUVECs between passage 5 and passage 8 were used for the following experiments to minimize the influence of cell senescence.

4.2.2 Low glucose and high glucose treatment

Dulbecco's Modified Eagle Medium (DMEM, Cat. #31885) containing 5.6 mmol/L of glucose was used as basal medium for the low glucose (LG) group. DMEM was purchased from the Thermo Fisher Scientific (Waltham, MA, USA). Sterile glucose solution (200 g/L, Cat. #A2494001) was purchased from the Gibco-Invitrogen Inc.

(Carlsbad, CA, USA). High glucose (HG) medium was prepared by adding 1.237 mL of sterile glucose solution to DMEM medium (final concentration = 33.3 mmol/L).

4.2.3 Irradiation

Cells were irradiated by X-ray irradiator (MultiRAD225, Surrey, UK) at the dose of 8 Gy or 16 Gy (dose rate of 2.5 Gy/min). Besides, HUVECs for the unirradiated sets (0 Gy) were taken to the irradiation room, but were kept away from the exposure of X-ray. Thus, all the manipulations kept consistence for all sets of cells, except for irradiation.

The experiments were divided into 6 groups:

	0 Gy	8 Gy	16 Gy
Low glucose	L0	L8	L16
High glucose	H0	H8	H16

4.2.4 Cell viability assay

Cell Counting Kit-8

Cell viability was determined by Cell Counting Kit-8 (CCK8, Dojindo, Kumamoto, Japan), according to the manufacturer's instructions with some optimizations. Briefly, HUVECs were harvest when they reached 80% confluence in T75 flasks and seeded

in 96-well plates (cell density1×10^4 M/well) and incubated overnight. The next day, HUVECs were exposed to low (5.6 mmol/L) or high (33.3 mmol/L) glucose medium.

Glucose medium was refreshed every 48 hours. After 72 hours treatment, the glucose medium was changed to culture medium (ECM). And cells were exposed to 0 Gy, 8 Gy or 16 Gy of radiation, and incubated for another 72 hours. This work flow was summarized as the time line below:

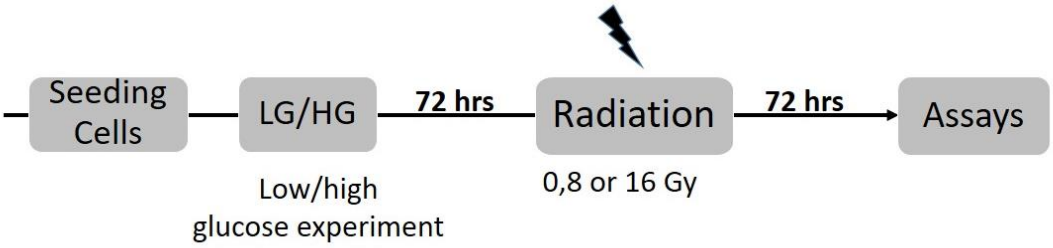

Figure 4.1 Schematic diagram for cell experiments

Cell viability was assayed after 72 hours of glucose treatment and 72 hours of post-radiation incubation. 10μL CCK-8 reagent was added to each well and the absorbance at 450 nm was measured by Benchmark PlusTM Microplate Reader (Bio-Rad, USA) after incubation at 37℃ for 3 hours. Cell viability is proportional to the absorbance at 450 nm. 4-5 replicated were included for each condition.

4.2.5 Tube formation assay

Tube formation assay was used to investigate the ability of capillary-like formation by endothelial cells. Endothelial cells were seeded on the Corning® Matrigel® Growth

Factor-Reduced Basement Membrane Matrix (BMM, Corning, Cat #356231, Bedford, MA). This basement membrane matrix was a soluble complex mixture extracted from the Engelbreth-Holm-Swarm (EHS) mouse sarcoma. Corning Matrigel matrix contained various proteins. They were Laminin (a major component), Collagen IV, heparan sulfate proteoglycans, entactin/nidogen, and a number of growth factors.

In brief, Matrigel was transferred to 4℃ a night in advance. The next day, 250 μL of the well-thawed Matrigel was aliquoted to 24-wells plate and incubated at 37℃ for 30 minutes, until the soluble Matrigel covered the well surface thoroughly as a gelation coating. The cells were suspended in culture medium at the density of 400 cells/ μL, and 300 μL of cell suspension was layered on the gelation evenly, avoiding over-densed cell cluster in the central area. Then, the capillary-like tubes were allow to form in 24 hours. Since tube formation could be affected by both intrinsic and extrinsic factors, the optimizing tube formation was confirmed by inverted phase contrast microscope (Eclipse TS100, Nikon, Japan). Subsequently, five areas in each well were randomly selected and photographed. All the images were analyzed by Angiogenesis Analyzer (ImageJ v1.52r, National Institute of Health, Bethesda, Maryland, USA) and manual count. The degree of capillary-like tube formation was investigated by quantifying the junctions and meshes (Lin et al., 2015; Marquez-Curtis et al., 2016).

4.2.6 Western blotting

4.2.6.1 Protein extraction

After exposure to LG/HG and different levels of radiation, cells were incubated for 72 hours. Then, the medium was collected and cells were rinsed by adding PBS and detached by Trypsin-EDTA 0.05%. The suspended cells were collected and

centrifuged at 1,000 rpm for 5 minutes. The cell pellets were re-suspended with ice-cold PBS after

discarding the supernatants. Cells were centrifuged for the second time (1,000 rpm for 5 minutes) and remove the supernatants. Cell pellets were lysed in RIPA buffer (50mM Tris, pH 8.0, 150mM NaCl, 1% Triton X-100, 0.5% sodium deoxycholate, and 0.1% SDS), supplemented with complete protease inhibitor cocktail (Roche Applied Science, Germany) and phosphatase inhibitors (Calbiochem, Merck Millipore, Germany). Cells were mixed with the buffer by pipetting up and down and the mixture was then maintained on ice for another 30 minutes. The cell lysate was centrifuged at 13,000 rpm for 30 minutes at 4°C. The clarified supernatant was collected carefully and stored at -70°C for further tests.

4.2.6.2 Protein concentration measurement

Protein concentration were detected by PierceTM BCA Protein Assay Kit (Thermo Fisher Scientific Inc., USA). The work mechanism of BCA (bicinchoninic acid) assay was mainly based on chemical response as below: Cu^{2+} can be reduced into Cu^{+} by proteins in an alkaline medium, and then each Cu^{+} ion can chelate with two BCA molecules, forming a colored complex with a strong absorbance at 562 nm. The absorbance of 562 nm showed an almost linear correlation to the protein concentration ranging from 20 to 2,000 μg/mL.

The BCA working reagent was pre-prepared by mixing Reagent A and Reagent B at the ratio of 50:1. Reagent A was an alkaline medium with bicinchoninic acid and Reagent B was a cupric sulfate solution. All the protein samples were diluted by 10 times in Milli-Q water and total volume of diluted samples were 300μL (30μL original

sample and 270μL Milli-Q water). A set of diluted BSA standards were also prepared according to the recipe in **Table 4.1**. Then, 200μL of prepared BCA working reagent was distributed into 96-well plate. 25μL of each diluted sample or BSA standard was added to each well and mixed with BSA standard reagents thoroughly. The plate was covered by silver paper to be avoid of light and incubated at 37°C. After 30 minutes' incubation, the absorbance at 562 nm was measured by Benchmark PlusTM Microplate Reader (Bio-Rad, USA). The protein concentration of each sample was then calculated according to the standard curve.

Table 4.1 Preparation of protein standards by serial dilution

	Volume of Milli-Q water (μL)	Volume and Source of BSA (μL)	Final BSA concentration (μL/mL)
A	0	120 of Stock	2000
B	60	60 of vial A dilution	1000
C	60	60 of vial B dilution	500
D	60	60 of vial C dilution	250
E	60	60 of vial D dilution	125
F	60	60 of vial E dilution	62.5
G	60	0	0=blank

4.2.6.3 Denature of samples

Protein samples were mixed with Laemmli 2 × buffer at the ratio 1:1. The mixture was then heated at 98℃ for 5 minutes to denature the protein. Unused samples were stored at -80 ℃.

Laemmli 2 × buffer

4% SDS

10% 2-mercaptoehtanol

20% glycerol

0.004% bromophenol blue

0.125 M Tris HCl

4.2.6.4 Preparation of PAGE-gels

Samples were separated according to their molecular weight by a technique called SDS-PAGE (Sodium Dodecyl Sulfate PolyAcrylamide Gel Electrophoresis). 6%, 8% and 12% resolving gels for Tris-glycine SDS-PAGE were used in this study. The components were mixed according to the following protocol (**Table 4.2**).

Table 4.2 Solutions for preparing resolving gels for Tris-glycine SDS-PAGE

	Volume of components required to cast gels of indicated volumes and concentrations		
Components	10ml	15ml	20ml
6% gel			
H2O	5.3	7.9	10.6
Acrylamide mix (30%)	2.0	3.0	4.0
Tris (1.5 M, pH 8.8)	2.5	3.8	5.0
SDS (10%)	0.1	0.15	0.2
Ammonium persulfate (10%)	0.1	0.15	0.2
TEMED	0.008	0.012	0.016
8% gel			
H2O	4.6	6.9	9.3
Acrylamide mix (30%)	2.7	4.0	5.3
Tris (1.5 M, pH 8.8)	2.5	3.8	5.0
SDS (10%)	0.1	0.15	0.2
Ammonium persulfate (10%)	0.1	0.15	0.2
TEMED	0.006	0.009	0.012
10% gel			
H2O	4.0	5.9	7.9
Acrylamide mix (30%)	3.3	5.0	6.7
Tris (1.5 M, pH 8.8)	2.5	3.8	5.0
SDS (10%)	0.1	0.15	0.2
Ammonium persulfate (10%)	0.1	0.15	0.2
TEMED	0.004	0.006	0.008

4.2.6.5 Electrophoresis and blotting

After casting the gel, equal amount of total protein from each sample was added to the wells (10-24 μg, optimized according to the different antibodies). Running of SDS-PAGE began with a slightly higher voltage (140v) to compress the sample for 5 minutes, and then maintained at 130v for another 90 minutes, until the band was completely separated within the ruler range.

Afterwards, proteins were transferred to a polyvinylidene difluoride (PVDF) membrane (Bio-rad, USA) at 100v for 120 minutes. To maintain a low temperature, the tank was immersed in ice until the protein were transferred completely.

The blocking buffer was prepared by Tris-buffer saline with 0.1% Tween-20 (TBST, pH 7.4) with 5% (w/v) bovine serum albumin (BSA) in advance. The membranes were blocked for 1 hour at room temperature with gentle shaking, and incubated with primary antibodies at 4℃ overnight with gentle agitation. The membranes were washed by TBST five times for 5 minutes each. The membranes were incubated with goat anti-rabbit IgG secondary antibody at the room temperature with gentle agitation for 2 hours, and washed by TBST five times for 5 minutes each. The bands were visualized by chemiluminescence substrates Western Lightning (Perkin Elmer, USA). The images were captured by the ChemiDoc MP System (Bio-Rad, USA) and quantified by ImageJ software (version 1.52r, NIH, USA).

The primary antibodies used for the current study were VEGF receptor 2 (55B11) Rabbit mAb [Cat. #2479, Cell Signaling Technology (CST), USA], phosphor-VEGF receptor 2 (Tyr1175) (19A10) Cat. #2478, CST, USA), FAK (Cat. #3285, CST, USA), phosho-FAK (Cat. #3281, CST, USA), cleaved Caspase-3 (Asp75) (5A1E) (Cat.

#9664, CST, USA), eNOS (49G3) Rabbit mAb (Cat. #9586, CST, USA), phosphor-eNOS (Ser1177) (C9C3) Rabbit mAb (Cat. #9570, CST, USA), iNOS (D6B6) Rabbit mAb (Cat. #13120S, CST, USA), and β-actin (D6A8) Rabbit mAb horseradish peroxidase (HRP) conjugated (Cat. #12620, CST, USA).

4.2.7 Data analysis

Data was presented as means ± SEM. Statistical analysis was performed by student's t-test (2 groups), Kruskal-Wallis test or ANOVA (≥3 groups) using SPSS version 22.0. $P < 0.05$(two tails) was considered as statistically significant.

4.3 Results

4.3.1 Morphological changes

The changes of cell density were observed as **Figure 4.2A**. Cultured by ECM (with the supplements of endothelial cell growth factors), the untreated HUVECs were round in cobblestone-like shape, and the 80% - 90% confluence was observed after 72 hours.

HUVECs under glucose (**Figure 4.2B)** were also round as cobblestone, but had only 40% - 50% cell confluence was observed after 72 hours, compared with cells cultured in ECM (**Figure 4.2A)**. Besides, when exposed to the same concentration of glucose, the irradiated HUVECs were spindle-like rather than cobblestone-like. When exposed to the same irradiation dosage, HG decreased the cell number, showing less cell confluence compared to the LG group. **(Figure 4. 2B)**

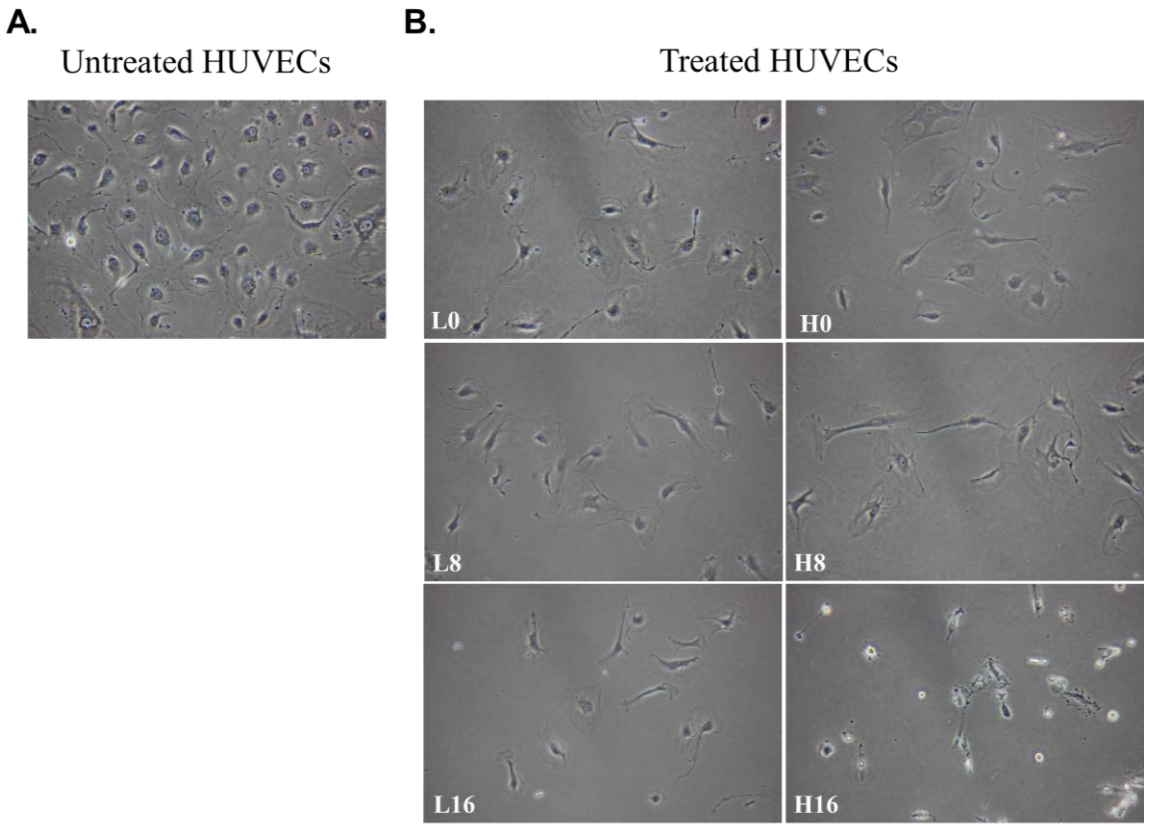

Figure 4.2 Morphological changes of HUVECs in response to different treatments. Untreated cells were incubated in completed endothelial medium and photographed when they reached 80% confluence. Treated cells were incubated in LG (5.6 mmol/L) or HG (33.3 mmol/L) medium for 72 hours, and irradiated by 0 Gy, 8 Gy or 16 Gy the next day. Images were captured 72 hours post-irradiation. Magnification: 100 times. **(A)** Representative images of untreated cells with a high density and cobblestone morphology **(B)** Representative images of treated cells show that 8 Gy and 16 Gy irradiation cause the more cell loss compared to the non-irradiated cells. HUVECs: human umbilical vein endothelial cells

4.3.2 Induction of cell death of irradiation on HUVECs

4.3.2.1 Cell viability

Cell viability were assessed by CCK8 as described in Section 4.2.3. HUVECs cultured in LG receiving 0 Gy were regarded as control group, standardizing its cell viability as 100%. A slightly decreased trend of cell viability was observed both in 0 Gy and 8 Gy irradiated HUVECs, as the glucose concentration increased from LG (5.6 mmol/L) to HG (33.3 mmol/L) (L0: 100% vs H0: 94.4%; L8: 86.5% vs H8: 79.8%). HUVECs receiving 16 Gy-irradiation in the presence of LG and HG showed a similar viability (L16: 81.3% vs H16: 81.5%). (**Figure 4.3**)

Under the LG condition, radiation significantly decrease the viability compared to the non-radiated counterpart (L8: 86.5% vs L0: 100% $p=0.006$; L16: 81.3% vs L0: 100% $p<0.001$). The same trend was observed under the HG condition (H8: 79.8% vs H0: 94.4% $p=0.004$; H16: 81.5% vs H0: 94.4% $p=0.007$).

It was reported that endothelial cell growth was suppressed by the increased radiation as dose-dependent manner (Annabi & Lee, 2003; Hess et al., 2001). However, cells treated by high glucose in combination of 8 Gy and 16 Gy showed a similar viability. (**Figure 4.3** H8: 79.8% vs H16: 81.5%, $p>0.5$). As 8 Gy showed the inhibitive effect of cell viability regardless of the concentration of glucose medium, 8 Gy was thereafter adopted to be used to irradiate cells in the subsequential assays.

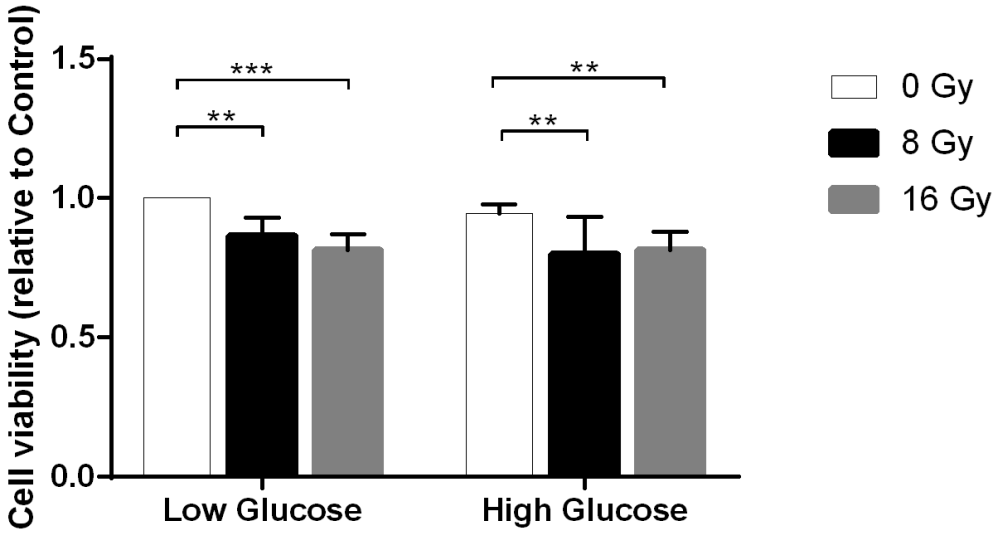

Figure 4.3 Exposure to irradiation dominantly decrease the cell viability. HUVECs were treated with 5.6 mmol/L (LG) or 33.3 mmol/L (HG) for 72 hours, and then exposed to 0 Gy (white), 8 Gy (black), and 16 Gy (grey) for another 72 hours. Cell viability was determined by CCK8 assay and analyzed by ANOVA with Prism 7 and expressed as a percentage of control (mean ± SEM, n=4). (***) indicates significant difference ($^{**}p<0.01$) compared to the control. HUVECs: human umbilical vein endothelial cells; SEM: standard error.

4.3.2.2 Active Caspase-3 levels

Radiation-induced apoptosis is mainly regulated by P53-mediated pathways, via the Caspase family (Venkatesulu et al., 2018). The effects of irradiation and high glucose alone and in combination on endothelial apoptosis were tested on HUVECs using Western blot to determine the levels of active Caspase-3. Higher levels of active Caspase-3 represented higher degree of cell apoptosis.

Quantifying by ImageJ, bands of IR and IR in combined of HG were much intensive than the bands of LG/HG alone, indicating that irradiation induced higher levels of active Caspase-3 than concentrated glucose. Moreover, with the exposure to radiation, HG in combination had an even stronger signals of active Caspase-3 than that of LG in combination, indicating that the accumulative effects of HG and IR inhibited the cell proliferation **(Figure 4.4A)**.

Exposure to radiation induced higher levels of the active Caspase-3 than untreated cells. However, the difference was not statistically significant (data represented active Caspase-3 levels relative to control, LG+IR: 1.9 / HG+IR: 2.175 vs HG: 1.018, $p>0.05$) **(Figure 4.4B)**.

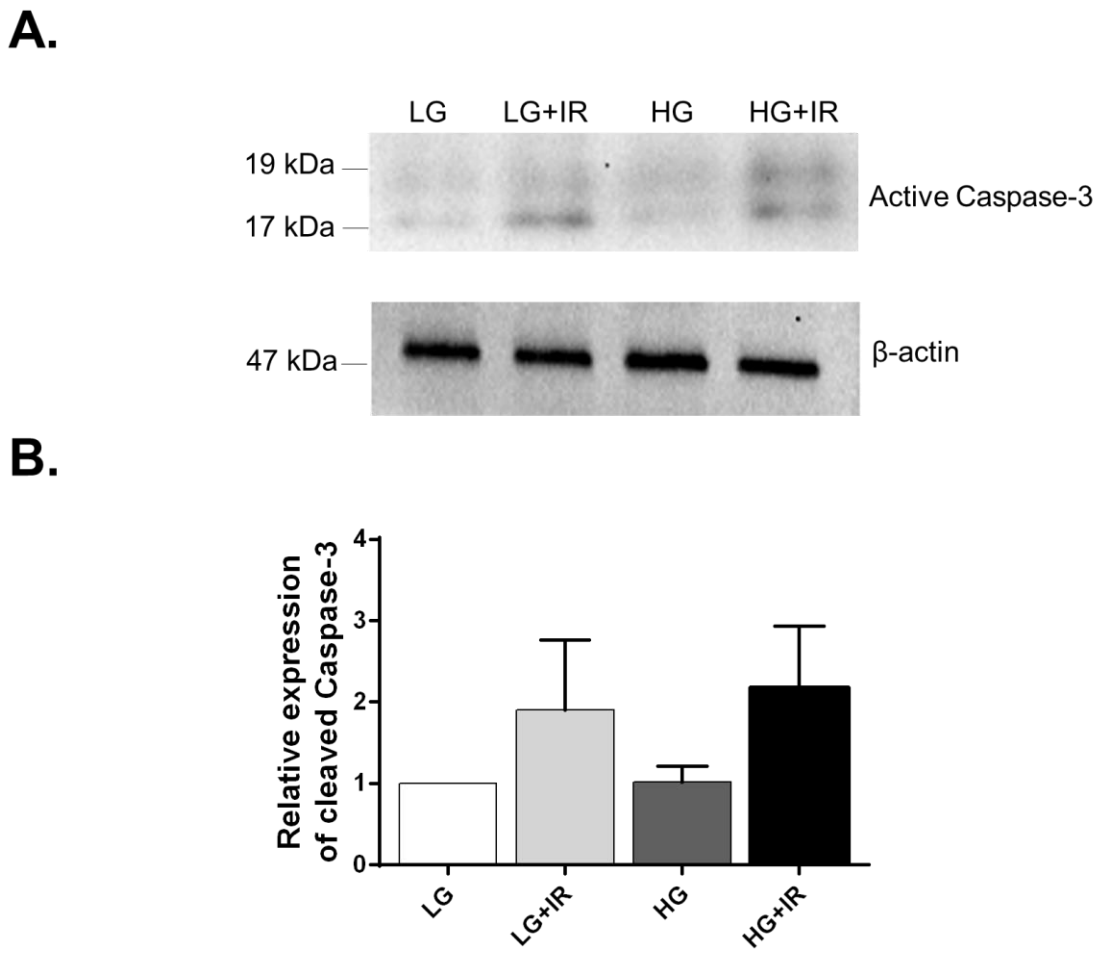

Figure 4.4 Irradiation dominantly increase active Capase-3 levels. HUVECs were treated with LG/HG for 72 hours. Protein expressions of cleaved Capase-3 were measured by western blot. The relative ratio of cleaved Capase-3 expressions were presented as mean ± SEM (n=4).

4.3.3 Effects of radiation on angiogenesis of HUVECs

4.3.3.1 Tube formation

Basement membrane (BM) plays a vital role on blood vessels structurally and functionally, by simulating a variety of signals and the corresponding regulations (Kalluri, 2003). Endothelial cells could specifically form the network structure when seeded on the BM, and be activated to a series of biological processes relating to angiogenesis (Kleinman & Martin, 2005). Therefore, Matrigel, as a special BM, can be used to study primary or stem cells angiogenesis (Hughes et al., 2010).

Cells formed tube-like structures in 3 hours after seeding. Images were captured post-seeding (**Figure 4.5A),** showing the effects of HG and IR (treated alone or in combination) on angiogenesis of HUVECs. **Figure 4.5B** summarised the results from tube formation experiments.

With the absence of IR, more tube-like structures were observed in the treatment of HG than that in LG (**Figure 4.5A**), but no statistical significance was found between the two groups (**Figure 4.5B and 4.5C**) (HG: 37.23 vs LG: 35.67, $p>0.05$, n=3).

Radiation induced more junctions, when compared to LG or HG alone (LG+IR: 42.00 vs LG: 35.67, $p>0.05$; HG+IR: 48.71 vs HG: 37.23, $p=0.004$). Moreover, the combination of HG and radiation had significantly more junctions than LG/HG alone (HG+IR: 48.71 vs LG: 35.67, $p=0.001$; HG+IR: 48.71 vs HG: 37.23, $p=0.004$, n=3) **(Figure 4.5B)**. With the exposure to radiation, the combination of HG had a greater number of junctions than the combination of LG, but the difference did not reach the statistical significance (HG+IR: 48.71 vs LG+IR: 42.00, $p>0.05$) **(Figure 4.5B)**.

Similar trends were found in terms of number of meshes. With no irradiation, HG group had more meshes than LG group, but no statistically significance was found (HG: 39.02 vs LG: 36.79, $p>0.5$) **(Figure 4.5C)**.The combined treatment of HG and IR induced more meshes than LG alone and HG alone (HG+IR: 50.69 vs LG: 36.79, $p<0.001$; HG+IR: 50.69 vs HG: 39.02, $p=0.002$) **(Figure 4.5C)**. With the exposure to IR, the combined treatment of HG induced slightly more meshes than the combined treatment of LG, but having no statistical significance (HG+IR: 50.69 vs LG+IR: 45.11, $p>0.5$) **(Figure 4.5C)**.

A.

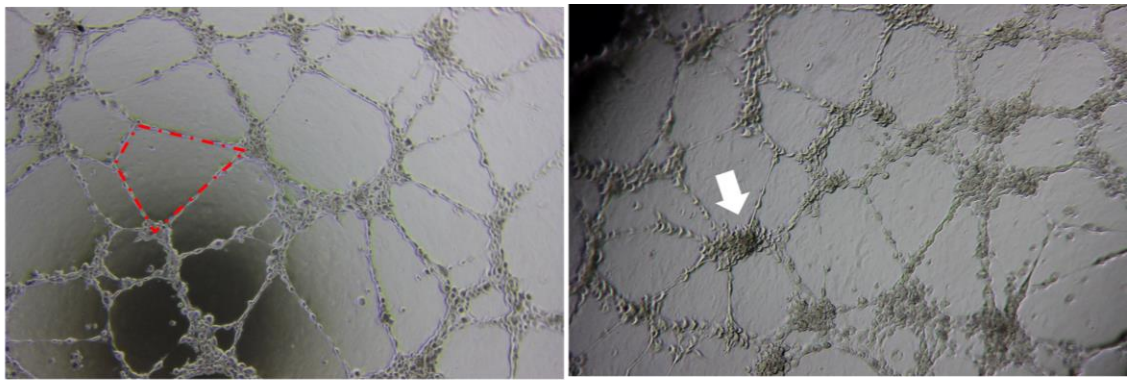

L0 L8

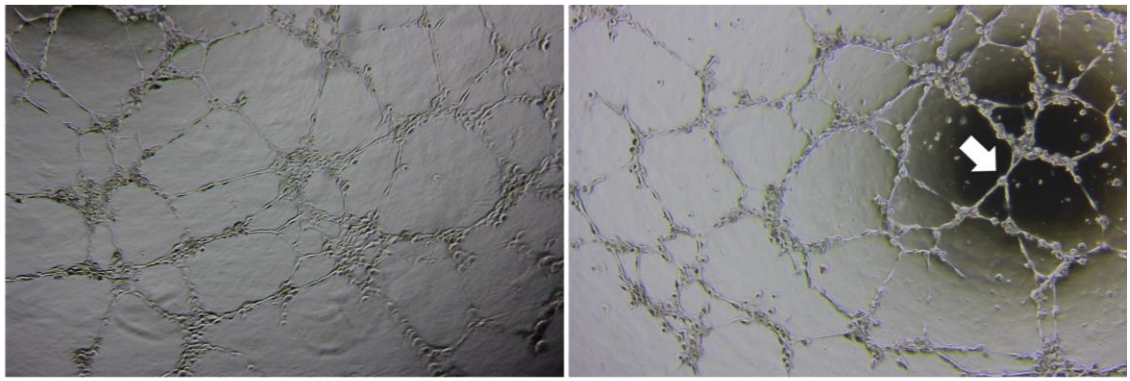

H0 H8

B.

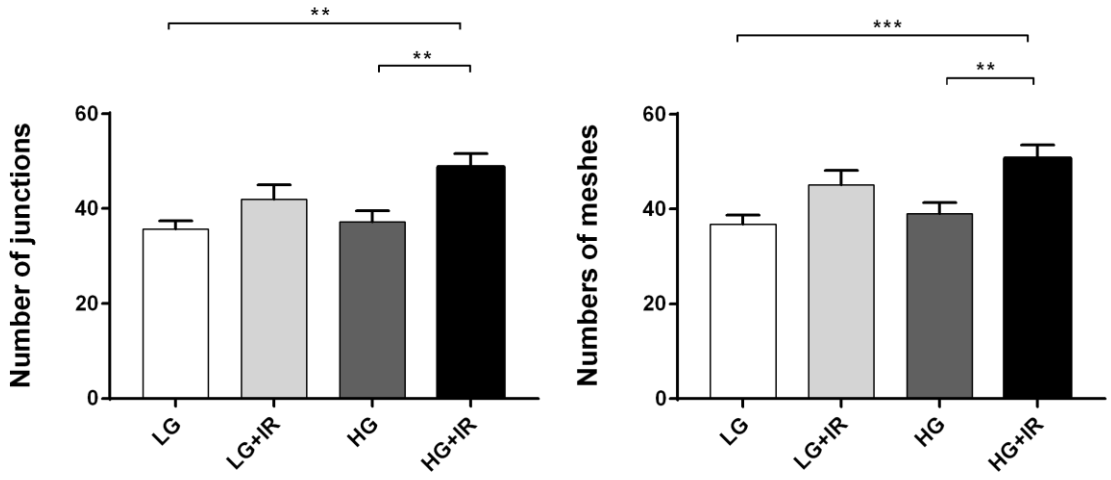

Figure 4.5 Tube formation of HUVECs in response to different treatments. HUVECs, with different treatments, were seeded on growth factor-reduced Matrigel, at the seeding density of 120,000 cells per well. Images were photographed at 18 hours after seeding, by 40 times magnification, dashed line: mesh; arrow: junction. **(A)** The images showed that HUVECs formed tube-like structures after seeding 18 hours. **(B)** Number of junctions was analyzed by ANOVA and presented by as mean ± SEM (n=3). Noted that combined effects of HG and IR induced significantly more junctions than LG alone (HG+IR: 48.71 vs LG: 35.67, $^{**}p<0.01$) and HG alone groups (HG+IR: 48.71 vs HG: 37.23, $^{**}p<0.01$). **(C)** Number of meshes was analyzed by ANOVA and presented by as mean ± SEM (n=3). Noted that the combined effects of HG and IR induced forming significantly more meshes than LG alone (HG+IR: 50.69 vs LG: 36.79, $^{***}p<0.001$) and HG alone (HG+IR: 50.69 vs HG: 39.02, $^{**}p<0.01$).

4.3.3.2 Angiogenesis-related protein expressions

FAK has been reported to be stimulated by the VEGFR2, when VEGFR2 combines with VEGF. FAK is responsible for cell migration in cellular signalling transduction through integrins and growth factors (such as VEGF), and thus modulates the downstream biological process, such as angiogenesis (Abbi & Guan, 2002; Abedi & Zachary, 1997; Parsons, 2003; Schaller, 2001; Sun et al., 2018). To investigate the potential mechanisms of radiation-induced and high glucose-induced tube formation, the levels of FAK and VEGFR2 were determined using western blot analysis after different treatments. Data was analysed by ANOVA test and displayed the trend that groups received IR has a higher levels of p-FAK/FAK, suggesting that radiation induced the phosphorylation of FAK, regardless the combination with LG or HG (relative levels of p-FAK/FAK to control: LG+IR: 1.340 folds; HG+IR: 1.234 folds, $p>0.05$) (**Figure 4.6A**). Though, HG also increased the protein expression of by 1.191 folds to control, it was less superior to IR in the up-regulation of p-FAK/FAK.

Results showed that there was no significant differences in the levels of activated VEGFR2 among different treatments of HUVECs (relative levels of p-VEGFR / VEGFR to control: HG: 1.067 folds; LG+IR: 1.050 folds; HG+IR: 1.080 folds, $p>0.05$) (**Figure 4.6A** and **B**), and the possible reasons would be discussed in 4.4.2.

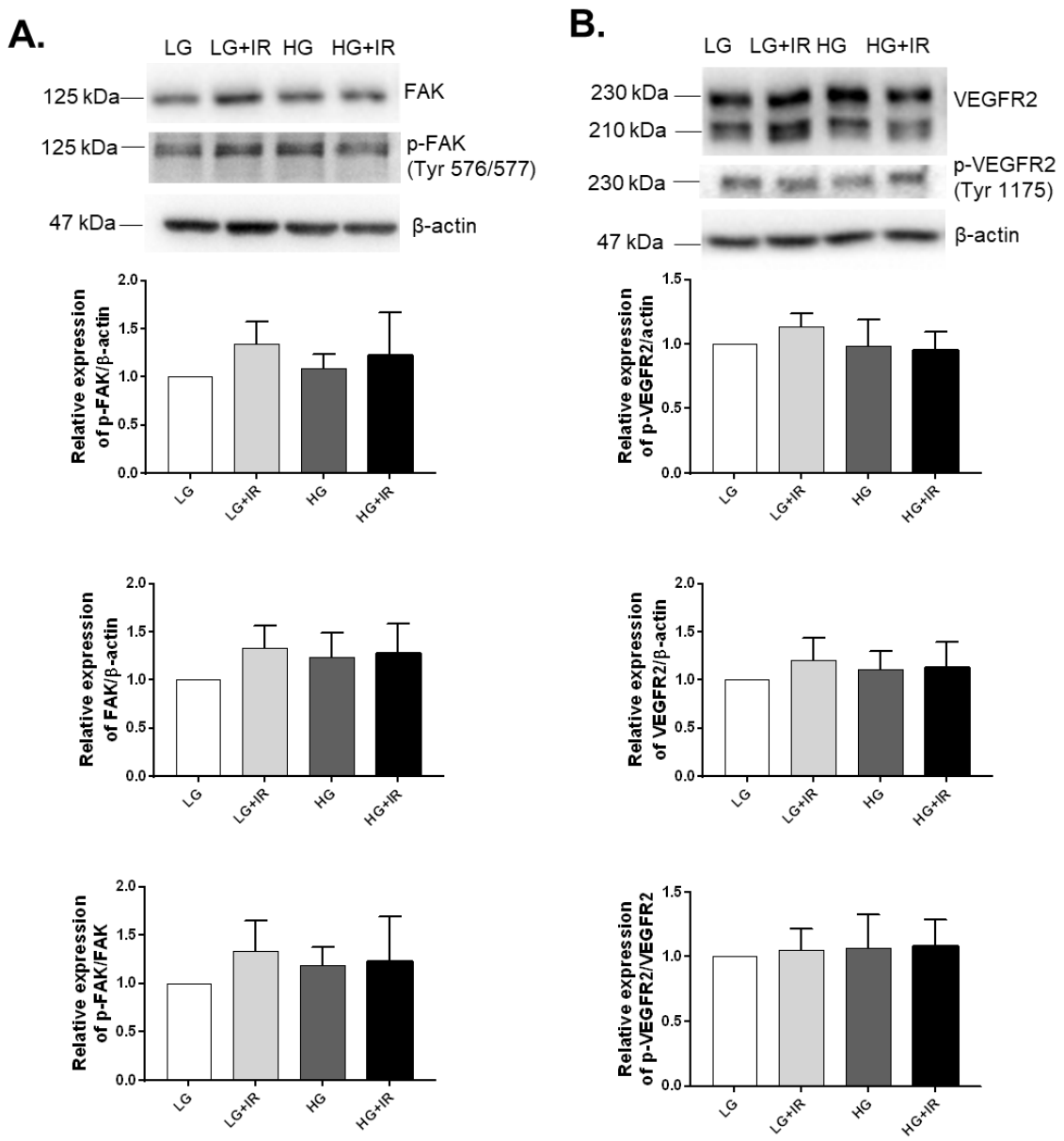

Figure 4.6 FAK. p-FAK, VEGFR2 and p-VEGFR2 expression levels of HUVECs in response to different stimulus. HUVECs were treated with LG (5.6 mmol/L) alone, HG (33.3 mmol/L) alone, and in combination with radiation. Protein expressions of FAK (n=7), p-FAK (n=7), VEGFR2 (n=6) and p-EGFR2 (n=6) were measured by western blotting (mean ± SEM). Noted that FAK and p-FAK levels (**A**) with radiation were higher, but did not reach significantly difference.

4.3.3.3 Nitric oxide production of HUVECs after treatments

NO is a liposoluble molecule, exerting versatile effects on vascular regulation. Physical concentration of NO is essential for maintaining endothelial function. NOS is constituted by constitutive NOS (cNOS) and inducible NOS (iNOS). The isoforms of cNOS in endothelial cells (eNOS) is the major source of NO production in endothelial cells (Bult, 1996).

Results of the present study showed that iNOS levels were similar under the treatment of LG combined with radiation, HG alone and HG combined with radiation, with no significant difference (relative levels of iNOS to control: LG+IR: 0.97 folds, HG: 1.104 folds; HG+IR: 1.202 folds, $p>0.05$) (**Figure 4.6A**).

The protein levels of eNOS showed a decreasing trend from radiation alone, HG alone, to HG in combination with radiation (relative levels were 1.137, 0.943, and 0.747, respectively). For the levels of p-eNOS, a strong signal of p-eNOS (Ser^{1177}) induced by HG was observed as shown in **Figure 4.6B**, with the corresponding statistical results of 1.213 folds to control. The relative levels of p-eNOS with combined treatment of LG /HG and radiation were 1.213 folds and 1.163, respectively. (**Figure 4.6B**). The protein expressions of p-eNOS/NOS were increased in a growing trend from IR alone, HG, to HG in combination with IR (relative levels were 1.217, 1.560, and 1.747, respectively). However, there was no significant differences in the ANOVA analysis ($p>0.05$) (**Figure 4. 6B**).

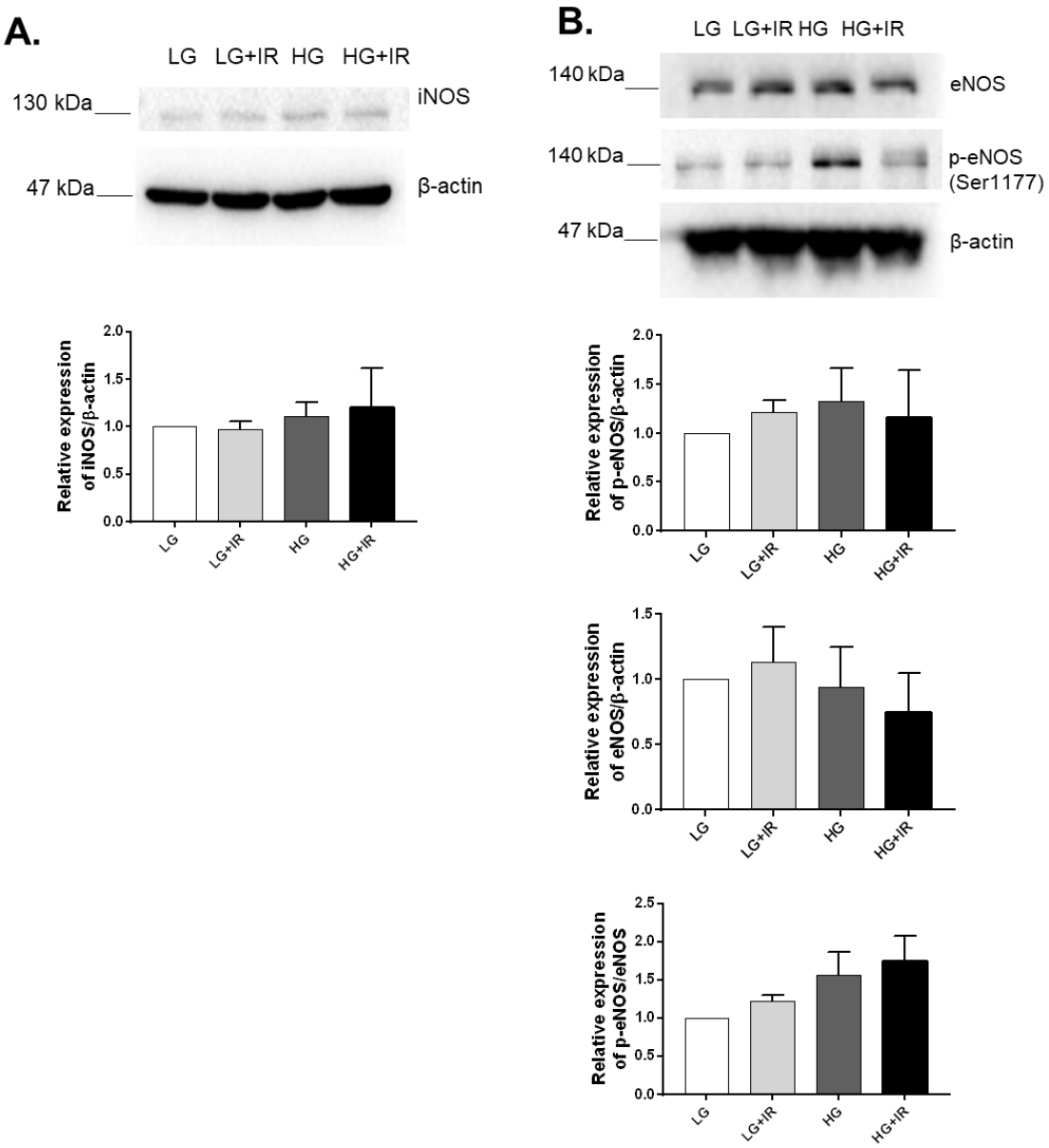

Figure 4.7 Nitric oxide production levels of HUVECs in response to different stimulus. HUVECs were treated with LG (5.6 mmol/L) alone, HG (33.3 mmol/L) alone, and in combination with radiation (8Gy). Protein expressions of iNOS (n=5), eNOS (n=4), p-eNOS (n=4) were measured by western blotting and presented as mean ± SEM. Noted that iNOS levels were similar under different treatments (**A**), and increasing levels of p-eNOS were found in LG alone, LG combined with radiation, and HG combined with radiation with no statistical difference (**B**).

4.4 Discussion

4.4.1 Overview

Endothelial cells are radiosensitive, multifunctional, and directly respond to stimulus. Besides, monolayer of endothelial cells is also a barrier between blood stream and vascular wall. Therefore, endothelial cells are both the structural and functional foundation of the vasculature, participating inflammation, cell proliferation, cell migration and angiogenesis (Lusis, 2000; Ross, 1999; Sumpio et al., 2002). Thus, the evaluation of endothelial dysfunction is important for understanding pathogenesis of carotid atherosclerosis. In this chapter, we incubated HUVECs with LG/HG, with or without radiation, and evaluated the cell viability, cell apoptosis, ability of tube formation, angiogenesis and nitric oxide synthesis (NOS) to simulate radiation-induced and hyperglycaemia-induced atherosclerosis, which reflected several important aspects of endothelial cell functions.

4.4.2 Tube formation

Vasculargenesis and angiogenesis are the two mechanisms for forming the new blood vessels, coordinated by growth factors, cytokines, various cell types and the extracellular matrix (Folkman, 1972; Ronca et al., 2017). After the normal vascular development in adult physiologically, angiogenesis usually happens in the injuried areas in blood vessels pathologically. Endothelial cells proliferation is observed in this region with the formation of new vessels. Therefore, angiogenesis is of primarily importance, because it is fundamental for reproduction, development, survival and repair (Carmeliet & Jain, 2000; Folkman, 2006; Kleinman & Martin, 2005). Previous

study demonstrated that intralesion angiogenesis was related to atherosclerotic plaques with risk of acute coronary syndrome (Tenaglia et al., 1998). Therefore, in carotid atherosclerosis, it is generally believed that carotid plaques with intra-plaque angiogenesis are vulnerable and tend to rupture, causing the occlusion and thereby leading to severer cerebrovascular events.

In the present study, we confirmed the damage of endothelial cells could be caused by HG and radiation. Apart from the impaired morphological changed triggered by both HG and radiation, radiation induced severer loss of cell viability and a trend of activating the cleaved caspase-3. These results provided the evidence that HG and radiation caused the endothelial damage.

Furthermore, we examined the junctions and meshes which represent the degree of tube formation induced by HG and IR. Our results showed that radiation in combination with HG induced significantly higher angiogenesis than HG/LG alone. Besides, with absence of radiation, a trend was notable that the angiogenic effect of HG was greater than LG. Similar trend could be observed with presence of radiation, that was radiation in combination with HG induced higher angiogenesis than to in combination with LG. These results indicated that radiation played the predominant role in angiogenesis in vitro amongst the treatments of both HG and radiation, and the combined effects exerted greater angiogenic influence on endothelial cells.

In addition, we investigated VEGF and FAK, which involve in angiogenesis and migration, to explore the possible signalling pathways. The results showed that endothelial damage caused by radiation with or without HG activated the FAK pathway, and resulted higher levels of p-FAK/FAK. This suggested that radiation

caused endothelial cells migration in vitro, thereby leading to angiogenesis in the process of atherosclerosis. However, the difference in the levels of activated VEGFR2 (Tyr^{1175}) was not statistically significant.

The results of the present study suggested that radiation exerted more significant effects on endothelial dysfunction, when stimulated by both non-radiation and radiation factor. Besides, radiation-induced angiogenesis in vitro may be mediated by caspase-3 and FAK-mediate pathway. Yet, the stimulation of FAK may not be resulted from VEGFR2, which is anchored on surface in charge of transmitting the signal intracellularly.

Similar previous study reported the role of VEGF and FAK in angiogenesis and atherosclerosis. Liu et al. found that carbon ion and X-ray radiation (2Gy, 4Gy and 8Gy) induced endothelial cells migration and tube formation. The supplement of VEGF induced a trend of higher levels of p-FAK (Tyr861) in human microvascular endothelial cells (HMECs), but noted with no significant difference compared to cells without VEGF165. They also used C6 glioma to investigate the effect of radiation on migration and angiogenesis and obtained the consistent results with HMEC's. Besides, the supplement of VEGF165 increased FAK phosphorylation at Tyr861. Therefore, they suggested that the inhibition of cell migration by carbon ion radiation may be regulated by VEGF-activated FAK pathway. Moreover, compared to carbon ion radiation, X-ray radiation played less important role in suppressing tumorigenesis and angiogenesis through regulation of VEGF in the glioma microenvironment (Liu et al., 2014). Recently, Sun et al. showed that down-regulation of FAK or its kinase activity inhibited proliferating endothelial cells and their migration, indicating the crucial role of FAK in governing the adult EC-mediated angiogenesis. Moreover, they also found

that nuclear FAK in RNA polymerase II complex was associated with VEGFR2 promoter, indicating the direct role of FAK in regulating VEGFR2 (Sun et al., 2018).

The result of our study and Liu's study were consistent in which X-ray radiation induced endothelial cells migration by activating FAK-mediated pathway. However, the results from Sun were different from ours, and the possible reason may due to the different cell lines used. We performed the assays on human endothelial cells, while Sun et al. studied on mouse cells and mouse animal model.

4.4.3 NOS synthesis

NO is produced by NOS, and is primarily responsible for vasomotion regulation to maintain the elasticity of blood vessel in response to physical and chemical stimuli. eNOS is known as constitutive NOS, while iNOS is inducible NOS. In the present study, we observed the trend that radiation and HG alone activated the eNOS, and radiation in combination with HG induced higher levels of p-eNOS.

Previous studies have reported that radiation induced stimulating NOS activity and phosphorylating eNOS (Ser1179), which is consistent with our findings on radiation-induced activation of eNOS. Nagane and colleagues found that Ataxia telangiectasia mutated (ATM) kinase inhibitor (ku-60019) and heat shock protein 90 (HSP90) inhibitor (geldanamycin) play independent and significant roles in suppressing the stimulation of NOS and phosphorylation of eNOS after radiation. Accordingly, they suggested that, in bovine aortic endothelial cells, radiation-induced eNOS stimulation was under the regulation of ATM and HSP90 (Nagane et al., 2015). Hong's in vitro study showed that radiation induced expression of iNOS and nitrotyrosine in HUVECs at the dose of 4 Gy (Hong et al., 2013). They also used rabbit models and found that

radiation suppressed the vasodilation at the dose 8Gy and 16Gy. In addition, some iNOS inhibitors (such as aminoguanidine) were revealed to be useful in ameliorating radiation-induced vascular endothelial damage (Hong et al., 2013). Consistently, we also demonstrated that radiation, and radiation in combination with HG were involved in the stimulation of iNOS. However, the increase was not statistically significant. The possible reasons may due to the different doses to HUVECs and the status of HUVECs, such as aging. HUVECs are primary cell lines, and thus their status were directly affected by various factors. HUVECs taken from different sites of the vasculature may perform differently in terms of proliferation, apoptosis and response to radiation (Venkatesulu et al., 2018). More importantly, a higher number of cell passages may lead to cell senescence, resulting in a decrease in sensitivity to stimulation. Therefore, the effects of HUVECs on radiation were affected by a variety of extrinsic and intrinsic factors.

4.4.4 Limitations

Though activation of FAK, VEGFR2 and iNOS were different with radiation, the difference did not reach statistical significance due to the variation between experiments. The variation may due to internal (cell passages) and external reasons. In this study, we used passage 5 to passage 7 to ensure the optimal condition and for consistency. Thus, further studies with smaller passages of cells and more repeated assays are suggested in order to decrease the variation and better optimization.

4.5 Conclusion

In conclusion, HUVECs were incubated in LG/HG, with or without the exposure to radiation, to examine the effects of radiation and high glucose on endothelial cell functions. Our results indicated that radiation induced the endothelial dysfunction in different aspects. Radiation had a larger effect on inhibiting cell viability, upregulating the expression of active caspase-3. Besides, the combined effects of radiation and high glucose induced angiogenesis. Moreover, eNOS-mediated and FAK-mediated signalling cellular transduction were the possible signalling pathways of radiation and hyperglycaemia-induced endothelial dysfunction. Therefore, caspase-mediated cell apoptosis and increased angiogenesis were the major cellular responses in radiation-induced endothelial dysfunction. Both radiation and hyperglycemia are risk factors for endothelial dysfunction which could potentially lead to atherosclerosis.

Chapter Five

Summary of the Thesis

5.1 Overall summary

Carotid atherosclerosis is a main cause of cerebrovascular events, commonly found in post-radiotherapy (post-RT) head and neck cancer patients, such as nasopharyngeal carcinoma (NPC) patients. It is generally believed that carotid atherosclerosis could be caused by the exposure of cardiovascular risk factors (CVRFs) and radiation. Carotid atherosclerosis is a chronic, progressive and inflammatory disease with different biological processes involving various cell types and cytokines. Therefore, detecting and evaluating the development of carotid atherosclerosis in both post-RT NPC and subjects with CVRFs is important, and exploring the underlying mechanisms of this vascular disorder could pave the way to an efficient therapeutic strategy in the future.

Ultrasound is commonly used in detecting and monitoring carotid atherosclerosis clinically, given that it is non-invasive, time-saving and easy-assessable for subjects. Carotid intima-media thickness (CIMT), incidence and grey-scale median (GSM) of carotid plaque are the common parameters to evaluate the degree of carotid atherosclerosis. Vulnerable carotid plaques are more likely to rupture, and thereby causing occlusion of intracranial blood vessels leading to cerebrovascular events or mortality.

Therefore, identifying the vulnerable carotid plaques and monitoring the changes of carotid plaques are of great clinical significance in patients with carotid atherosclerosis. The research study in Chapter 3 investigated the feasibility of using a computer-assisted method to evaluate and differentiate the carotid plaque characteristics in radiation-induced and non-radiation-induced carotid atherosclerosis.

This study included 107 post-RT NPC patients and 110 CVRF subjects. Each participant had a carotid ultrasound examination, and carotid plaques and carotid intima-media thickness (CIMT) were evaluated with grey scale ultrasound. The carotid plaque characteristics were evaluated for GSM and detailed plaque texture analysis (DPTA) using specific computer software. In DPTA, five different intra-plaque components were color-coded according to different grey scale ranges. Multivariate regression model was used to evaluate the correlation of risk factors and carotid plaque characteristics.

The results of this study showed that post-RT NPC patients had significantly higher CIMT, higher incidence of carotid plaque formation and more carotid plaques than CVRF subjects. Among the five intra-plaque components, radiation-induced carotid plaques had significantly larger area of calcification, but lesser area of lipid when compared to non-radiation-induced carotid plaques. Age, radiation and number of CVRF were significantly associated with the carotid atherosclerosis burden. Besides, age was significantly associated with the amount of lipid and calcification within carotid plaques.

In conclusion, compared to CVRF subjects, post-RT NPC patients were more susceptible to carotid plaque formation with less lipid content. Considering both carotid

atherosclerosis burden and plaque component, both post-RT NPC patients and individuals with CVRF have a high risk of cerebrovascular diseases.

Carotid atherosclerosis is complex and systemic disease. The underlying mechanisms of radiation-carotid atherosclerosis have not been fully revealed. Previous literature suggested that atherosclerosis involves oxidized low-density lipoprotein (oxLDL), migration and differentiation of macrophages, migration of smooth muscle cells, lymphocytes, formation of foam cells, and proliferation of extracellular matrix. Endothelial cells are mono-layer cells, lining on the inner wall of blood vessel and are sensitive to radiation. These cells would be injured by physical or chemical stimuli leading to endothelial dysfunction. To investigate the possible mechanisms of radiation-induced carotid atherosclerosis, and to study the individual and combined effects of radiation and high glucose level (a CVRF leading to atherosclerosis) on endothelial dysfunction, we conducted a cell study (Chapter 4) using human umbilical vascular endothelial cells (HUVECs). HUVECs were exposed to radiation and high-glucose, followed by observing the morphological changes, detecting cells viability, examining tube formation and different proteins' level. These proteins are related to apoptosis (cleaved capses-3), migration (focal adhesion kinase, FAK), angiogenesis (vascular endothelial growth factor receptor 2, VEGFR2) and vasomotion relation, nitric oxide synthesis (NOS), including iNOS and eNOS. The results of this study showed that the combination of radiation and high glucose induced severer endothelial dysfunction, by presenting the activation of caspase-3, phosphorylation of FAK and stimulation of iNOS and eNOS. Therefore, the potential mechanism of radiation-induced carotid atherosclerosis may involve in caspase-3-FAK-mediated pathway and the activation of NOS.

In summary, the thesis is composed of two major research studies, the human study (in vivo) and cell study (in vitro), which answered important research questions in radiation-induced and non-radiation-induced carotid atherosclerosis. The findings of the human study provided evidence to apply computer-assisted ultrasound image analysis to evaluate the characteristics of radiation-induced and non-radiation-induced carotid plaques. This study also demonstrated that radiation caused higher carotid atherosclerosis burden than CVRF. Moreover, the in vitro cell line study revealed the possible mechanisms, and thereby offered a better understanding of the pathogenesis of carotid atherosclerosis.

5.2 Overall implications and clinical significance

Considering carotid atherosclerosis burden, plaque components, both post-RT NPC patients and CVRF subjects have a high risk of cerebrovascular diseases.

The findings of the human study provided evidence to apply computer-assisted ultrasound image analysis to evaluate the characteristics of radiation-induced and non-radiation-induced carotid plaques. This study also demonstrated that radiation caused higher carotid atherosclerosis burden than CVRF. Moreover, the clinical significance in vitro cell line study was that radiation cast a strong effect on endothelial cell dysfunction especially in patients with high blood glucose levels.

References

Abbi, S., & Guan, J. L. (2002). Focal adhesion kinase: protein interactions and cellular functions. Histol Histopathol, 17(4), 1163-1171. doi:10.14670/HH-17.1163

Abedi, H., & Zachary, I. (1997). Vascular endothelial growth factor stimulates tyrosine phosphorylation and recruitment to new focal adhesions of focal adhesion kinase and paxillin in endothelial cells. J Biol Chem, 272(24), 15442-15451. doi:10.1074/jbc.272.24.15442

AbuRahma, A. F., Wulu, J. T., Jr., & Crotty, B. (2002). Carotid plaque ultrasonic heterogeneity and severity of stenosis. Stroke, 33(7), 1772-1775. doi:10.1161/01.str.0000019127.11189.b5

Adams, J. M., & Cory, S. (2002). Apoptosomes: engines for caspase activation. Curr Opin Cell Biol, 14(6), 715-720. doi:10.1016/s0955-0674(02)00381-2

Ajduk, M., Pavic, L., Bulimbasic, S., Sarlija, M., Pavic, P., Patrlj, L., & Brkljacic, B. (2009). Multidetector-row computed tomography in evaluation of atherosclerotic carotid plaques complicated with intraplaque hemorrhage. Ann Vasc Surg, 23(2), 186-193. doi:10.1016/j.avsg.2008.05.008

Alberti, K. G., & Zimmet, P. Z. (1998). Definition, diagnosis and classification of diabetes mellitus and its complications. Part 1: diagnosis and classification of diabetes mellitus provisional report of a WHO consultation. Diabet Med, 15(7), 539-553. doi:10.1002/(SICI)1096-9136(199807)15:7<539::AID-DIA668>3.0.CO;2-S

Alberti, Kurt George Matthew Mayer, & Zimmet, PZ ft. (1998). Definition, diagnosis and classification of diabetes mellitus and its complications. Part 1: diagnosis and classification of diabetes mellitus. Provisional report of a WHO consultation. Diabetic medicine, 15(7), 539-553.

Allen, J. D., Ham, K. L., Dumont, D. M., Sileshi, B., Trahey, G. E., & Dahl, J. J. (2011). The development and potential of acoustic radiation force impulse (ARFI) imaging for carotid artery plaque characterization. Vasc Med, 16(4), 302-311. doi:10.1177/1358863X11400936

Ambale Venkatesh, B., Volpe, G. J., Donekal, S., Mewton, N., Liu, C. Y., Shea, S., Liu, K., Burke, G., Wu, C., Bluemke, D. A., & Lima, J. A. (2014). Association of longitudinal changes in left ventricular structure and function with myocardial fibrosis: the Multi-Ethnic Study of Atherosclerosis study. Hypertension, 64(3), 508-515. doi:10.1161/HYPERTENSIONAHA.114.03697

Annabi, Borhane, & Lee, Ying-Ta. (2003). Radiation Induced-Tubulogenesis in Endothelial Cells is Antagonized by the Antiangiogenic Properties of Green Tea Polyphenol (-) Epigallocatechin-3-Gallate. Cancer Biology & Therapy, 2(6), 640-647. doi:10.4161/cbt.2.6.529

Apter, S., Shemesh, J., Raanani, P., Portnoy, O., Thaler, M., Zissin, R., Ezra, D., Rozenman, J., Pfeffer, R., & Hertz, M. (2006). Cardiovascular calcifications after radiation therapy for Hodgkin lymphoma: computed tomography detection and clinical correlation. Coron Artery Dis, 17(2), 145-151. doi:10.1097/00019501-200603000-00008

Azzam, E. I., Jay-Gerin, J. P., & Pain, D. (2012). Ionizing radiation-induced metabolic oxidative stress and prolonged cell injury. Cancer Lett, 327(1-2), 48-60. doi:10.1016/j.canlet.2011.12.012

Babic, M., Schuchardt, M., Tolle, M., & van der Giet, M. (2019). In times of tobacco-free nicotine consumption: The influence of nicotine on vascular calcification. Eur J Clin Invest, 49(4), e13077. doi:10.1111/eci.13077

Bae, J. H., Kim, W. S., Lee, M. S., Kim, K. S., Park, J. B., Youn, H. J., Park, C. G., Hong, K. S., Kim, J. Y., Jeong, J. W., Park, J. C., Lim, D. S., Kim, M. H., & Woo, J. T. (2016). The changes of individual carotid artery wall layer by aging and carotid intima-media thickness value for high risk. Cardiovasc Ther, 34(6), 397-403. doi:10.1111/1755-5922.12209

Baldassarre, D., Amato, M., Bondioli, A., Sirtori, C. R., & Tremoli, E. (2000). Carotid artery intima-media thickness measured by ultrasonography in normal clinical practice correlates well with atherosclerosis risk factors. Stroke, 31(10), 2426-2430. doi:10.1161/01.str.31.10.2426

Barrett, D., Ploner, A., Chang, E. T., Liu, Z., Zhang, C. X., Liu, Q., Cai, Y., Zhang, Z., Chen, G., Huang, Q. H., Xie, S. H., Cao, S. M., Shao, J. Y., Jia, W. H., Zheng, Y., Liao, J., Chen, Y., Lin, L., Ernberg, I., Adami, H. O., Huang, G., Zeng, Y., Zeng, Y. X., & Ye, W. (2019). Past and Recent Salted Fish and Preserved Food Intakes Are Weakly Associated with Nasopharyngeal Carcinoma Risk in Adults in Southern China. J Nutr, 149(9), 1596-1605. doi:10.1093/jn/nxz095

Bassiouny, H. S., Sakaguchi, Y., Mikucki, S. A., McKinsey, J. F., Piano, G., Gewertz, B. L., & Glagov, S. (1997). Juxtalumenal location of plaque necrosis and neoformation in symptomatic carotid stenosis. J Vasc Surg, 26(4), 585-594. doi:10.1016/s0741-5214(97)70056-9

Beer, A. J., Pelisek, J., Heider, P., Saraste, A., Reeps, C., Metz, S., Seidl, S., Kessler, H., Wester, H. J., Eckstein, H. H., & Schwaiger, M. (2014). PET/CT imaging of

integrin alphavbeta3 expression in human carotid atherosclerosis. JACC Cardiovasc Imaging, 7(2), 178-187. doi:10.1016/j.jcmg.2013.12.003

Ben David, D., Reznick, A. Z., Srouji, S., & Livne, E. (2008). Exposure to pro-inflammatory cytokines upregulates MMP-9 synthesis by mesenchymal stem cells-derived osteoprogenitors. Histochem Cell Biol, 129(5), 589-597. doi:10.1007/s00418-008-0391-1

Bentzon, J. F., Otsuka, F., Virmani, R., & Falk, E. (2014). Mechanisms of plaque formation and rupture. Circ Res, 114(12), 1852-1866. doi:10.1161/CIRCRESAHA.114.302721

Bergmann, O., Zdunek, S., Felker, A., Salehpour, M., Alkass, K., Bernard, S., Sjostrom, S. L., Szewczykowska, M., Jackowska, T., Dos Remedios, C., Malm, T., Andra, M., Jashari, R., Nyengaard, J. R., Possnert, G., Jovinge, S., Druid, H., & Frisen, J. (2015). Dynamics of Cell Generation and Turnover in the Human Heart. Cell, 161(7), 1566-1575. doi:10.1016/j.cell.2015.05.026

Bernelot Moens, S. J., Neele, A. E., Kroon, J., van der Valk, F. M., Van den Bossche, J., Hoeksema, M. A., Hoogeveen, R. M., Schnitzler, J. G., Baccara-Dinet, M. T., Manvelian, G., de Winther, M. P. J., & Stroes, E. S. G. (2017). PCSK9 monoclonal antibodies reverse the pro-inflammatory profile of monocytes in familial hypercholesterolaemia. Eur Heart J, 38(20), 1584-1593. doi:10.1093/eurheartj/ehx002

Biasi, G. M., Sampaolo, A., Mingazzini, P., De Amicis, P., El-Barghouty, N., & Nicolaides, A. N. (1999). Computer analysis of ultrasonic plaque echolucency in identifying high risk carotid bifurcation lesions. Eur J Vasc Endovasc Surg, 17(6), 476-479. doi:10.1053/ejvs.1999.0789

Biau, J., Lapeyre, M., Troussier, I., Budach, W., Giralt, J., Grau, C., Kazmierska, J., Langendijk, J. A., Ozsahin, M., O'Sullivan, B., Bourhis, J., & Gregoire, V. (2019). Selection of lymph node target volumes for definitive head and neck radiation therapy: a 2019 Update. Radiother Oncol, 134, 1-9. doi:10.1016/j.radonc.2019.01.018

Bilora, F., Pietrogrande, F., Petrobelli, F., Polato, G., Pomerri, F., & Muzzio, P. C. (2006). Is radiation a risk factor for atherosclerosis? An echo-color Doppler study on Hodgkin and non-Hodgkin patients. Tumori, 92(4), 295-298.

Blacher, J., Pannier, B., Guerin, A. P., Marchais, S. J., Safar, M. E., & London, G. M. (1998). Carotid arterial stiffness as a predictor of cardiovascular and all-cause mortality in end-stage renal disease. Hypertension, 32(3), 570-574. doi:10.1161/01.hyp.32.3.570

Blann, A. D. (2000). Endothelial cell activation, injury, damage and dysfunction: separate entities or mutual terms? Blood Coagul Fibrinolysis, 11(7), 623-630. doi:10.1097/00001721-200010000-00006

Borghini, A., Gianicolo, E. A., Picano, E., & Andreassi, M. G. (2013). Ionizing radiation and atherosclerosis: current knowledge and future challenges. Atherosclerosis, 230(1), 40-47. doi:10.1016/j.atherosclerosis.2013.06.010

Bray, F., Ferlay, J., Soerjomataram, I., Siegel, R. L., Torre, L. A., & Jemal, A. (2018). Global cancer statistics 2018: GLOBOCAN estimates of incidence and mortality worldwide for 36 cancers in 185 countries. CA Cancer J Clin, 68(6), 394-424. doi:10.3322/caac.21492

Brinjikji, W., Rabinstein, A. A., Lanzino, G., Murad, M. H., Williamson, E. E., DeMarco, J. K., & Huston, J., 3rd. (2015). Ultrasound Characteristics of Symptomatic Carotid Plaques: A Systematic Review and Meta-Analysis. Cerebrovasc Dis, 40(3-4), 165-174. doi:10.1159/000437339

Buell, P. (1974). The effect of migration on the risk of nasopharyngeal cancer among Chinese. Cancer Res, 34(5), 1189-1191.

Bult, H. (1996). Nitric oxide and atherosclerosis: possible implications for therapy. Mol Med Today, 2(12), 510-518. doi:10.1016/s1357-4310(97)81455-4

Burridge, K., Turner, C. E., & Romer, L. H. (1992). Tyrosine phosphorylation of paxillin and pp125FAK accompanies cell adhesion to extracellular matrix: a role in cytoskeletal assembly. J Cell Biol, 119(4), 893-903. doi:10.1083/jcb.119.4.893

Cai, J. M., Hatsukami, T. S., Ferguson, M. S., Small, R., Polissar, N. L., & Yuan, C. (2002). Classification of human carotid atherosclerotic lesions with in vivo multicontrast magnetic resonance imaging. Circulation, 106(11), 1368-1373. doi:10.1161/01.cir.0000028591.44554.f9

Calalb, M. B., Polte, T. R., & Hanks, S. K. (1995). Tyrosine phosphorylation of focal adhesion kinase at sites in the catalytic domain regulates kinase activity: a role for Src family kinases. Mol Cell Biol, 15(2), 954-963. doi:10.1128/mcb.15.2.954

Campisi, J. (2013). Aging, cellular senescence, and cancer. Annu Rev Physiol, 75, 685-705. doi:10.1146/annurev-physiol-030212-183653

Cao, J. J., Arnold, A. M., Manolio, T. A., Polak, J. F., Psaty, B. M., Hirsch, C. H., Kuller, L. H., & Cushman, M. (2007). Association of carotid artery intima-media thickness, plaques, and C-reactive protein with future cardiovascular disease and

all-cause mortality: the Cardiovascular Health Study. Circulation, 116(1), 32-38. doi:10.1161/CIRCULATIONAHA.106.645606

Carmeliet, P., & Jain, R. K. (2000). Angiogenesis in cancer and other diseases. nature, 407(6801), 249-257. doi:10.1038/35025220

Carr, S., Farb, A., Pearce, W. H., Virmani, R., & Yao, J. S. (1996). Atherosclerotic plaque rupture in symptomatic carotid artery stenosis. J Vasc Surg, 23(5), 755-765; discussion 765-756. doi:10.1016/s0741-5214(96)70237-9

Carretero, O. A., & Oparil, S. (2000). Essential hypertension. Part I: definition and etiology. Circulation, 101(3), 329-335. doi:10.1161/01.cir.101.3.329

Carretero, Oscar A, & Oparil, Suzanne. (2000). Essential hypertension part I: definition and etiology. Circulation, 101(3), 329-335.

Chambless, L. E., Heiss, G., Folsom, A. R., Rosamond, W., Szklo, M., Sharrett, A. R., & Clegg, L. X. (1997). Association of coronary heart disease incidence with carotid arterial wall thickness and major risk factors: the Atherosclerosis Risk in Communities (ARIC) Study, 1987-1993. Am J Epidemiol, 146(6), 483-494. doi:10.1093/oxfordjournals.aje.a009302

Chan, A. T., Hsu, M. M., Goh, B. C., Hui, E. P., Liu, T. W., Millward, M. J., Hong, R. L., Whang-Peng, J., Ma, B. B., To, K. F., Mueser, M., Amellal, N., Lin, X., & Chang, A. Y. (2005). Multicenter, phase II study of cetuximab in combination with carboplatin in patients with recurrent or metastatic nasopharyngeal carcinoma. J Clin Oncol, 23(15), 3568-3576. doi:10.1200/JCO.2005.02.147

Chan, K. C., Hung, E. C., Woo, J. K., Chan, P. K., Leung, S. F., Lai, F. P., Cheng, A. S., Yeung, S. W., Chan, Y. W., Tsui, T. K., Kwok, J. S., King, A. D., Chan, A. T., van Hasselt, A. C., & Lo, Y. M. (2013). Early detection of nasopharyngeal carcinoma by plasma Epstein-Barr virus DNA analysis in a surveillance program. cancer, 119(10), 1838-1844. doi:10.1002/cncr.28001

Chang, Y. J., Chang, T. C., Lee, T. H., & Ryu, S. J. (2009). Predictors of carotid artery stenosis after radiotherapy for head and neck cancers. J Vasc Surg, 50(2), 280-285. doi:10.1016/j.jvs.2009.01.033

Chen, P. Y., Qin, L., Baeyens, N., Li, G., Afolabi, T., Budatha, M., Tellides, G., Schwartz, M. A., & Simons, M. (2015). Endothelial-to-mesenchymal transition drives atherosclerosis progression. J Clin Invest, 125(12), 4514-4528. doi:10.1172/JCI82719

Chen, Q. Y., Wen, Y. F., Guo, L., Liu, H., Huang, P. Y., Mo, H. Y., Li, N. W., Xiang, Y. Q., Luo, D. H., Qiu, F., Sun, R., Deng, M. Q., Chen, M. Y., Hua, Y. J., Guo, X., Cao, K. J., Hong, M. H., Qian, C. N., & Mai, H. Q. (2011). Concurrent chemoradiotherapy vs radiotherapy alone in stage II nasopharyngeal carcinoma: phase III randomized trial. J Natl Cancer Inst, 103(23), 1761-1770. doi:10.1093/jnci/djr432

Chen, Y. P., Chan, A. T. C., Le, Q. T., Blanchard, P., Sun, Y., & Ma, J. (2019). Nasopharyngeal carcinoma. Lancet, 394(10192), 64-80. doi:10.1016/S0140-6736(19)30956-0

Chen, Y., Sun, Y., Liang, S. B., Zong, J. F., Li, W. F., Chen, M., Chen, L., Mao, Y. P., Tang, L. L., Guo, Y., Lin, A. H., Liu, M. Z., & Ma, J. (2013). Progress report of a randomized trial comparing long-term survival and late toxicity of concurrent chemoradiotherapy with adjuvant chemotherapy versus radiotherapy alone in patients with stage III to IVB nasopharyngeal carcinoma from endemic regions of China. cancer, 119(12), 2230-2238. doi:10.1002/cncr.28049

Chen, Yu-Pei, Chan, Anthony T. C., Le, Quynh-Thu, Blanchard, Pierre, Sun, Ying, & Ma, Jun. (2019). Nasopharyngeal carcinoma. The Lancet, 394(10192), 64-80. doi:10.1016/s0140-6736(19)30956-0

Cheng, S. W., Ting, A. C., & Wu, L. L. (2002). Ultrasonic analysis of plaque characteristics and intimal-medial thickness in radiation-induced atherosclerotic carotid arteries. Eur J Vasc Endovasc Surg, 24(6), 499-504. doi:10.1053/ejvs.2002.1752

Cheng, S. W., Wu, L. L., Ting, A. C., Lau, H., Lam, L. K., & Wei, W. I. (1999). Irradiation-induced extracranial carotid stenosis in patients with head and neck malignancies. Am J Surg, 178(4), 323-328. doi:10.1016/s0002-9610(99)00184-1

Cheruvu, P. K., Finn, A. V., Gardner, C., Caplan, J., Goldstein, J., Stone, G. W., Virmani, R., & Muller, J. E. (2007). Frequency and distribution of thin-cap fibroatheroma and ruptured plaques in human coronary arteries: a pathologic study. J Am Coll Cardiol, 50(10), 940-949. doi:10.1016/j.jacc.2007.04.086

Chia, W. K., Wang, W. W., Teo, M., Tai, W. M., Lim, W. T., Tan, E. H., Leong, S. S., Sun, L., Chen, J. J., Gottschalk, S., & Toh, H. C. (2012). A phase II study evaluating the safety and efficacy of an adenovirus-DeltaLMP1-LMP2 transduced dendritic cell vaccine in patients with advanced metastatic nasopharyngeal carcinoma. Ann Oncol, 23(4), 997-1005. doi:10.1093/annonc/mdr341

Childs, B. G., Durik, M., Baker, D. J., & van Deursen, J. M. (2015). Cellular senescence in aging and age-related disease: from mechanisms to therapy. Nat Med, 21(12), 1424-1435. doi:10.1038/nm.4000

Cho, C. H., Kammerer, R. A., Lee, H. J., Yasunaga, K., Kim, K. T., Choi, H. H., Kim, W., Kim, S. H., Park, S. K., Lee, G. M., & Koh, G. Y. (2004). Designed angiopoietin-1 variant, COMP-Ang1, protects against radiation-induced endothelial cell apoptosis. Proc Natl Acad Sci U S A, 101(15), 5553-5558. doi:10.1073/pnas.0307575101

Choi, A. O., Cho, S. J., Desbarats, J., Lovric, J., & Maysinger, D. (2007). Quantum dot-induced cell death involves Fas upregulation and lipid peroxidation in human neuroblastoma cells. J Nanobiotechnology, 5, 1. doi:10.1186/1477-3155-5-1

Chong, V. F., & Ong, C. K. (2008). Nasopharyngeal carcinoma. Eur J Radiol, 66(3), 437-447. doi:10.1016/j.ejrad.2008.03.029

Choy, J. C., Granville, D. J., Hunt, D. W., & McManus, B. M. (2001). Endothelial cell apoptosis: biochemical characteristics and potential implications for atherosclerosis. J Mol Cell Cardiol, 33(9), 1673-1690. doi:10.1006/jmcc.2001.1419

Christensen, J. J., Osnes, L. T., Halvorsen, B., Retterstol, K., Bogsrud, M. P., Wium, C., Svilaas, A., Narverud, I., Ulven, S. M., Aukrust, P., & Holven, K. B. (2017). Altered leukocyte distribution under hypercholesterolemia: A cross-sectional study in children with familial hypercholesterolemia. Atherosclerosis, 256, 67-74. doi:10.1016/j.atherosclerosis.2016.11.031

Chu, B., Kampschulte, A., Ferguson, M. S., Kerwin, W. S., Yarnykh, V. L., O'Brien, K. D., Polissar, N. L., Hatsukami, T. S., & Yuan, C. (2004). Hemorrhage in the atherosclerotic carotid plaque: a high-resolution MRI study. Stroke, 35(5), 1079-1084. doi:10.1161/01.STR.0000125856.25309.86

Cines, D. B., Pollak, E. S., Buck, C. A., Loscalzo, J., Zimmerman, G. A., McEver, R. P., Pober, J. S., Wick, T. M., Konkle, B. A., Schwartz, B. S., Barnathan, E. S., McCrae, K. R., Hug, B. A., Schmidt, A. M., & Stern, D. M. (1998). Endothelial cells in physiology and in the pathophysiology of vascular disorders. Blood, 91(10), 3527-3561.

Cleland, S. J., Sattar, N., Petrie, J. R., Forouhi, N. G., Elliott, H. L., & Connell, J. M. (2000). Endothelial dysfunction as a possible link between C-reactive protein levels and cardiovascular disease. Clin Sci (Lond), 98(5), 531-535.

Cochain, C., & Zernecke, A. (2015). Macrophages and immune cells in atherosclerosis: recent advances and novel concepts. Basic Res Cardiol, 110(4), 34. doi:10.1007/s00395-015-0491-8

Cumming, M. J., & Morrow, I. M. (1994). Carotid artery stenosis: a prospective comparison of CT angiography and conventional angiography. AJR Am J Roentgenol, 163(3), 517-523. doi:10.2214/ajr.163.3.8079836

Czernuszewicz, T. J., Homeister, J. W., Caughey, M. C., Farber, M. A., Fulton, J. J., Ford, P. F., Marston, W. A., Vallabhaneni, R., Nichols, T. C., & Gallippi, C. M. (2015). Non-invasive in vivo characterization of human carotid plaques with acoustic radiation force impulse ultrasound: comparison with histology after endarterectomy. Ultrasound Med Biol, 41(3), 685-697. doi:10.1016/j.ultrasmedbio.2014.09.016

Damjanov, Ivan. (2011). Pathology for the Health Professions (4 ed.).

Damjanov, Ivan. (2012). Pathology for the health professions (4th ed.). St. Louis, Mo.: Elsevier/Saunders.

Davies, M. J., & Woolf, N. (1993). Atherosclerosis: what is it and why does it occur? Br Heart J, 69(1 Suppl), S3-11. doi:10.1136/hrt.69.1_suppl.s3

Davis, S., Aldrich, T. H., Jones, P. F., Acheson, A., Compton, D. L., Jain, V., Ryan, T. E., Bruno, J., Radziejewski, C., Maisonpierre, P. C., & Yancopoulos, G. D. (1996). Isolation of angiopoietin-1, a ligand for the TIE2 receptor, by secretion-trap expression cloning. Cell, 87(7), 1161-1169. doi:10.1016/s0092-8674(00)81812-7

Dawson, C. W., Port, R. J., & Young, L. S. (2012). The role of the EBV-encoded latent membrane proteins LMP1 and LMP2 in the pathogenesis of nasopharyngeal carcinoma (NPC). Semin Cancer Biol, 22(2), 144-153. doi:10.1016/j.semcancer.2012.01.004

de Freitas, E. V., Brandao, A. A., Pozzan, R., Magalhies, M. E., Castier, M., & Brandao, A. P. (2008). Study of the intima-media thickening in carotid arteries of healthy elderly with high blood pressure and elderly with high blood pressure and dyslipidemia. Clin Interv Aging, 3(3), 525-534. doi:10.2147/cia.s213

de Korte, C. L., Pasterkamp, G., van der Steen, A. F., Woutman, H. A., & Bom, N. (2000). Characterization of plaque components with intravascular ultrasound elastography in human femoral and coronary arteries in vitro. Circulation, 102(6), 617-623. doi:10.1161/01.cir.102.6.617

de Korte, C. L., van der Steen, A. F., Cepedes, E. I., Pasterkamp, G., Carlier, S. G., Mastik, F., Schoneveld, A. H., Serruys, P. W., & Bom, N. (2000). Characterization of plaque components and vulnerability with intravascular ultrasound elastography. Phys Med Biol, 45(6), 1465-1475. doi:10.1088/0031-9155/45/6/305

De Meyer, G. R., Bult, H., Ustunes, L., Kockx, M. M., Feelisch, M., & Herman, A. G. (1995). Effect of nitric oxide donors on neointima formation and vascular reactivity in the collared carotid artery of rabbits. J Cardiovasc Pharmacol, 26(2), 272-279. doi:10.1097/00005344-199508000-00013

Deng, L., Jing, N., Tan, G., Zhou, M., Zhan, F., Xie, Y., Cao, L., & Li, G. (1998). A common region of allelic loss on chromosome region 3p25.3-26.3 in nasopharyngeal carcinoma. Genes Chromosomes Cancer, 23(1), 21-25. doi:10.1002/(sici)1098-2264(199809)23:1<21::aid-gcc4>3.0.co;2-8

Dewey, W. C., Ling, C. C., & Meyn, R. E. (1995). Radiation-induced apoptosis: relevance to radiotherapy. Int J Radiat Oncol Biol Phys, 33(4), 781-796. doi:10.1016/0360-3016(95)00214-8

Dickson, R. I., & Flores, A. D. (1985). Nasopharyngeal carcinoma: an evaluation of 134 patients treated between 1971-1980. Laryngoscope, 95(3), 276-283. doi:10.1288/00005537-198503000-00007

Dijk, J. M., Algra, A., van der Graaf, Y., Grobbee, D. E., Bots, M. L., & group, Smart study. (2005). Carotid stiffness and the risk of new vascular events in patients with manifest cardiovascular disease. The SMART study. Eur Heart J, 26(12), 1213-1220. doi:10.1093/eurheartj/ehi254

Dimitrievich, G. S., Fischer-Dzoga, K., & Griem, M. L. (1984). Radiosensitivity of vascular tissue. I. Differential radiosensitivity of capillaries: a quantitative in vivo study. Radiat Res, 99(3), 511-535.

Ding, N., Sang, Y., Chen, J., Ballew, S. H., Kalbaugh, C. A., Salameh, M. J., Blaha, M. J., Allison, M., Heiss, G., Selvin, E., Coresh, J., & Matsushita, K. (2019). Cigarette Smoking, Smoking Cessation, and Long-Term Risk of 3 Major Atherosclerotic Diseases. J Am Coll Cardiol, 74(4), 498-507. doi:10.1016/j.jacc.2019.05.049

Dong, X., Tong, F., Qian, C., Zhang, R., Dong, J., Wu, G., & Hu, Y. (2015). NEMO modulates radiation-induced endothelial senescence of human umbilical veins through NF-kappaB signal pathway. Radiat Res, 183(1), 82-93. doi:10.1667/RR13682.1

Dong, Xiaorong, Tong, Fan, Qian, Cai, Zhang, Ruiguang, Dong, Jihua, Wu, Gang, & Hu, Yu. (2014). NEMO Modulates Radiation-Induced Endothelial Senescence of

Human Umbilical Veins Through NF-κB Signal Pathway. Radiation Research, 183(1), 82-93. doi:10.1667/RR13682.1

Doran, A. C., Meller, N., & McNamara, C. A. (2008). Role of smooth muscle cells in the initiation and early progression of atherosclerosis. Arterioscler Thromb Vasc Biol, 28(5), 812-819. doi:10.1161/ATVBAHA.107.159327

Dorresteijn, L. D., Kappelle, A. C., Boogerd, W., Klokman, W. J., Balm, A. J., Keus, R. B., van Leeuwen, F. E., & Bartelink, H. (2002). Increased risk of ischemic stroke after radiotherapy on the neck in patients younger than 60 years. J Clin Oncol, 20(1), 282-288. doi:10.1200/JCO.2002.20.1.282

Doyle, A. E. (1991). Hypertension and vascular disease. Am J Hypertens, 4(2 Pt 2), 103S-106S. doi:10.1093/ajh/4.2.103s

Du, Y. Y., Luo, D. H., Sun, X. S., Tang, L. Q., Mai, H. Q., Chen, Q. Y., Zhong, J. H., Mai, D. M., Zhang, W. R., Chen, W. H., & Mo, H. Y. (2019). Combining pretreatment plasma Epstein-Barr virus DNA level and cervical node necrosis improves prognostic stratification in patients with nasopharyngeal carcinoma: A cohort study. Cancer Med, 8(16), 6841-6852. doi:10.1002/cam4.2481

Dunmore, B. J., McCarthy, M. J., Naylor, A. R., & Brindle, N. P. (2007). Carotid plaque instability and ischemic symptoms are linked to immaturity of microvessels within plaques. J Vasc Surg, 45(1), 155-159. doi:10.1016/j.jvs.2006.08.072

el-Barghouty, N., Nicolaides, A., Bahal, V., Geroulakos, G., & Androulakis, A. (1996). The identification of the high risk carotid plaque. Eur J Vasc Endovasc Surg, 11(4), 470-478. doi:10.1016/s1078-5884(96)80184-5

Elatrozy, T., Nicolaides, A., Tegos, T., & Griffin, M. (1998). The objective characterisation of ultrasonic carotid plaque features. Eur J Vasc Endovasc Surg, 16(3), 223-230. doi:10.1016/s1078-5884(98)80224-4

Elatrozy, T., Nicolaides, A., Tegos, T., Zarka, A. Z., Griffin, M., & Sabetai, M. (1998). The effect of B-mode ultrasonic image standardisation on the echodensity of symptomatic and asymptomatic carotid bifurcation plaques. Int Angiol, 17(3), 179-186.

Eriksson, D., & Stigbrand, T. (2010). Radiation-induced cell death mechanisms. Tumour Biol, 31(4), 363-372. doi:10.1007/s13277-010-0042-8

Espeland, M. A., O'Leary D, H., Terry, J. G., Morgan, T., Evans, G., & Mudra, H. (2005). Carotid intimal-media thickness as a surrogate for cardiovascular disease events

in trials of HMG-CoA reductase inhibitors. Curr Control Trials Cardiovasc Med, 6(1), 3. doi:10.1186/1468-6708-6-3

Fayad, Z. A., & Fuster, V. (2000). Characterization of atherosclerotic plaques by magnetic resonance imaging. Ann N Y Acad Sci, 902, 173-186. doi:10.1111/j.1749-6632.2000.tb06312.x

Fernandez-Alvarez, V., Lopez, F., Suarez, C., Strojan, P., Eisbruch, A., Silver, C. E., Mendenhall, W. M., Langendijk, J. A., Rinaldo, A., Lee, A. W. M., Beitler, J. J., Smee, R., Alvarez, J., & Ferlito, A. (2018). Radiation-induced carotid artery lesions. Strahlenther Onkol, 194(8), 699-710. doi:10.1007/s00066-018-1304-4

Ferrara, N., & Davis-Smyth, T. (1997). The biology of vascular endothelial growth factor. Endocr Rev, 18(1), 4-25. doi:10.1210/edrv.18.1.0287

Folkman, J. (1972). Anti-angiogenesis: new concept for therapy of solid tumors. Ann Surg, 175(3), 409-416. doi:10.1097/00000658-197203000-00014

Folkman, J. (2006). Angiogenesis. Annu Rev Med, 57, 1-18. doi:10.1146/annurev.med.57.121304.131306

Folsom, A. R., Kronmal, R. A., Detrano, R. C., O'Leary, D. H., Bild, D. E., Bluemke, D. A., Budoff, M. J., Liu, K., Shea, S., Szklo, M., Tracy, R. P., Watson, K. E., & Burke, G. L. (2008). Coronary artery calcification compared with carotid intima-media thickness in the prediction of cardiovascular disease incidence: the Multi-Ethnic Study of Atherosclerosis (MESA). Arch Intern Med, 168(12), 1333-1339. doi:10.1001/archinte.168.12.1333

Ford, Earl S, Li, Chaoyang, Pearson, William S, Zhao, Guixiang, & Mokdad, Ali H. (2010). Trends in hypercholesterolemia, treatment and control among United States adults. International journal of cardiology, 140(2), 226-235.

Fridman, J. S., & Lowe, S. W. (2003). Control of apoptosis by p53. Oncogene, 22(56), 9030-9040. doi:10.1038/sj.onc.1207116

Frost, D., Friedl, A., & Beischer, W. (1998). [Determination of intima-media thickness of the carotid artery: influences of methods, proband and examination variables]. Ultraschall Med, 19(4), 168-173. doi:10.1055/s-2007-1000484

Fuks, Z., Persaud, R. S., Alfieri, A., McLoughlin, M., Ehleiter, D., Schwartz, J. L., Seddon, A. P., Cordon-Cardo, C., & Haimovitz-Friedman, A. (1994). Basic fibroblast growth factor protects endothelial cells against radiation-induced programmed cell death in vitro and in vivo. Cancer Res, 54(10), 2582-2590.

Gepner, A. D., Young, R., Delaney, J. A., Tattersall, M. C., Blaha, M. J., Post, W. S., Gottesman, R. F., Kronmal, R., Budoff, M. J., Burke, G. L., Folsom, A. R., Liu, K., Kaufman, J., & Stein, J. H. (2015). Comparison of coronary artery calcium presence, carotid plaque presence, and carotid intima-media thickness for cardiovascular disease prediction in the Multi-Ethnic Study of Atherosclerosis. Circ Cardiovasc Imaging, 8(1). doi:10.1161/CIRCIMAGING.114.002262

Ghiadoni, L., Taddei, S., Virdis, A., Sudano, I., Di Legge, V., Meola, M., Di Venanzio, L., & Salvetti, A. (1998). Endothelial function and common carotid artery wall thickening in patients with essential hypertension. Hypertension, 32(1), 25-32. doi:10.1161/01.hyp.32.1.25

Giannarelli, C., Bianchini, E., Bruno, R. M., Magagna, A., Landini, L., Faita, F., Gemignani, V., Penno, G., Taddei, S., & Ghiadoni, L. (2012). Local carotid stiffness and intima-media thickness assessment by a novel ultrasound-based system in essential hypertension. Atherosclerosis, 223(2), 372-377. doi:10.1016/j.atherosclerosis.2012.05.027

Glagov, S., Weisenberg, E., Zarins, C. K., Stankunavicius, R., & Kolettis, G. J. (1987). Compensatory enlargement of human atherosclerotic coronary arteries. N Engl J Med, 316(22), 1371-1375. doi:10.1056/NEJM198705283162204

Glastonbury, C. M. (2007). Nasopharyngeal carcinoma: the role of magnetic resonance imaging in diagnosis, staging, treatment, and follow-up. Top Magn Reson Imaging, 18(4), 225-235. doi:10.1097/RMR.0b013e3181572b3a

GM., Cooper. (2000). The Cell: A Molecular Approach. 2nd edition.

. In The Cell: A Molecular Approach. 2nd edition. : Sunderland (MA): Sinauer Associates;.

Golledge, J., Greenhalgh, R. M., & Davies, A. H. (2000). The symptomatic carotid plaque. Stroke, 31(3), 774-781. doi:10.1161/01.str.31.3.774

Goncalves, I., Moses, J., Pedro, L. M., Dias, N., Fernandes e Fernandes, J., Nilsson, J., & Ares, M. P. (2003). Echolucency of carotid plaques correlates with plaque cellularity. Eur J Vasc Endovasc Surg, 26(1), 32-38. doi:10.1053/ejvs.2002.1907

Gorski, David H, Beckett, Michael A, Jaskowiak, Nora T, Calvin, Douglas P, Mauceri, Helena J, Salloum, Rabih M, Seetharam, Saraswathy, Koons, Ann, Hari, Danielle M, & Kufe, Donald W. (1999). Blockade of the vascular endothelial growth factor stress response increases the antitumor effects of ionizing radiation. Cancer research, 59(14), 3374-3378.

Gray-Weale, A. C., Graham, J. C., Burnett, J. R., Byrne, K., & Lusby, R. J. (1988). Carotid artery atheroma: comparison of preoperative B-mode ultrasound appearance with carotid endarterectomy specimen pathology. J Cardiovasc Surg (Torino), 29(6), 676-681.

Gray, K., & Bennett, M. (2011). Role of DNA damage in atherosclerosis--bystander or participant? Biochem Pharmacol, 82(7), 693-700. doi:10.1016/j.bcp.2011.06.025

Gronholdt, M. L., Nordestgaard, B. G., Bentzon, J., Wiebe, B. M., Zhou, J., Falk, E., & Sillesen, H. (2002). Macrophages are associated with lipid-rich carotid artery plaques, echolucency on B-mode imaging, and elevated plasma lipid levels. J Vasc Surg, 35(1), 137-145.

Gross, S. S., & Wolin, M. S. (1995). Nitric oxide: pathophysiological mechanisms. Annu Rev Physiol, 57, 737-769. doi:10.1146/annurev.ph.57.030195.003513

Group, European Carotid Surgery Trialists' Collaborative. (1991). MRC European Carotid Surgery Trial: interim results for symptomatic patients with severe (70-99%) or with mild (0-29%) carotid stenosis. European Carotid Surgery Trialists' Collaborative Group. Lancet, 337(8752), 1235-1243.

Guan, Y., Yu, C., Shi, M., Ni, J., Wu, Y., Gu, H., Bai, L., Liu, J., Tu, J., Wang, J., & Ning, X. (2017). The association between elevated fasting plasma glucose levels and carotid intima-media thickness in non-diabetic adults: a population-based cross-sectional study. Oncotarget, 8(67), 111053-111063. doi:10.18632/oncotarget.22302

Gujral, D. M., Chahal, N., Senior, R., Harrington, K. J., & Nutting, C. M. (2014). Radiation-induced carotid artery atherosclerosis. Radiother Oncol, 110(1), 31-38. doi:10.1016/j.radonc.2013.08.009

Gujral, D. M., Shah, B. N., Chahal, N. S., Bhattacharyya, S., Hooper, J., Senior, R., Harrington, K. J., & Nutting, C. M. (2016). Carotid intima-medial thickness as a marker of radiation-induced carotid atherosclerosis. Radiother Oncol, 118(2), 323-329. doi:10.1016/j.radonc.2015.11.025

Gujral, D. M., Shah, B. N., Chahal, N. S., Bhattacharyya, S., Senior, R., Harrington, K. J., & Nutting, C. M. (2016). Arterial Stiffness as a Biomarker of Radiation-Induced Carotid Atherosclerosis. Angiology, 67(3), 266-271. doi:10.1177/0003319715589520

Gujral, D. M., Shah, B. N., Chahal, N. S., Senior, R., Harrington, K. J., & Nutting, C. M. (2014). Clinical features of radiation-induced carotid atherosclerosis. Clin Oncol (R Coll Radiol), 26(2), 94-102. doi:10.1016/j.clon.2013.10.002

Gupta, V. K., Jaskowiak, N. T., Beckett, M. A., Mauceri, H. J., Grunstein, J., Johnson, R. S., Calvin, D. A., Nodzenski, E., Pejovic, M., Kufe, D. W., Posner, M. C., & Weichselbaum, R. R. (2002). Vascular endothelial growth factor enhances endothelial cell survival and tumor radioresistance. Cancer J, 8(1), 47-54.

Gupta, Vinay K., Jaskowiak, Nora T., Beckett, Michael A., Mauceri, Helena J., Grunstein, Jeremy, Johnson, Randall S., Calvin, Douglas A., Nodzenski, Edwardine, Pejovic, Marija, Kufe, Donald W., Posner, Mitchell C., & Weichselbaum, Ralph R. (2002). Vascular Endothelial Growth Factor Enhances Endothelial Cell Survival and Tumor Radioresistance. The Cancer Journal, 8(1), 47-54.

Haasdijk, R. A., Den Dekker, W. K., Cheng, C., Tempel, D., Szulcek, R., Bos, F. L., Hermkens, D. M., Chrifi, I., Brandt, M. M., Van Dijk, C., Xu, Y. J., Van De Kamp, E. H., Blonden, L. A., Van Bezu, J., Sluimer, J. C., Biessen, E. A., Van Nieuw Amerongen, G. P., & Duckers, H. J. (2016). THSD1 preserves vascular integrity and protects against intraplaque haemorrhaging in ApoE-/- mice. Cardiovasc Res, 110(1), 129-139. doi:10.1093/cvr/cvw015

Haigis, M. C., & Guarente, L. P. (2006). Mammalian sirtuins--emerging roles in physiology, aging, and calorie restriction. Genes Dev, 20(21), 2913-2921. doi:10.1101/gad.1467506

Han, X. B., Tan, Y., Fang, Y. Q., & Li, F. (2018). Protective effects of celastrol against gamma irradiation-induced oxidative stress in human umbilical vein endothelial cells. Exp Ther Med, 16(2), 685-694. doi:10.3892/etm.2018.6270

Hanahan, D., & Folkman, J. (1996). Patterns and emerging mechanisms of the angiogenic switch during tumorigenesis. Cell, 86(3), 353-364. doi:10.1016/s0092-8674(00)80108-7

Harwood-Nash, D. C., & Reilly, B. J. (1970). Calcification of the basal ganglia following radiation therapy. Am J Roentgenol Radium Ther Nucl Med, 108(2), 392-395. doi:10.2214/ajr.108.2.392

Hau, P. M., Lung, H. L., Wu, M., Tsang, C. M., Wong, K. L., Mak, N. K., & Lo, K. W. (2020). Targeting Epstein-Barr Virus in Nasopharyngeal Carcinoma. Front Oncol, 10, 600. doi:10.3389/fonc.2020.00600

Heiland, V. M., Forsell, C., Roy, J., Hedin, U., & Gasser, T. C. (2013). Identification of carotid plaque tissue properties using an experimental-numerical approach. J Mech Behav Biomed Mater, 27, 226-238. doi:10.1016/j.jmbbm.2013.05.001

Hellings, W. E., Moll, F. L., de Kleijn, D. P., & Pasterkamp, G. (2012). 10-years experience with the Athero-Express study. Cardiovasc Diagn Ther, 2(1), 63-73. doi:10.3978/j.issn.2223-3652.2012.02.01

Hellings, W. E., Peeters, W., Moll, F. L., Piers, S. R., van Setten, J., Van der Spek, P. J., de Vries, J. P., Seldenrijk, K. A., De Bruin, P. C., Vink, A., Velema, E., de Kleijn, D. P., & Pasterkamp, G. (2010). Composition of carotid atherosclerotic plaque is associated with cardiovascular outcome: a prognostic study. Circulation, 121(17), 1941-1950. doi:10.1161/CIRCULATIONAHA.109.887497

Hess, C., Vuong, V., Hegyi, I., Riesterer, O., Wood, J., Fabbro, D., Glanzmann, C., Bodis, S., & Pruschy, M. (2001). Effect of VEGF receptor inhibitor PTK787/ZK222584 [correction of ZK222548] combined with ionizing radiation on endothelial cells and tumour growth. Br J Cancer, 85(12), 2010-2016. doi:10.1054/bjoc.2001.2166

Ho, F. C., Tham, I. W., Earnest, A., Lee, K. M., & Lu, J. J. (2012). Patterns of regional lymph node metastasis of nasopharyngeal carcinoma: a meta-analysis of clinical evidence. BMC Cancer, 12, 98. doi:10.1186/1471-2407-12-98

Holdsworth, R. J., McCollum, P. T., Bryce, J. S., & Harrison, D. K. (1995). Symptoms, stenosis and carotid plaque morphology. Is plaque morphology relevant? Eur J Vasc Endovasc Surg, 9(1), 80-85. doi:10.1016/s1078-5884(05)80229-1

Hollander, M., Bots, M. L., Del Sol, A. I., Koudstaal, P. J., Witteman, J. C., Grobbee, D. E., Hofman, A., & Breteler, M. M. (2002). Carotid plaques increase the risk of stroke and subtypes of cerebral infarction in asymptomatic elderly: the Rotterdam study. Circulation, 105(24), 2872-2877. doi:10.1161/01.cir.0000018650.58984.75

Holven, K. B., Ulven, S. M., & Bogsrud, M. P. (2017). Hyperlipidemia and cardiovascular disease with focus on familial hypercholesterolemia. Curr Opin Lipidol, 28(5), 445-447. doi:10.1097/MOL.0000000000000449

Hong, C. W., Kim, Y. M., Pyo, H., Lee, J. H., Kim, S., Lee, S., & Noh, J. M. (2013). Involvement of inducible nitric oxide synthase in radiation-induced vascular endothelial damage. J Radiat Res, 54(6), 1036-1042. doi:10.1093/jrr/rrt066

Howard, G., Burke, G. L., Evans, G. W., Crouse, J. R., 3rd, Riley, W., Arnett, D., de Lacy, R., & Heiss, G. (1994). Relations of intimal-medial thickness among sites within the carotid artery as evaluated by B-mode ultrasound. ARIC Investigators. Atherosclerosis Risk in Communities. Stroke, 25(8), 1581-1587. doi:10.1161/01.str.25.8.1581

Hu, S., Liu, Y., You, T., & Zhu, L. (2018). Semaphorin 7A Promotes VEGFA/VEGFR2-Mediated Angiogenesis and Intraplaque Neovascularization in ApoE(-/-) Mice. Front Physiol, 9, 1718. doi:10.3389/fphys.2018.01718

Huang, T. L., Hsu, H. C., Chen, H. C., Lin, H. C., Chien, C. Y., Fang, F. M., Huang, C. C., Chang, H. W., Chang, W. N., Huang, C. R., Tsai, N. W., Kung, C. T., Wang, H. C., Lin, W. C., Cheng, B. C., Su, Y. J., Chang, Y. T., Chang, C. R., Tan, T. Y., & Lu, C. H. (2013). Long-term effects on carotid intima-media thickness after radiotherapy in patients with nasopharyngeal carcinoma. Radiat Oncol, 8, 261. doi:10.1186/1748-717X-8-261

Huang, Y. S., Lee, C. C., Chang, T. S., Ho, H. C., Su, Y. C., Hung, S. K., Lee, M. S., Chou, P., Chang, Y. H., & Lee, C. C. (2011). Increased risk of stroke in young head and neck cancer patients treated with radiotherapy or chemotherapy. Oral Oncol, 47(11), 1092-1097. doi:10.1016/j.oraloncology.2011.07.024

Huang, Yan, Zhang, Li, Pan, Jian-ji, Hu, Guoqing, Gang, Wu, Xiong, Jian ping, Hu, Chaosu, Lin, Lizhu, Yu, Hao, & Jiang, Haoyuan. (2013). A phase II, multicenter, open-label, single-arm trial of famitinib in patients with advanced recurrent and/or metastatic nasopharyngeal carcinoma (NPC) after two previous treatment regimens. Journal of Clinical Oncology, 31(15_suppl), 6026-6026. doi:10.1200/jco.2013.31.15_suppl.6026

Hughes, C. S., Postovit, L. M., & Lajoie, G. A. (2010). Matrigel: a complex protein mixture required for optimal growth of cell culture. Proteomics, 10(9), 1886-1890. doi:10.1002/pmic.200900758

Hui, E. P., Lui, V. W., Wong, C. S., Ma, B. B., Lau, C. P., Cheung, C. S., Ho, K., Cheng, S. H., Ng, M. H., & Chan, A. T. (2011). Preclinical evaluation of sunitinib as single agent or in combination with chemotherapy in nasopharyngeal carcinoma. Invest New Drugs, 29(6), 1123-1131. doi:10.1007/s10637-010-9451-1

Hui, E. P., Ma, B. B., King, A. D., Mo, F., Chan, S. L., Kam, M. K., Loong, H. H., Ahuja, A. T., Zee, B. C., & Chan, A. T. (2011). Hemorrhagic complications in a phase II study of sunitinib in patients of nasopharyngeal carcinoma who has previously received high-dose radiation. Ann Oncol, 22(6), 1280-1287. doi:10.1093/annonc/mdq629

Hui, Edwin Pun, Lui, Vivian WY, Hui, Connie WC, Lau, Cecilia PY, Loong, Herbert HF, Wong, Cesar SC, Wong, Eric CH, & Chan, Anthony TC. (2012). Abstract 1373: Preclinical activity of axitinib and its associated change of serum biomarkers in nasopharyngeal carcinoma (NPC). Cancer research, 72(8 Supplement), 1373-1373. doi:10.1158/1538-7445.Am2012-1373

Huibers, A., de Borst, G. J., Wan, S., Kennedy, F., Giannopoulos, A., Moll, F. L., & Richards, T. (2015). Non-invasive Carotid Artery Imaging to Identify the Vulnerable Plaque: Current Status and Future Goals. Eur J Vasc Endovasc Surg, 50(5), 563-572. doi:10.1016/j.ejvs.2015.06.113

Hurtubise, J., McLellan, K., Durr, K., Onasanya, O., Nwabuko, D., & Ndisang, J. F. (2016). The Different Facets of Dyslipidemia and Hypertension in Atherosclerosis. Curr Atheroscler Rep, 18(12), 82. doi:10.1007/s11883-016-0632-z

Iannuzzi, A., Wilcosky, T., Mercuri, M., Rubba, P., Bryan, F. A., & Bond, M. G. (1995). Ultrasonographic correlates of carotid atherosclerosis in transient ischemic attack and stroke. Stroke, 26(4), 614-619. doi:10.1161/01.str.26.4.614

Ibrahimi, P., Jashari, F., Johansson, E., Gronlund, C., Bajraktari, G., Wester, P., & Henein, M. Y. (2015). Common carotid intima-media features determine distal disease phenotype and vulnerability in asymptomatic patients. Int J Cardiol, 196, 22-28. doi:10.1016/j.ijcard.2015.05.168

Igney, F. H., & Krammer, P. H. (2002). Death and anti-death: tumour resistance to apoptosis. Nat Rev Cancer, 2(4), 277-288. doi:10.1038/nrc776

Ijas, P., Saksi, J., Soinne, L., Tuimala, J., Jauhiainen, M., Jula, A., Kahonen, M., Kesaniemi, Y. A., Kovanen, P. T., Kaste, M., & Lindsberg, P. J. (2013). Haptoglobin 2 allele associates with unstable carotid plaque and major cardiovascular events. Atherosclerosis, 230(2), 228-234. doi:10.1016/j.atherosclerosis.2013.07.008

Insull, W., Jr. (2009). The pathology of atherosclerosis: plaque development and plaque responses to medical treatment. Am J Med, 122(1 Suppl), S3-S14. doi:10.1016/j.amjmed.2008.10.013

Istvan, E. S., & Deisenhofer, J. (2001). Structural mechanism for statin inhibition of HMG-CoA reductase. Science, 292(5519), 1160-1164. doi:10.1126/science.1059344

Ito, T., Yagi, S., & Yamakuchi, M. (2010). MicroRNA-34a regulation of endothelial senescence. Biochem Biophys Res Commun, 398(4), 735-740. doi:10.1016/j.bbrc.2010.07.012

Ji, M. F., Huang, Q. H., Yu, X., Liu, Z., Li, X., Zhang, L. F., Wang, P., Xie, S. H., Rao, H. L., Fang, F., Guo, X., Liu, Q., Hong, M. H., Ye, W., Zeng, Y. X., & Cao, S. M. (2014). Evaluation of plasma Epstein-Barr virus DNA load to distinguish nasopharyngeal carcinoma patients from healthy high-risk populations in Southern China. cancer, 120(9), 1353-1360. doi:10.1002/cncr.28564

Jin, Y. W., Jeong, M., Moon, K., Jo, M. H., & Kang, S. K. (2010). Ionizing radiation-induced diseases in Korea. J Korean Med Sci, 25(Suppl), S70-76. doi:10.3346/jkms.2010.25.S.S70

JM, U. King-Im, Fox, A. J., Aviv, R. I., Howard, P., Yeung, R., Moody, A. R., & Symons, S. P. (2010). Characterization of carotid plaque hemorrhage: a CT angiography and MR intraplaque hemorrhage study. Stroke, 41(8), 1623-1629. doi:10.1161/STROKEAHA.110.579474

Kalluri, R. (2003). Basement membranes: structure, assembly and role in tumour angiogenesis. Nat Rev Cancer, 3(6), 422-433. doi:10.1038/nrc1094

Kardoulas, D. G., Katsamouris, A. N., Gallis, P. T., Philippides, T. P., Anagnostakos, N. K., Gorgoyannis, D. S., & Gourtsoyannis, N. C. (1996). Ultrasonographic and histologic characteristics of symptom-free and symptomatic carotid plaque. Cardiovasc Surg, 4(5), 580-590. doi:10.1016/0967-2109(96)00030-0

Kasliwal, R. R., Bansal, M., Desai, N., Kotak, B., Raza, A., Vasnawala, H., Kumar, A., & collaborators, S. CORE-India. (2016). A Study to derive distribution of carotid intima media thickness and to determine its COrrelation with cardiovascular Risk factors in asymptomatic nationwidE Indian population (SCORE-India). Indian Heart J, 68(6), 821-827. doi:10.1016/j.ihj.2016.04.009

Kastelein, J. J., van Leuven, S. I., Burgess, L., Evans, G. W., Kuivenhoven, J. A., Barter, P. J., Revkin, J. H., Grobbee, D. E., Riley, W. A., Shear, C. L., Duggan, W. T., Bots, M. L., & Investigators, Radiance. (2007). Effect of torcetrapib on carotid atherosclerosis in familial hypercholesterolemia. N Engl J Med, 356(16), 1620-1630. doi:10.1056/NEJMoa071359

Kennedy, Ann R., Maity, Amit, & Sanzari, Jenine K. (2016). A Review of Radiation-Induced Coagulopathy and New Findings to Support Potential Prevention Strategies and Treatments. Radiation Research, 186(2), 121-140. doi:10.1667/RR14406.1

Kerwin, W. S., O'Brien, K. D., Ferguson, M. S., Polissar, N., Hatsukami, T. S., & Yuan, C. (2006). Inflammation in carotid atherosclerotic plaque: a dynamic contrast-enhanced MR imaging study. Radiology, 241(2), 459-468. doi:10.1148/radiol.2412051336

Khalil, A., Poelvoorde, P., Fayyad-Kazan, M., Rousseau, A., Nuyens, V., Uzureau, S., Biston, P., El-Makhour, Y., Badran, B., Van Antwerpen, P., Boudjeltia, K. Z., & Vanhamme, L. (2018). Apoliporotein L3 interferes with endothelial tube formation via regulation of ERK1/2, FAK and Akt signaling pathway. Atherosclerosis, 279, 73-87. doi:10.1016/j.atherosclerosis.2018.10.023

Kiang., Juliann G., Fukumoto., Risaku, & Gorbunov., Nikolai V. (2012). Lipid Peroxidation After Ionizing Irradiation Leads to Apoptosis and Autophagy. In A. Catala (Ed.): IntechOpen.

Kietselaer, Bas L. J. H., Reutelingsperger, Chris P. M., Heidendal, Guido A. K., Daemen, Mat J. A. P., Mess, Werner H., Hofstra, Leonard, & Narula, Jagat. (2004). Noninvasive Detection of Plaque Instability with Use of Radiolabeled Annexin A5 in Patients with Carotid-Artery Atherosclerosis. New England Journal of Medicine, 350(14), 1472-1473. doi:10.1056/NEJM200404013501425

Kim, M., Choi, S. H., Jin, Y. B., Lee, H. J., Ji, Y. H., Kim, J., Lee, Y. S., & Lee, Y. J. (2013). The effect of oxidized low-density lipoprotein (ox-LDL) on radiation-induced endothelial-to-mesenchymal transition. Int J Radiat Biol, 89(5), 356-363. doi:10.3109/09553002.2013.763193

Kim, T. J., Shin, H. Y., Chang, Y., Kang, M., Jee, J., Choi, Y. H., Ahn, H. S., Ahn, S. H., Son, H. J., & Ryu, S. (2017). Metabolically healthy obesity and the risk for subclinical atherosclerosis. Atherosclerosis. doi:10.1016/j.atherosclerosis.2017.03.035

Kim, W., Lee, S., Seo, D., Kim, D., Kim, K., Kim, E., Kang, J., Seong, K. M., Youn, H., & Youn, B. (2019). Cellular Stress Responses in Radiotherapy. Cells, 8(9). doi:10.3390/cells8091105

Kingstone, Lysa Legault, Torres, Carlos, & Currie, Geoff. (2012). A Systematic Literature Review of Ultrasonography for Morphology and Characterization of Vulnerable Carotid Artery Plaques. Journal for Vascular Ultrasound, 36(3), 191-198. doi:10.1177/154431671203600301

Kinlay, S., Creager, M. A., Fukumoto, M., Hikita, H., Fang, J. C., Selwyn, A. P., & Ganz, P. (2001). Endothelium-derived nitric oxide regulates arterial elasticity in human arteries in vivo. Hypertension, 38(5), 1049-1053. doi:10.1161/hy1101.095329

Kleinman, H. K., & Martin, G. R. (2005). Matrigel: basement membrane matrix with biological activity. Semin Cancer Biol, 15(5), 378-386. doi:10.1016/j.semcancer.2005.05.004

Kockx, M. M., DeMeyer, G. R. Y., Muhring, J., Bult, H., Bultinck, J., & Herman, A. G. (1996). Distribution of cell replication and apoptosis in atherosclerotic plaques of cholesterol-fed rabbits. Atherosclerosis, 120(1-2), 115-124. doi:Doi 10.1016/0021-9150(95)05691-2

Kolesnick, R., & Fuks, Z. (2003). Radiation and ceramide-induced apoptosis. Oncogene, 22(37), 5897-5906. doi:10.1038/sj.onc.1206702

Kolodgie, F. D., Yahagi, K., Mori, H., Romero, M. E., Trout, H. H. Rd, Finn, A. V., & Virmani, R. (2017). High-risk carotid plaque: lessons learned from histopathology. Semin Vasc Surg, 30(1), 31-43. doi:10.1053/j.semvascsurg.2017.04.008

Kong, F., Zhou, J., Du, C., He, X., Kong, L., Hu, C., & Ying, H. (2018). Long-term survival and late complications of intensity-modulated radiotherapy for recurrent nasopharyngeal carcinoma. BMC Cancer, 18(1), 1139. doi:10.1186/s12885-018-5055-5

Kruglikova, A. S., Strazhesko, I. D., Plokhova, E. V., Pyhtina, V. S., Akasheva, D. U., Isaykina, O. U., Tkacheva, O. N., & Boytsov, S. A. (2013). P3.10 GENETIC FACTORS VS CARDIOVASCULAR RISK FACTORS. WHAT IS MORE SIGNIFICANT IN VASCULAR AGING? Artery Research, 7(3-4), 129-129. doi:https://doi.org/10.1016/j.artres.2013.10.098

Kwong, D. L., Sham, J. S., Au, G. K., Chua, D. T., Kwong, P. W., Cheng, A. C., Wu, P. M., Law, M. W., Kwok, C. C., Yau, C. C., Wan, K. Y., Chan, R. T., & Choy, D. D. (2004). Concurrent and adjuvant chemotherapy for nasopharyngeal carcinoma: a factorial study. J Clin Oncol, 22(13), 2643-2653. doi:10.1200/JCO.2004.05.173

Lal, B. K., Hobson, R. W., 2nd, Pappas, P. J., Kubicka, R., Hameed, M., Chakhtoura, E. Y., Jamil, Z., Padberg, F. T., Jr., Haser, P. B., & Duran, W. N. (2002). Pixel distribution analysis of B-mode ultrasound scan images predicts histologic features of atherosclerotic carotid plaques. J Vasc Surg, 35(6), 1210-1217. doi:10.1067/mva.2002.122888

Lam, W. W., Leung, S. F., So, N. M., Wong, K. S., Liu, K. H., Ku, P. K., Yuen, H. Y., & Metreweli, C. (2001). Incidence of carotid stenosis in nasopharyngeal carcinoma patients after radiotherapy. cancer, 92(9), 2357-2363. doi:10.1002/1097-0142(20011101)92:9<2357::aid-cncr1583>3.0.co;2-k

Larrivee, B., & Karsan, A. (2000). Signaling pathways induced by vascular endothelial growth factor (review). Int J Mol Med, 5(5), 447-456. doi:10.3892/ijmm.5.5.447

Lau, P. P., Li, L., Merched, A. J., Zhang, A. L., Ko, K. W., & Chan, L. (2006). Nicotine induces proinflammatory responses in macrophages and the aorta leading to acceleration of atherosclerosis in low-density lipoprotein receptor(-/-) mice. Arterioscler Thromb Vasc Biol, 26(1), 143-149. doi:10.1161/01.ATV.0000193510.19000.10

Leborgne, L., Fournadjiev, J., Pakala, R., Dilcher, C., Cheneau, E., Wolfram, R., Hellinga, D., Seaborn, R., O'Tio, F., & Waksman, R. (2003). Antioxidants attenuate atherosclerotic plaque development in a balloon-denuded and -radiated

hypercholesterolemic rabbit. Cardiovasc Radiat Med, 4(1), 25-28. doi:10.1016/s1522-1865(03)00113-6

Leborgne, L., Pakala, R., Dilcher, C., Hellinga, D., Seabron, R., Tio, F. O., & Waksman, R. (2005). Effect of antioxidants on atherosclerotic plaque formation in balloon-denuded and irradiated hypercholesterolemic rabbits. J Cardiovasc Pharmacol, 46(4), 540-547. doi:10.1097/01.fjc.0000179436.03502.26

Lee, A. W., Foo, W., Mang, O., Sze, W. M., Chappell, R., Lau, W. H., & Ko, W. M. (2003). Changing epidemiology of nasopharyngeal carcinoma in Hong Kong over a 20-year period (1980-99): an encouraging reduction in both incidence and mortality. Int J Cancer, 103(5), 680-685. doi:10.1002/ijc.10894

Lee, A. W., Lin, J. C., & Ng, W. T. (2012). Current management of nasopharyngeal cancer. Semin Radiat Oncol, 22(3), 233-244. doi:10.1016/j.semradonc.2012.03.008

Lee, A. W., Ma, B. B., Ng, W. T., & Chan, A. T. (2015). Management of Nasopharyngeal Carcinoma: Current Practice and Future Perspective. J Clin Oncol, 33(29), 3356-3364. doi:10.1200/JCO.2015.60.9347

Lee, A. W., Poon, Y. F., Foo, W., Law, S. C., Cheung, F. K., Chan, D. K., Tung, S. Y., Thaw, M., & Ho, J. H. (1992). Retrospective analysis of 5037 patients with nasopharyngeal carcinoma treated during 1976-1985: overall survival and patterns of failure. Int J Radiat Oncol Biol Phys, 23(2), 261-270. doi:10.1016/0360-3016(92)90740-9

Lee, A. W., Tung, S. Y., Chan, A. T., Chappell, R., Fu, Y. T., Lu, T. X., Tan, T., Chua, D. T., O'Sullivan, B., Tung, R., Ng, W. T., Leung, T. W., Leung, S. F., Yau, S., Zhao, C., Tan, E. H., Au, G. K., Siu, L., Fung, K. K., & Lau, W. H. (2011). A randomized trial on addition of concurrent-adjuvant chemotherapy and/or accelerated fractionation for locally-advanced nasopharyngeal carcinoma. Radiother Oncol, 98(1), 15-22. doi:10.1016/j.radonc.2010.09.023

Lee, A. W., Tung, S. Y., Chua, D. T., Ngan, R. K., Chappell, R., Tung, R., Siu, L., Ng, W. T., Sze, W. K., Au, G. K., Law, S. C., O'Sullivan, B., Yau, T. K., Leung, T. W., Au, J. S., Sze, W. M., Choi, C. W., Fung, K. K., Lau, J. T., & Lau, W. H. (2010). Randomized trial of radiotherapy plus concurrent-adjuvant chemotherapy vs radiotherapy alone for regionally advanced nasopharyngeal carcinoma. J Natl Cancer Inst, 102(15), 1188-1198. doi:10.1093/jnci/djq258

Lee, A. W., Tung, S. Y., Ngan, R. K., Chappell, R., Chua, D. T., Lu, T. X., Siu, L., Tan, T., Chan, L. K., Ng, W. T., Leung, T. W., Fu, Y. T., Au, G. K., Zhao, C., O'Sullivan, B., Tan, E. H., & Lau, W. H. (2011). Factors contributing to the efficacy of concurrent-adjuvant chemotherapy for locoregionally advanced nasopharyngeal

carcinoma: combined analyses of NPC-9901 and NPC-9902 Trials. Eur J Cancer, 47(5), 656-666. doi:10.1016/j.ejca.2010.10.026

Lee, Chang-Geol, Heijn, Marcus, di Tomaso, Emmanuelle, Griffon-Etienne, Genevieve, Ancukiewicz, M, Koike, Chieko, Park, KR, Ferrara, Napoleone, Jain, Rakesh K, & Suit, Herman D. (2000). Anti-vascular endothelial growth factor treatment augments tumor radiation response under normoxic or hypoxic conditions. Cancer research, 60(19), 5565-5570.

Leopold, Jane A. (2013). Chapter 2 - The Endothelium. In M. A. Creager, J. A. Beckman, & J. Loscalzo (Eds.), Vascular Medicine: A Companion to Braunwald's Heart Disease (Second Edition) (pp. 14-24). Philadelphia: W.B. Saunders.

Leung, T. W., Tung, S. Y., Sze, W. K., Wong, F. C., Yuen, K. K., Lui, C. M., Lo, S. H., Ng, T. Y., & O, S. K. (2005). Treatment results of 1070 patients with nasopharyngeal carcinoma: an analysis of survival and failure patterns. Head Neck, 27(7), 555-565. doi:10.1002/hed.20189

Lewis, G. D., Holliday, E. B., Kocak-Uzel, E., Hernandez, M., Garden, A. S., Rosenthal, D. I., & Frank, S. J. (2016). Intensity-modulated proton therapy for nasopharyngeal carcinoma: Decreased radiation dose to normal structures and encouraging clinical outcomes. Head Neck, 38 Suppl 1, E1886-1895. doi:10.1002/hed.24341

Li, Y. Q., Chen, P., Haimovitz-Friedman, A., Reilly, R. M., & Wong, C. S. (2003). Endothelial apoptosis initiates acute blood-brain barrier disruption after ionizing radiation. Cancer Res, 63(18), 5950-5956.

Libby, P. (2012). Inflammation in atherosclerosis. Arterioscler Thromb Vasc Biol, 32(9), 2045-2051. doi:10.1161/ATVBAHA.108.179705

Liebowitz, D. (1994). Nasopharyngeal carcinoma: the Epstein-Barr virus association. Semin Oncol, 21(3), 376-381.

Lim, W. T., Ng, Q. S., Ivy, P., Leong, S. S., Singh, O., Chowbay, B., Gao, F., Thng, C. H., Goh, B. C., Tan, D. S., Koh, T. S., Toh, C. K., & Tan, E. H. (2011). A Phase II study of pazopanib in Asian patients with recurrent/metastatic nasopharyngeal carcinoma. Clin Cancer Res, 17(16), 5481-5489. doi:10.1158/1078-0432.CCR-10-3409

Lin, J. R., Shen, W. L., Yan, C., & Gao, P. J. (2015). Downregulation of dynamin-related protein 1 contributes to impaired autophagic flux and angiogenic function in senescent endothelial cells. Arterioscler Thromb Vasc Biol, 35(6), 1413-1422. doi:10.1161/ATVBAHA.115.305706

Lin, R., Chen, S., Liu, G., Xue, Y., & Zhao, X. (2017). Association Between Carotid Atherosclerotic Plaque Calcification and Intraplaque Hemorrhage: A Magnetic Resonance Imaging Study. Arterioscler Thromb Vasc Biol, 37(6), 1228-1233. doi:10.1161/ATVBAHA.116.308360

Lindemann, S., Kramer, B., Seizer, P., & Gawaz, M. (2007). Platelets, inflammation and atherosclerosis. Journal of Thrombosis and Haemostasis, 5 Suppl 1, 203-211. doi:10.1111/j.1538-7836.2007.02517.x

Liu, B., Ni, J., Shi, M., Bai, L., Zhan, C., Lu, H., Wu, Y., Tu, J., Ning, X., Hao, J., & Wang, J. (2017). Carotid Intima-media Thickness and its Association with Conventional Risk Factors in Low-income Adults: A Population-based Cross-Sectional Study in China. Sci Rep, 7, 41500. doi:10.1038/srep41500

Liu, Y., Liu, Y., Sun, C., Gan, L., Zhang, L., Mao, A., Du, Y., Zhou, R., & Zhang, H. (2014). Carbon ion radiation inhibits glioma and endothelial cell migration induced by secreted VEGF. PLoS One, 9(6), e98448. doi:10.1371/journal.pone.0098448

Liu, Y., Wang, M., Zhang, B., Wang, W., Xu, Y., Han, Y., Yuan, C., & Zhao, X. (2019). Size of carotid artery intraplaque hemorrhage and acute ischemic stroke: a cardiovascular magnetic resonance Chinese atherosclerosis risk evaluation study. J Cardiovasc Magn Reson, 21(1), 36. doi:10.1186/s12968-019-0548-1

Lo, K. W., Teo, P. M., Hui, A. B., To, K. F., Tsang, Y. S., Chan, S. Y., Mak, K. F., Lee, J. C., & Huang, D. P. (2000). High resolution allelotype of microdissected primary nasopharyngeal carcinoma. Cancer Res, 60(13), 3348-3353.

Loong, H. H., Ma, B. B., Leung, S. F., Mo, F., Hui, E. P., Kam, M. K., Chan, S. L., Yu, B. K., & Chan, A. T. (2012). Prognostic significance of the total dose of cisplatin administered during concurrent chemoradiotherapy in patients with locoregionally advanced nasopharyngeal carcinoma. Radiother Oncol, 104(3), 300-304. doi:10.1016/j.radonc.2011.12.022

Louis, C. U., Straathof, K., Bollard, C. M., Ennamuri, S., Gerken, C., Lopez, T. T., Huls, M. H., Sheehan, A., Wu, M. F., Liu, H., Gee, A., Brenner, M. K., Rooney, C. M., Heslop, H. E., & Gottschalk, S. (2010). Adoptive transfer of EBV-specific T cells results in sustained clinical responses in patients with locoregional nasopharyngeal carcinoma. J Immunother, 33(9), 983-990. doi:10.1097/CJI.0b013e3181f3cbf4

Low Wang, C. C., Hess, C. N., Hiatt, W. R., & Goldfine, A. B. (2016). Clinical Update: Cardiovascular Disease in Diabetes Mellitus: Atherosclerotic Cardiovascular Disease and Heart Failure in Type 2 Diabetes Mellitus - Mechanisms,

Management, and Clinical Considerations. Circulation, 133(24), 2459-2502. doi:10.1161/CIRCULATIONAHA.116.022194

Lu, J., Ma, Y., Chen, J., Wang, L., Zhang, G., Zhao, M., & Yin, Y. (2014). Assessment of anatomical and dosimetric changes by a deformable registration method during the course of intensity-modulated radiotherapy for nasopharyngeal carcinoma. J Radiat Res, 55(1), 97-104. doi:10.1093/jrr/rrt076

Lusby, R. J., Ferrell, L. D., Ehrenfeld, W. K., Stoney, R. J., & Wylie, E. J. (1982). Carotid plaque hemorrhage. Its role in production of cerebral ischemia. Arch Surg, 117(11), 1479-1488. doi:10.1001/archsurg.1982.01380350069010

Lusis, A. J. (2000). Atherosclerosis. nature, 407(6801), 233-241. doi:10.1038/35025203

Lv, J. W., Qi, Z. Y., Zhou, G. Q., He, X. J., Chen, Y. P., Mao, Y. P., Chen, L., Tang, L. L., Li, W. F., Lin, A. H., Ma, J., & Sun, Y. (2018). Optimal cumulative cisplatin dose in nasopharyngeal carcinoma patients receiving additional induction chemotherapy. Cancer Sci, 109(3), 751-763. doi:10.1111/cas.13474

Ma, B. B. Y., Lim, W. T., Goh, B. C., Hui, E. P., Lo, K. W., Pettinger, A., Foster, N. R., Riess, J. W., Agulnik, M., Chang, A. Y. C., Chopra, A., Kish, J. A., Chung, C. H., Adkins, D. R., Cullen, K. J., Gitlitz, B. J., Lim, D. W., To, K. F., Chan, K. C. A., Lo, Y. M. D., King, A. D., Erlichman, C., Yin, J., Costello, B. A., & Chan, A. T. C. (2018). Antitumor Activity of Nivolumab in Recurrent and Metastatic Nasopharyngeal Carcinoma: An International, Multicenter Study of the Mayo Clinic Phase 2 Consortium (NCI-9742). J Clin Oncol, 36(14), 1412-1418. doi:10.1200/JCO.2017.77.0388

Madycki, G., Staszkiewicz, W., & Gabrusiewicz, A. (2006). Carotid plaque texture analysis can predict the incidence of silent brain infarcts among patients undergoing carotid endarterectomy. Eur J Vasc Endovasc Surg, 31(4), 373-380. doi:10.1016/j.ejvs.2005.10.010

Maisonpierre, P. C., Suri, C., Jones, P. F., Bartunkova, S., Wiegand, S. J., Radziejewski, C., Compton, D., McClain, J., Aldrich, T. H., Papadopoulos, N., Daly, T. J., Davis, S., Sato, T. N., & Yancopoulos, G. D. (1997). Angiopoietin-2, a natural antagonist for Tie2 that disrupts in vivo angiogenesis. Science, 277(5322), 55-60. doi:10.1126/science.277.5322.55

Makita, S., Nakamura, M., & Hiramori, K. (2005). The association of C-reactive protein levels with carotid intima-media complex thickness and plaque formation in the general population. Stroke, 36(10), 2138-2142. doi:10.1161/01.STR.0000181740.74005.ee

Mao, Y. P., Tang, L. L., Chen, L., Sun, Y., Qi, Z. Y., Zhou, G. Q., Liu, L. Z., Li, L., Lin, A. H., & Ma, J. (2016). Prognostic factors and failure patterns in non-metastatic nasopharyngeal carcinoma after intensity-modulated radiotherapy. Chin J Cancer, 35(1), 103. doi:10.1186/s40880-016-0167-2

Marini, M. A., Fiorentino, T. V., Succurro, E., Pedace, E., Andreozzi, F., Sciacqua, A., Perticone, F., & Sesti, G. (2017). Association between hemoglobin glycation index with insulin resistance and carotid atherosclerosis in non-diabetic individuals. PLoS One, 12(4), e0175547. doi:10.1371/journal.pone.0175547

Marks, D. S., Vita, J. A., Folts, J. D., Keaney, J. F., Jr., Welch, G. N., & Loscalzo, J. (1995). Inhibition of neointimal proliferation in rabbits after vascular injury by a single treatment with a protein adduct of nitric oxide. J Clin Invest, 96(6), 2630-2638. doi:10.1172/JCI118328

Marnane, M., Prendeville, S., McDonnell, C., Noone, I., Barry, M., Crowe, M., Mulligan, N., & Kelly, P. J. (2014). Plaque inflammation and unstable morphology are associated with early stroke recurrence in symptomatic carotid stenosis. Stroke, 45(3), 801-806. doi:10.1161/STROKEAHA.113.003657

Marquez-Curtis, L. A., Sultani, A. B., McGann, L. E., & Elliott, J. A. (2016). Beyond membrane integrity: Assessing the functionality of human umbilical vein endothelial cells after cryopreservation. Cryobiology, 72(3), 183-190. doi:10.1016/j.cryobiol.2016.05.005

Martinez-Sanchez, P., Fernandez-Dominguez, J., Ruiz-Ares, G., Fuentes, B., Alexandrov, A. V., & Diez-Tejedor, E. (2012). Changes in carotid plaque echogenicity with time since the stroke onset: an early marker of plaque remodeling? Ultrasound Med Biol, 38(2), 231-237. doi:10.1016/j.ultrasmedbio.2011.10.025

Matsumoto, K., Sera, Y., Nakamura, H., Ueki, Y., & Miyake, S. (2002). Correlation between common carotid arterial wall thickness and ischemic stroke in patients with type 2 diabetes mellitus. Metabolism, 51(2), 244-247. doi:10.1053/meta.2002.28971

Mattace-Raso, F. U., van der Cammen, T. J., van der Meer, I. M., Schalekamp, M. A., Asmar, R., Hofman, A., & Witteman, J. C. (2004). C-reactive protein and arterial stiffness in older adults: the Rotterdam Study. Atherosclerosis, 176(1), 111-116. doi:10.1016/j.atherosclerosis.2004.04.014

Mayer, F. J., Gruenberger, D., Schillinger, M., Mannhalter, C., Minar, E., Koppensteiner, R., Arbesu, I., Niessner, A., & Hoke, M. (2013). Prognostic value of neutrophils in patients with asymptomatic carotid artery disease (2013/11/26 ed. Vol. 231).

Mayer, F. J., Gruenberger, D., Schillinger, M., Mannhalter, C., Minar, E., Koppensteiner, R., Arbesu, I., Niessner, A., & Hoke, M. (2013). Prognostic value of neutrophils in patients with asymptomatic carotid artery disease. Atherosclerosis, 231(2), 274-280. doi:10.1016/j.atherosclerosis.2013.10.002

Mehta, A., Yang, B. C., Khan, S., Hendricks, J. B., Stephen, C., & Mehta, J. L. (1995). Oxidized Low-Density Lipoproteins Facilitate Leukocyte Adhesion to Aortic Intima without Affecting Endothelium-Dependent Relaxation - Role of P-Selectin. Arteriosclerosis Thrombosis and Vascular Biology, 15(11), 2076-2083. doi:Doi 10.1161/01.Atv.15.11.2076

Menghini, R., Casagrande, V., Cardellini, M., Martelli, E., Terrinoni, A., Amati, F., Vasa-Nicotera, M., Ippoliti, A., Novelli, G., Melino, G., Lauro, R., & Federici, M. (2009). MicroRNA 217 modulates endothelial cell senescence via silent information regulator 1. Circulation, 120(15), 1524-1532. doi:10.1161/CIRCULATIONAHA.109.864629

Meredith, I. T., Yeung, A. C., Weidinger, F. F., Anderson, T. J., Uehata, A., Ryan, T. J., Selwyn, A. P., & Ganz, P. (1993). Role of Impaired Endothelium-Dependent Vasodilation in Ischemic Manifestations of Coronary-Artery Disease. Circulation, 87(5), 56-66.

Michel, J. B., Tedgui, A., Salzmann, J. L., Belmain, J., & Levy, B. (1989). [Function and structure of the vascular wall in experimental arterial hypertension. Effect of treatment]. Nephrologie, 10(2), 55-57.

Michiels, C. (2003). Endothelial cell functions. J Cell Physiol, 196(3), 430-443. doi:10.1002/jcp.10333

Mitchell, C. C., Stein, J. H., Cook, T. D., Salamat, S., Wang, X., Varghese, T., Jackson, D. C., Sandoval Garcia, C., Wilbrand, S. M., & Dempsey, R. J. (2017). Histopathologic Validation of Grayscale Carotid Plaque Characteristics Related to Plaque Vulnerability. Ultrasound Med Biol, 43(1), 129-137. doi:10.1016/j.ultrasmedbio.2016.08.011

Miyagawa, M., Yokoyama, R., Nishiyama, Y., Ogimoto, A., Higaki, J., & Mochizuki, T. (2014). Positron emission tomography-computed tomography for imaging of inflammatory cardiovascular diseases. Circ J, 78(6), 1302-1310.

Molloy, J., & Markus, H. S. (1999). Asymptomatic embolization predicts stroke and TIA risk in patients with carotid artery stenosis. Stroke, 30(7), 1440-1443. doi:10.1161/01.str.30.7.1440

Moreno, P. R., Purushothaman, K. R., Zias, E., Sanz, J., & Fuster, V. (2006). Neovascularization in human atherosclerosis. Curr Mol Med, 6(5), 457-477. doi:10.2174/156652406778018635

Moulder, J. E., Fish, B. L., Regner, K. R., & Cohen, E. P. (2002). Angiotensin II blockade reduces radiation-induced proliferation in experimental radiation nephropathy. Radiat Res, 157(4), 393-401. doi:10.1667/0033-7587(2002)157[0393:aibrri]2.0.co;2

Mudau, M., Genis, A., Lochner, A., & Strijdom, H. (2012). Endothelial dysfunction: the early predictor of atherosclerosis. Cardiovasc J Afr, 23(4), 222-231. doi:10.5830/CVJA-2011-068

Nagane, M., Yasui, H., Sakai, Y., Yamamori, T., Niwa, K., Hattori, Y., Kondo, T., & Inanami, O. (2015). Activation of eNOS in endothelial cells exposed to ionizing radiation involves components of the DNA damage response pathway. Biochem Biophys Res Commun, 456(1), 541-546. doi:10.1016/j.bbrc.2014.12.002

Naim, C., Douziech, M., Therasse, E., Robillard, P., Giroux, M. F., Arsenault, F., Cloutier, G., & Soulez, G. (2014). Vulnerable atherosclerotic carotid plaque evaluation by ultrasound, computed tomography angiography, and magnetic resonance imaging: an overview. Can Assoc Radiol J, 65(3), 275-286. doi:10.1016/j.carj.2013.05.003

Naqvi, T. Z., & Lee, M. S. (2014). Carotid intima-media thickness and plaque in cardiovascular risk assessment. JACC Cardiovasc Imaging, 7(10), 1025-1038. doi:10.1016/j.jcmg.2013.11.014

Naqvi, T. Z., Mendoza, F., Rafii, F., Gransar, H., Guerra, M., Lepor, N., Berman, D. S., & Shah, P. K. (2010). High prevalence of ultrasound detected carotid atherosclerosis in subjects with low Framingham risk score: potential implications for screening for subclinical atherosclerosis. J Am Soc Echocardiogr, 23(8), 809-815. doi:10.1016/j.echo.2010.05.005

Neufeld, G., Cohen, T., Gengrinovitch, S., & Poltorak, Z. (1999). Vascular endothelial growth factor (VEGF) and its receptors. FASEB J, 13(1), 9-22.

Ng, Eugene W. M., Shima, David T., Calias, Perry, Cunningham, Emmett T., Guyer, David R., & Adamis, Anthony P. (2006). Pegaptanib, a targeted anti-VEGF aptamer for ocular vascular disease. Nat Rev Drug Discov, 5(2), 123-132.

Ng, W. T., Yau, T. K., Yung, R. W., Sze, W. M., Tsang, A. H., Law, A. L., & Lee, A. W. (2005). Screening for family members of patients with nasopharyngeal carcinoma. Int J Cancer, 113(6), 998-1001. doi:10.1002/ijc.20672

Nicolaides, A. N., Kakkos, S. K., Kyriacou, E., Griffin, M., Sabetai, M., Thomas, D. J., Tegos, T., Geroulakos, G., Labropoulos, N., Dore, C. J., Morris, T. P., Naylor, R., Abbott, A. L., Asymptomatic Carotid, Stenosis, & Risk of Stroke Study, Group. (2010). Asymptomatic internal carotid artery stenosis and cerebrovascular risk stratification. J Vasc Surg, 52(6), 1486-1496 e1481-1485. doi:10.1016/j.jvs.2010.07.021

Nighoghossian, N., Derex, L., & Douek, P. (2005). The vulnerable carotid artery plaque: current imaging methods and new perspectives. Stroke, 36(12), 2764-2772. doi:10.1161/01.STR.0000190895.51934.43

North American Symptomatic Carotid Endarterectomy Trial, Collaborators, Barnett, H. J. M., Taylor, D. W., Haynes, R. B., Sackett, D. L., Peerless, S. J., Ferguson, G. G., Fox, A. J., Rankin, R. N., Hachinski, V. C., Wiebers, D. O., & Eliasziw, M. (1991). Beneficial effect of carotid endarterectomy in symptomatic patients with high-grade carotid stenosis. N Engl J Med, 325(7), 445-453. doi:10.1056/NEJM199108153250701

Omisore, A. D., Famurewa, O. C., Komolafe, M. A., Asaleye, C. M., Fawale, M. B., & Afolabi, B. I. (2018). Association of traditional cardiovascular risk factors with carotid atherosclerosis among adults at a teaching hospital in south-western Nigeria. Cardiovasc J Afr, 29(3), 183-188. doi:10.5830/CVJA-2018-014

Owen, J. D., Ruest, P. J., Fry, D. W., & Hanks, S. K. (1999). Induced focal adhesion kinase (FAK) expression in FAK-null cells enhances cell spreading and migration requiring both auto- and activation loop phosphorylation sites and inhibits adhesion-dependent tyrosine phosphorylation of Pyk2. Mol Cell Biol, 19(7), 4806-4818. doi:10.1128/mcb.19.7.4806

Owolabi, M. O., Agunloye, A. M., Umeh, E. O., & Akpa, O. M. (2015). Can common carotid intima media thickness serve as an indicator of both cardiovascular phenotype and risk among black Africans? Eur J Prev Cardiol, 22(11), 1442-1451. doi:10.1177/2047487314547656

Parcell, Stephen W. (2013). Preventive Cardiology The value of evaluating plaque burden using calcium scoring and carotid intima media thickness testing. Natural medicine journal, 5(9).

Paris, F., Fuks, Z., Kang, A., Capodieci, P., Juan, G., Ehleiter, D., Haimovitz-Friedman, A., Cordon-Cardo, C., & Kolesnick, R. (2001). Endothelial apoptosis as the primary lesion initiating intestinal radiation damage in mice. Science, 293(5528), 293-297. doi:10.1126/science.1060191

Park, T. H. (2016). Evaluation of Carotid Plaque Using Ultrasound Imaging. J Cardiovasc Ultrasound, 24(2), 91-95. doi:10.4250/jcu.2016.24.2.91

Parsons, J. T. (2003). Focal adhesion kinase: the first ten years. J Cell Sci, 116(Pt 8), 1409-1416. doi:10.1242/jcs.00373

Pathmanathan, R., Prasad, U., Chandrika, G., Sadler, R., Flynn, K., & Raab-Traub, N. (1995). Undifferentiated, nonkeratinizing, and squamous cell carcinoma of the nasopharynx. Variants of Epstein-Barr virus-infected neoplasia. Am J Pathol, 146(6), 1355-1367.

Pedro, L. M., Pedro, M. M., Goncalves, I., Carneiro, T. F., Balsinha, C., Fernandes e Fernandes, R., & Fernandes e Fernandes, J. (2000). Computer-assisted carotid plaque analysis: characteristics of plaques associated with cerebrovascular symptoms and cerebral infarction. Eur J Vasc Endovasc Surg, 19(2), 118-123. doi:10.1053/ejvs.1999.0952

Peeters, W., Hellings, W. E., de Kleijn, D. P., de Vries, J. P., Moll, F. L., Vink, A., & Pasterkamp, G. (2009). Carotid atherosclerotic plaques stabilize after stroke: insights into the natural process of atherosclerotic plaque stabilization. Arterioscler Thromb Vasc Biol, 29(1), 128-133. doi:10.1161/ATVBAHA.108.173658

Peng, Gang, Wang, Tao, Yang, Kun-yu, Zhang, Sheng, Zhang, Tao, Li, Qin, Han, Jun, & Wu, Gang. (2012). A prospective, randomized study comparing outcomes and toxicities of intensity-modulated radiotherapy vs. conventional two-dimensional radiotherapy for the treatment of nasopharyngeal carcinoma. Radiotherapy and Oncology, 104(3), 286-293. doi:http://dx.doi.org/10.1016/j.radonc.2012.08.013

Peng, H., Chen, L., Zhang, Y., Li, W. F., Mao, Y. P., Zhang, F., Guo, R., Liu, L. Z., Lin, A. H., Sun, Y., & Ma, J. (2016). Prognostic Value of the Cumulative Cisplatin Dose During Concurrent Chemoradiotherapy in Locoregionally Advanced Nasopharyngeal Carcinoma: A Secondary Analysis of a Prospective Phase III Clinical Trial. Oncologist, 21(11), 1369-1376. doi:10.1634/theoncologist.2016-0105

Peters, S. A., Lind, L., Palmer, M. K., Grobbee, D. E., Crouse, J. R., 3rd, O'Leary, D. H., Evans, G. W., Raichlen, J., Bots, M. L., den Ruijter, H. M., & group, Meteor study. (2012). Increased age, high body mass index and low HDL-C levels are related to an echolucent carotid intima-media: the METEOR study. J Intern Med, 272(3), 257-266. doi:10.1111/j.1365-2796.2011.02505.x

Petrie, J. R., Guzik, T. J., & Touyz, R. M. (2018). Diabetes, Hypertension, and Cardiovascular Disease: Clinical Insights and Vascular Mechanisms. Can J Cardiol, 34(5), 575-584. doi:10.1016/j.cjca.2017.12.005

Pignoli, P., Tremoli, E., Poli, A., Oreste, P., & Paoletti, R. (1986). Intimal plus medial thickness of the arterial wall: a direct measurement with ultrasound imaging. Circulation, 74(6), 1399-1406. doi:10.1161/01.cir.74.6.1399

Pipili-Synetos, E., Sakkoula, E., & Maragoudakis, M. E. (1993). Nitric oxide is involved in the regulation of angiogenesis. Br J Pharmacol, 108(4), 855-857. doi:10.1111/j.1476-5381.1993.tb13476.x

Pletsch-Borba, L., Selwaness, M., van der Lugt, A., Hofman, A., Franco, O. H., & Vernooij, M. W. (2018). Change in Carotid Plaque Components: A 4-Year Follow-Up Study With Serial MR Imaging. JACC Cardiovasc Imaging, 11(2 Pt 1), 184-192. doi:10.1016/j.jcmg.2016.12.026

Polak, J. F., & O'Leary, D. H. (2015). Edge-detected common carotid artery intima-media thickness and incident coronary heart disease in the multi-ethnic study of atherosclerosis. J Am Heart Assoc, 4(6), e001492. doi:10.1161/JAHA.114.001492

Polak, J. F., O'Leary, D. H., Kronmal, R. A., Wolfson, S. K., Bond, M. G., Tracy, R. P., Gardin, J. M., Kittner, S. J., Price, T. R., & Savage, P. J. (1993). Sonographic evaluation of carotid artery atherosclerosis in the elderly: relationship of disease severity to stroke and transient ischemic attack. Radiology, 188(2), 363-370. doi:10.1148/radiology.188.2.8327679

Prati, P., Vanuzzo, D., Casaroli, M., Di Chiara, A., De Biasi, F., Feruglio, G. A., & Touboul, P. J. (1992). Prevalence and determinants of carotid atherosclerosis in a general population. Stroke, 23(12), 1705-1711. doi:10.1161/01.str.23.12.1705

Price, J. F., Tzoulaki, I., Lee, A. J., & Fowkes, F. G. (2007). Ankle brachial index and intima media thickness predict cardiovascular events similarly and increased prediction when combined. J Clin Epidemiol, 60(10), 1067-1075. doi:10.1016/j.jclinepi.2007.01.011

Prochaska, J. J., & Benowitz, N. L. (2015). Smoking cessation and the cardiovascular patient. Curr Opin Cardiol, 30(5), 506-511. doi:10.1097/HCO.0000000000000204

Qi, Mei, Guangyuan, Hu, Guoxian, Long, Hong, Qiu, Qiang, Fu, & Guoqing, Hu. (2011). A prospective study on therapeutic gain by concurrent chemoradiotherapy for stage II–IV a nasopharyngeal carcinoma. Journal of Huazhong University of

Science and Technology [Medical Sciences], 31(1), 58-61. doi:10.1007/s11596-011-0150-8

Radford, I. R., Murphy, T. K., Radley, J. M., & Ellis, S. L. (1994). Radiation response of mouse lymphoid and myeloid cell lines. Part II. Apoptotic death is shown by all lines examined. Int J Radiat Biol, 65(2), 217-227. doi:10.1080/09553009414550251

Raitoharju, E., Lyytikainen, L. P., Levula, M., Oksala, N., Mennander, A., Tarkka, M., Klopp, N., Illig, T., Kahonen, M., Karhunen, P. J., Laaksonen, R., & Lehtimaki, T. (2011). miR-21, miR-210, miR-34a, and miR-146a/b are up-regulated in human atherosclerotic plaques in the Tampere Vascular Study. Atherosclerosis, 219(1), 211-217. doi:10.1016/j.atherosclerosis.2011.07.020

Rebner, M., Pennes, D. R., Adler, D. D., Helvie, M. A., & Lichter, A. S. (1989). Breast microcalcifications after lumpectomy and radiation therapy. Radiology, 170(3 Pt 1), 691-693. doi:10.1148/radiology.170.3.2492670

Reilly, L. M., Lusby, R. J., Hughes, L., Ferrell, L. D., Stoney, R. J., & Ehrenfeld, W. K. (1983). Carotid plaque histology using real-time ultrasonography. Clinical and therapeutic implications. Am J Surg, 146(2), 188-193. doi:10.1016/0002-9610(83)90370-7

Rizzo, M. T. (2004). Focal adhesion kinase and angiogenesis. Where do we go from here? Cardiovasc Res, 64(3), 377-378. doi:10.1016/j.cardiores.2004.09.011

Roh, Y. N., Woo, S. Y., Kim, N., Kim, S., Kim, Y. W., & Kim, D. I. (2011). Prevalence of asymptomatic carotid stenosis in Korea based on health screening population. J Korean Med Sci, 26(9), 1173-1177. doi:10.3346/jkms.2011.26.9.1173

Ronca, R., Benkheil, M., Mitola, S., Struyf, S., & Liekens, S. (2017). Tumor angiogenesis revisited: Regulators and clinical implications. Med Res Rev, 37(6), 1231-1274. doi:10.1002/med.21452

Ross, R. (1999). Atherosclerosis--an inflammatory disease. N Engl J Med, 340(2), 115-126. doi:10.1056/NEJM199901143400207

Rothwell, P. M., Gibson, R. J., Slattery, J., Sellar, R. J., & Warlow, C. P. (1994). Equivalence of measurements of carotid stenosis. A comparison of three methods on 1001 angiograms. European Carotid Surgery Trialists' Collaborative Group. Stroke, 25(12), 2435-2439. doi:10.1161/01.str.25.12.2435

Rothwell, P. M., Villagra, R., Gibson, R., Donders, R. C., & Warlow, C. P. (2000). Evidence of a chronic systemic cause of instability of atherosclerotic plaques. Lancet, 355(9197), 19-24. doi:10.1016/s0140-6736(99)04470-0

Rots, M. L., Timmerman, N., de Kleijn, D. P. V., Pasterkamp, G., Brown, M. M., Bonati, L. H., & de Borst, G. J. (2019). Magnetic Resonance Imaging Identified Brain Ischaemia in Symptomatic Patients Undergoing Carotid Endarterectomy Is Related to Histologically Apparent Intraplaque Haemorrhage. Eur J Vasc Endovasc Surg, 58(6), 796-804. doi:10.1016/j.ejvs.2019.07.017

Ruest, P. J., Shin, N. Y., Polte, T. R., Zhang, X., & Hanks, S. K. (2001). Mechanisms of CAS substrate domain tyrosine phosphorylation by FAK and Src. Mol Cell Biol, 21(22), 7641-7652. doi:10.1128/MCB.21.22.7641-7652.2001

Ryu, S. H., Park, E. Y., Kwak, S., Heo, S. H., Ryu, J. W., Park, J. H., Choi, K. C., & Lee, S. W. (2016). Protective effect of alpha-lipoic acid against radiation-induced fibrosis in mice. Oncotarget, 7(13), 15554-15565. doi:10.18632/oncotarget.6952

Saam, T., Hetterich, H., Hoffmann, V., Yuan, C., Dichgans, M., Poppert, H., Koeppel, T., Hoffmann, U., Reiser, M. F., & Bamberg, F. (2013). Meta-analysis and systematic review of the predictive value of carotid plaque hemorrhage on cerebrovascular events by magnetic resonance imaging. J Am Coll Cardiol, 62(12), 1081-1091. doi:10.1016/j.jacc.2013.06.015

Sabetai, M. M., Tegos, T. J., Nicolaides, A. N., El-Atrozy, T. S., Dhanjil, S., Griffin, M., Belcaro, G., & Geroulakos, G. (2000). Hemispheric symptoms and carotid plaque echomorphology. J Vasc Surg, 31(1 Pt 1), 39-49. doi:10.1016/s0741-5214(00)70066-8

Sadler, J. E. (1997). Thrombomodulin structure and function. Thromb Haemost, 78(1), 392-395.

Sakata, K., Kondo, T., Mizuno, N., Shoji, M., Yasui, H., Yamamori, T., Inanami, O., Yokoo, H., Yoshimura, N., & Hattori, Y. (2015). Roles of ROS and PKC-betaII in ionizing radiation-induced eNOS activation in human vascular endothelial cells. Vascul Pharmacol, 70, 55-65. doi:10.1016/j.vph.2015.03.016

Salonen, J. T., & Salonen, R. (1991). Ultrasonographically assessed carotid morphology and the risk of coronary heart disease. Arterioscler Thromb, 11(5), 1245-1249.

Santoso, S., Sachs, U. J., Kroll, H., Linder, M., Ruf, A., Preissner, K. T., & Chavakis, T. (2002). The junctional adhesion molecule 3 (JAM-3) on human platelets is a counterreceptor for the leukocyte integrin Mac-1. J Exp Med, 196(5), 679-691. doi:10.1084/jem.20020267

Sanz, J., & Fayad, Z. A. (2008). Imaging of atherosclerotic cardiovascular disease. nature, 451(7181), 953-957. doi:10.1038/nature06803

Schaller, M. D. (2001). Biochemical signals and biological responses elicited by the focal adhesion kinase. Biochim Biophys Acta, 1540(1), 1-21. doi:10.1016/s0167-4889(01)00123-9

Schaller, M. D., & Parsons, J. T. (1995). pp125FAK-dependent tyrosine phosphorylation of paxillin creates a high-affinity binding site for Crk. Mol Cell Biol, 15(5), 2635-2645. doi:10.1128/mcb.15.5.2635

Schlaepfer, D. D., & Mitra, S. K. (2004). Multiple connections link FAK to cell motility and invasion. Curr Opin Genet Dev, 14(1), 92-101. doi:10.1016/j.gde.2003.12.002

Shah, P. K. (1997). Inflammation, metalloproteinases, and increased proteolysis: an emerging pathophysiological paradigm in aortic aneurysm. Circulation, 96(7), 2115-2117. doi:10.1161/01.cir.96.7.2115

Sham, J. S., Choy, D., & Choi, P. H. (1990). Nasopharyngeal carcinoma: the significance of neck node involvement in relation to the pattern of distant failure. Br J Radiol, 63(746), 108-113. doi:10.1259/0007-1285-63-746-108

Shanmugaratnam, K. (1978). Histological typing of nasopharyngeal carcinoma. IARC Sci Publ(20), 3-12.

Shi, Y. (2002). Mechanisms of caspase activation and inhibition during apoptosis. Mol Cell, 9(3), 459-470. doi:10.1016/s1097-2765(02)00482-3

Song, P. K., Li, H., Man, Q. Q., Jia, S. S., Li, L. X., & Zhang, J. (2017). Trends in Determinants of Hypercholesterolemia among Chinese Adults between 2002 and 2012: Results from theNational Nutrition Survey. Nutrients, 9(3). doi:10.3390/nu9030279

Spanos, K., Petrocheilou, G., Karathanos, C., Labropoulos, N., Mikhailidis, D., & Giannoukas, A. (2017). Carotid Bifurcation Geometry and Atherosclerosis. Angiology, 68(9), 757-764. doi:10.1177/0003319716678741

Stary, H. C., Chandler, A. B., Glagov, S., Guyton, J. R., Insull, W., Jr., Rosenfeld, M. E., Schaffer, S. A., Schwartz, C. J., Wagner, W. D., & Wissler, R. W. (1994). A definition of initial, fatty streak, and intermediate lesions of atherosclerosis. A report from the Committee on Vascular Lesions of the Council on Arteriosclerosis, American Heart Association. Arterioscler Thromb, 14(5), 840-856. doi:10.1161/01.atv.14.5.840

Stein, J. H., Korcarz, C. E., Hurst, R. T., Lonn, E., Kendall, C. B., Mohler, E. R., Najjar, S. S., Rembold, C. M., Post, W. S., & American Society of Echocardiography Carotid Intima-Media Thickness Task, Force. (2008). Use of carotid ultrasound to identify subclinical vascular disease and evaluate cardiovascular disease risk: a consensus statement from the American Society of Echocardiography Carotid Intima-Media Thickness Task Force. Endorsed by the Society for Vascular Medicine. J Am Soc Echocardiogr, 21(2), 93-111; quiz 189-190. doi:10.1016/j.echo.2007.11.011

Steinberg, D., & Witztum, J. L. (1990). Lipoproteins and atherogenesis. Current concepts. JAMA, 264(23), 3047-3052.

Stenmark, K. R., Yeager, M. E., El Kasmi, K. C., Nozik-Grayck, E., Gerasimovskaya, E. V., Li, M., Riddle, S. R., & Frid, M. G. (2013). The adventitia: essential regulator of vascular wall structure and function. Annu Rev Physiol, 75, 23-47. doi:10.1146/annurev-physiol-030212-183802

Stewart, F. A., Heeneman, S., Te Poele, J., Kruse, J., Russell, N. S., Gijbels, M., & Daemen, M. (2006). Ionizing radiation accelerates the development of atherosclerotic lesions in ApoE-/- mice and predisposes to an inflammatory plaque phenotype prone to hemorrhage. Am J Pathol, 168(2), 649-658. doi:10.2353/ajpath.2006.050409

Su, T. C., Jeng, J. S., Chien, K. L., Sung, F. C., Hsu, H. C., & Lee, Y. T. (2001). Hypertension status is the major determinant of carotid atherosclerosis: a community-based study in Taiwan. Stroke, 32(10), 2265-2271.

Sumpio, B. E., Riley, J. T., & Dardik, A. (2002). Cells in focus: endothelial cell. Int J Biochem Cell Biol, 34(12), 1508-1512.

Sun, J., Canton, G., Balu, N., Hippe, D. S., Xu, D., Liu, J., Hatsukami, T. S., & Yuan, C. (2016). Blood Pressure Is a Major Modifiable Risk Factor Implicated in Pathogenesis of Intraplaque Hemorrhage: An In Vivo Magnetic Resonance Imaging Study. Arterioscler Thromb Vasc Biol, 36(4), 743-749. doi:10.1161/ATVBAHA.115.307043

Sun, S., Wu, H. J., & Guan, J. L. (2018). Nuclear FAK and its kinase activity regulate VEGFR2 transcription in angiogenesis of adult mice. Sci Rep, 8(1), 2550. doi:10.1038/s41598-018-20930-z

Suri, C., Jones, P. F., Patan, S., Bartunkova, S., Maisonpierre, P. C., Davis, S., Sato, T. N., & Yancopoulos, G. D. (1996). Requisite role of angiopoietin-1, a ligand for the TIE2 receptor, during embryonic angiogenesis. Cell, 87(7), 1171-1180. doi:10.1016/s0092-8674(00)81813-9

Suzuki, S., Nishio, S., Takata, K., Morioka, T., & Fukui, M. (2000). Radiation-induced brain calcification: paradoxical high signal intensity in T1-weighted MR images. Acta Neurochir (Wien), 142(7), 801-804. doi:10.1007/s007010070095

Takahashi, W., Ohnuki, T., Honma, K., Kawada, S., & Takagi, S. (2007). The significance of multiple risk factors for early carotid atherosclerosis in Japanese subjects. Intern Med, 46(20), 1679-1684. doi:10.2169/internalmedicine.46.0240

Tang, L., Li, L., Mao, Y., Liu, L., Liang, S., Chen, Y., Sun, Y., Liao, X., Tian, L., Lin, A., Liu, M., & Ma, J. (2008). Retropharyngeal lymph node metastasis in nasopharyngeal carcinoma detected by magnetic resonance imaging : prognostic value and staging categories. cancer, 113(2), 347-354. doi:10.1002/cncr.23555

Tang, L. Q., Chen, D. P., Guo, L., Mo, H. Y., Huang, Y., Guo, S. S., Qi, B., Tang, Q. N., Wang, P., Li, X. Y., Li, J. B., Liu, Q., Gao, Y. H., Xie, F. Y., Liu, L. T., Li, Y., Liu, S. L., Xie, H. J., Liang, Y. J., Sun, X. S., Yan, J. J., Wu, Y. S., Luo, D. H., Huang, P. Y., Xiang, Y. Q., Sun, R., Chen, M. Y., Lv, X., Wang, L., Xia, W. X., Zhao, C., Cao, K. J., Qian, C. N., Guo, X., Hong, M. H., Nie, Z. Q., Chen, Q. Y., & Mai, H. Q. (2018). Concurrent chemoradiotherapy with nedaplatin versus cisplatin in stage II-IVB nasopharyngeal carcinoma: an open-label, non-inferiority, randomised phase 3 trial. Lancet Oncol, 19(4), 461-473. doi:10.1016/S1470-2045(18)30104-9

Tang, R., Hennig, M., Thomasson, B., Scherz, R., Ravinetto, R., Catalini, R., Rubba, P., Zanchetti, A., & Bond, M. G. (2000). Baseline reproducibility of B-mode ultrasonic measurement of carotid artery intima-media thickness: the European Lacidipine Study on Atherosclerosis (ELSA). J Hypertens, 18(2), 197-201. doi:10.1097/00004872-200018020-00010

Taylor, G. S., Haigh, T. A., Gudgeon, N. H., Phelps, R. J., Lee, S. P., Steven, N. M., & Rickinson, A. B. (2004). Dual stimulation of Epstein-Barr Virus (EBV)-specific CD4+- and CD8+-T-cell responses by a chimeric antigen construct: potential therapeutic vaccine for EBV-positive nasopharyngeal carcinoma. J Virol, 78(2), 768-778. doi:10.1128/jvi.78.2.768-778.2004

Tazawa, H., Tsuchiya, N., Izumiya, M., & Nakagama, H. (2007). Tumor-suppressive miR-34a induces senescence-like growth arrest through modulation of the E2F pathway in human colon cancer cells. Proc Natl Acad Sci U S A, 104(39), 15472-15477. doi:10.1073/pnas.0707351104

Tegos, T. J., Sabetai, M. M., Nicolaides, A. N., Pare, G., Elatrozy, T. S., Dhanjil, S., & Griffin, M. (2000). Comparability of the ultrasonic tissue characteristics of carotid plaques. J Ultrasound Med, 19(6), 399-407. doi:10.7863/jum.2000.19.6.399

Tegos, T. J., Stavropoulos, P., Sabetai, M. M., Khodabakhsh, P., Sassano, A., & Nicolaides, A. N. (2001). Determinants of carotid plaque instability: echoicity versus heterogeneity. Eur J Vasc Endovasc Surg, 22(1), 22-30. doi:10.1053/ejvs.2001.1412

Tenaglia, A. N., Peters, K. G., Sketch, M. H., Jr., & Annex, B. H. (1998). Neovascularization in atherectomy specimens from patients with unstable angina: implications for pathogenesis of unstable angina. Am Heart J, 135(1), 10-14. doi:10.1016/s0002-8703(98)70336-9

Terrazzino, S., Deantonio, L., Cargnin, S., Donis, L., Pisani, C., Masini, L., Gambaro, G., Canonico, P. L., Genazzani, A. A., & Krengli, M. (2016). DNA Methyltransferase Gene Polymorphisms for Prediction of Radiation-induced Skin Fibrosis after Treatment of Breast Cancer: a Multifactorial Genetic Approach. Cancer Res Treat. doi:10.4143/crt.2016.256

Tjia, W. M., Sham, J. S., Hu, L., Tai, A. L., & Guan, X. Y. (2005). Characterization of 3p, 5p, and 3q in two nasopharyngeal carcinoma cell lines, using region-specific multiplex fluorescence in situ hybridization probes. Cancer Genet Cytogenet, 158(1), 61-66. doi:10.1016/j.cancergencyto.2004.08.024

Toprak, U., Aytas, I., Ustuner, E., Habiboglu, R., Aslan, N., Pasaoglu, E., & Karademir, A. (2012). Sonographic assessment of acute changes in plaque size and echogenicity and in intima-media thickness of carotid arteries after neck radiation therapy. J Clin Ultrasound, 40(9), 566-571. doi:10.1002/jcu.21971

Torzewski, M., Rist, C., Mortensen, R. F., Zwaka, T. P., Bienek, M., Waltenberger, J., Koenig, W., Schmitz, G., Hombach, V., & Torzewski, J. (2000). C-reactive protein in the arterial intima: role of C-reactive protein receptor-dependent monocyte recruitment in atherogenesis. Arterioscler Thromb Vasc Biol, 20(9), 2094-2099. doi:10.1161/01.atv.20.9.2094

Touboul, P. J., Hennerici, M. G., Meairs, S., Adams, H., Amarenco, P., Bornstein, N., Csiba, L., Desvarieux, M., Ebrahim, S., Hernandez Hernandez, R., Jaff, M., Kownator, S., Naqvi, T., Prati, P., Rundek, T., Sitzer, M., Schminke, U., Tardif, J. C., Taylor, A., Vicaut, E., & Woo, K. S. (2012). Mannheim carotid intima-media thickness and plaque consensus (2004-2006-2011). An update on behalf of the advisory board of the 3rd, 4th and 5th watching the risk symposia, at the 13th, 15th and 20th European Stroke Conferences, Mannheim, Germany, 2004, Brussels, Belgium, 2006, and Hamburg, Germany, 2011. Cerebrovasc Dis, 34(4), 290-296. doi:10.1159/000343145

Touboul, P. J., Hernandez-Hernandez, R., Kucukoglu, S., Woo, K. S., Vicaut, E., Labreuche, J., Migom, C., Silva, H., Vinueza, R., & Investigators, Parc-Aala.

(2007). Carotid artery intima media thickness, plaque and Framingham cardiovascular score in Asia, Africa/Middle East and Latin America: the PARC-AALA study. Int J Cardiovasc Imaging, 23(5), 557-567. doi:10.1007/s10554-006-9197-1

Tribble, D. L., Barcellos-Hoff, M. H., Chu, B. M., & Gong, E. L. (1999). Ionizing radiation accelerates aortic lesion formation in fat-fed mice via SOD-inhibitable processes. Arterioscler Thromb Vasc Biol, 19(6), 1387-1392. doi:10.1161/01.atv.19.6.1387

Tricot, O., Mallat, Z., Heymes, C., Belmin, J., Leseche, G., & Tedgui, A. (2000). Relation between endothelial cell apoptosis and blood flow direction in human atherosclerotic plaques. Circulation, 101(21), 2450-2453. doi:10.1161/01.cir.101.21.2450

Tsang, C. M., Lui, V. W. Y., Bruce, J. P., Pugh, T. J., & Lo, K. W. (2020). Translational genomics of nasopharyngeal cancer. Semin Cancer Biol, 61, 84-100. doi:10.1016/j.semcancer.2019.09.006

Tsao, P. S., Mcevoy, L. M., Drexler, H., Butcher, E. C., & Cooke, J. P. (1994). Enhanced Endothelial Adhesiveness in Hypercholesterolemia Is Attenuated by L-Arginine. Circulation, 89(5), 2176-2182. doi:Doi 10.1161/01.Cir.89.5.2176

Tsao, S. W., Yip, Y. L., Tsang, C. M., Pang, P. S., Lau, V. M., Zhang, G., & Lo, K. W. (2014). Etiological factors of nasopharyngeal carcinoma. Oral Oncol, 50(5), 330-338. doi:10.1016/j.oraloncology.2014.02.006

Tyurina, Y. Y., Tyurin, V. A., Kapralova, V. I., Wasserloos, K., Mosher, M., Epperly, M. W., Greenberger, J. S., Pitt, B. R., & Kagan, V. E. (2011). Oxidative lipidomics of gamma-radiation-induced lung injury: mass spectrometric characterization of cardiolipin and phosphatidylserine peroxidation. In Radiat Res (2011/02/23 ed., Vol. 175, pp. 610-621).

Upchurch, G. R., Jr., Welch, G. N., Fabian, A. J., Freedman, J. E., Johnson, J. L., Keaney, J. F., Jr., & Loscalzo, J. (1997). Homocyst(e)ine decreases bioavailable nitric oxide by a mechanism involving glutathione peroxidase. J Biol Chem, 272(27), 17012-17017.

van den Munckhof, I. C. L., Jones, H., Hopman, M. T. E., de Graaf, J., Nyakayiru, J., van Dijk, B., Eijsvogels, T. M. H., & Thijssen, D. H. J. (2018). Relation between age and carotid artery intima-medial thickness: a systematic review. Clin Cardiol, 41(5), 698-704. doi:10.1002/clc.22934

van der Meer, I. M., Bots, M. L., Hofman, A., del Sol, A. I., van der Kuip, D. A., & Witteman, J. C. (2004). Predictive value of noninvasive measures of atherosclerosis for incident myocardial infarction: the Rotterdam Study. Circulation, 109(9), 1089-1094. doi:10.1161/01.CIR.0000120708.59903.1B

Velazquez, F., Berna, J. D., Abellan, J. L., Serrano, L., Escribano, A., & Canteras, M. (2008). Reproducibility of sonographic measurements of carotid intima-media thickness. Acta Radiol, 49(10), 1162-1166. doi:10.1080/02841850802438520

Venkatesulu, B. P., Mahadevan, L. S., Aliru, M. L., Yang, X., Bodd, M. H., Singh, P. K., Yusuf, S. W., Abe, J. I., & Krishnan, S. (2018). Radiation-Induced Endothelial Vascular Injury: A Review of Possible Mechanisms. JACC Basic Transl Sci, 3(4), 563-572. doi:10.1016/j.jacbts.2018.01.014

Verheij, M., & Bartelink, H. (2000). Radiation-induced apoptosis. Cell Tissue Res, 301(1), 133-142. doi:10.1007/s004410000188

Verheij, M., Dewit, L. G., Boomgaard, M. N., Brinkman, H. J., & van Mourik, J. A. (1994). Ionizing radiation enhances platelet adhesion to the extracellular matrix of human endothelial cells by an increase in the release of von Willebrand factor. Radiat Res, 137(2), 202-207.

Virmani, R., Kolodgie, F. D., Burke, A. P., Farb, A., & Schwartz, S. M. (2000). Lessons from sudden coronary death: a comprehensive morphological classification scheme for atherosclerotic lesions. Arterioscler Thromb Vasc Biol, 20(5), 1262-1275. doi:10.1161/01.atv.20.5.1262

Voo, S., Kwee, R. M., Sluimer, J. C., Schreuder, F. H., Wierts, R., Bauwens, M., Heeneman, S., Cleutjens, J. P., van Oostenbrugge, R. J., Daemen, J. W., Daemen, M. J., Mottaghy, F. M., & Kooi, M. E. (2016). Imaging Intraplaque Inflammation in Carotid Atherosclerosis With 18F-Fluorocholine Positron Emission Tomography-Computed Tomography: Prospective Study on Vulnerable Atheroma With Immunohistochemical Validation. Circ Cardiovasc Imaging, 9(5). doi:10.1161/CIRCIMAGING.115.004467

Vuori, K., Hirai, H., Aizawa, S., & Ruoslahti, E. (1996). Introduction of p130cas signaling complex formation upon integrin-mediated cell adhesion: a role for Src family kinases. Mol Cell Biol, 16(6), 2606-2613. doi:10.1128/mcb.16.6.2606

Wang, H. Y., Chang, Y. L., To, K. F., Hwang, J. S., Mai, H. Q., Feng, Y. F., Chang, E. T., Wang, C. P., Kam, M. K., Cheah, S. L., Lee, M., Gao, L., Zhang, H. Z., He, J. H., Jiang, H., Ma, P. Q., Zhu, X. D., Zeng, L., Chen, C. Y., Chen, G., Huang, M. Y., Fu, S., Shao, Q., Han, A. J., Li, H. G., Shao, C. K., Huang, P. Y., Qian, C. N., Lu, T. X., Li, J. T., Ye, W., Ernberg, I., Ng, H. K., Wee, J. T., Zeng, Y. X., Adami, H.

O., Chan, A. T., & Shao, J. Y. (2016). A new prognostic histopathologic classification of nasopharyngeal carcinoma. Chin J Cancer, 35, 41. doi:10.1186/s40880-016-0103-5

Wang, Tony J. C., Riaz, Nadeem, Cheng, Simon K., Lu, Jiade J., & Lee, Nancy Y. (2012). Intensity-modulated radiation therapy for nasopharyngeal carcinoma: a review. Journal of Radiation Oncology, 1(2), 129-146. doi:10.1007/s13566-012-0020-4

Wang, X., Hu, C., Ying, H., He, X., Zhu, G., Kong, L., & Ding, J. (2015). Patterns of lymph node metastasis from nasopharyngeal carcinoma based on the 2013 updated consensus guidelines for neck node levels. Radiother Oncol, 115(1), 41-45. doi:10.1016/j.radonc.2015.02.017

Wang, Y., Wang, L., Ai, X., Zhao, J., Hao, X., Lu, Y., & Qiao, Z. (2004). Nicotine could augment adhesion molecule expression in human endothelial cells through macrophages secreting TNF-alpha, IL-1beta. Int Immunopharmacol, 4(13), 1675-1686. doi:10.1016/j.intimp.2004.07.028

Wang, Z., Liu, B., Zhu, J., Wang, D., & Wang, Y. (2019). Nicotine-mediated autophagy of vascular smooth muscle cell accelerates atherosclerosis via nAChRs/ROS/NF-kappaB signaling pathway. Atherosclerosis, 284, 1-10. doi:10.1016/j.atherosclerosis.2019.02.008

Ward, W. F., Molteni, A., & Ts'ao, C. H. (1989). Radiation-induced endothelial dysfunction and fibrosis in rat lung: modification by the angiotensin converting enzyme inhibitor CL242817. Radiat Res, 117(2), 342-350.

Wasay, M., Dai, A., Dubey, N., & Kamran, S. (2007). Acute stroke secondary to internal carotid artery pseudoaneurysm: MRI findings and treatment with endovascular coiling. J Pak Med Assoc, 57(7), 377-378.

Watanabe, Y., Nagayama, M., Sakata, A., Okumura, A., Amoh, Y., Ishimori, T., Nakashita, S., & Dodo, Y. (2014). Evaluation of Fibrous Cap Rupture of Atherosclerotic Carotid Plaque with Thin-Slice Source Images of Time-of-Flight MR Angiography. Ann Vasc Dis, 7(2), 127-133. doi:10.3400/avd.oa.13-00101

Wee, J., Tan, E. H., Tai, B. C., Wong, H. B., Leong, S. S., Tan, T., Chua, E. T., Yang, E., Lee, K. M., Fong, K. W., Tan, H. S., Lee, K. S., Loong, S., Sethi, V., Chua, E. J., & Machin, D. (2005). Randomized trial of radiotherapy versus concurrent chemoradiotherapy followed by adjuvant chemotherapy in patients with American Joint Committee on Cancer/International Union against cancer stage III and IV nasopharyngeal cancer of the endemic variety. J Clin Oncol, 23(27), 6730-6738. doi:10.1200/JCO.2005.16.790

Wendelhag, I., Gustavsson, T., Suurkula, M., Berglund, G., & Wikstrand, J. (1991). Ultrasound measurement of wall thickness in the carotid artery: fundamental principles and description of a computerized analysing system. Clin Physiol, 11(6), 565-577. doi:10.1111/j.1475-097x.1991.tb00676.x

Wikstrand, J. (2007). Methodological considerations of ultrasound measurement of carotid artery intima-media thickness and lumen diameter. Clin Physiol Funct Imaging, 27(6), 341-345. doi:10.1111/j.1475-097X.2007.00757.x

Williams, M. A., & Nicolaides, A. N. (1987). Predicting the normal dimensions of the internal and external carotid arteries from the diameter of the common carotid. Eur J Vasc Surg, 1(2), 91-96. doi:10.1016/s0950-821x(87)80004-x

Winn, R. K., & Harlan, J. M. (2005). The role of endothelial cell apoptosis in inflammatory and immune diseases. Journal of Thrombosis and Haemostasis, 3(8), 1815-1824. doi:10.1111/j.1538-7836.2005.01378.x

Winn, R. K., & Harlan, J. M. (2005). The role of endothelial cell apoptosis in inflammatory and immune diseases. Journal of Thrombosis and Haemostasis, 3(8), 1815-1824. doi:DOI 10.1111/j.1538-7836.2005.01378.x

Witztum, J. L. (1993). Role of oxidised low density lipoprotein in atherogenesis. British heart journal., 69(1 Suppl), S12-S18. doi:10.1136/hrt.69.1_suppl.s12

Woo, S. Y., Joh, J. H., Han, S. A., & Park, H. C. (2017). Prevalence and risk factors for atherosclerotic carotid stenosis and plaque: A population-based screening study. Medicine (Baltimore), 96(4), e5999. doi:10.1097/MD.0000000000005999

Woodcock, J. P. (1989). Characterisation of the atheromatous plaque in the carotid arteries. Clin Phys Physiol Meas, 10 Suppl A, 45-49. doi:10.1088/0143-0815/10/4a/006

Wu, K., Chen, Z., Peng, Q., Chen, G., Yan, W., & Chen, X. (2019). Ku86 alleviates human umbilical vein endothelial cellular apoptosis and senescence induced by a low dose of ionizing radiation. J Int Med Res, 47(2), 893-904. doi:10.1177/0300060518805302

Wu, L. S. H. (2006). Construction of evolutionary tree models for nasopharyngeal carcinoma using comparative genomic hybridization data. Cancer Genet Cytogenet, 168(2), 105-108. doi:10.1016/j.cancergencyto.2006.02.017

Wu, X., Gan, B., Yoo, Y., & Guan, J. L. (2005). FAK-mediated src phosphorylation of endophilin A2 inhibits endocytosis of MT1-MMP and promotes ECM degradation. Dev Cell, 9(2), 185-196. doi:10.1016/j.devcel.2005.06.006

Wu, X., Huang, P. Y., Peng, P. J., Lu, L. X., Han, F., Wu, S. X., Hou, X., Zhao, H. Y., Huang, Y., Fang, W. F., Zhao, Y. Y., Xue, C., Hu, Z. H., Zhang, J., Zhang, J. W., Ma, Y. X., Liang, W. H., Zhao, C., & Zhang, L. (2013). Long-term follow-up of a phase III study comparing radiotherapy with or without weekly oxaliplatin for locoregionally advanced nasopharyngeal carcinoma. Ann Oncol, 24(8), 2131-2136. doi:10.1093/annonc/mdt163

Wu, Yu-Xia, Zhang, Xi, Xu, Xiao-Pan, Liu, Yang, Zhang, Guo-Peng, Li, Bao-Juan, Chen, Hui-Jun, & Lu, Hong-Bing. (2017). Multi-contrast MRI registration of carotid arteries based on cross-sectional images and lumen boundaries.

Wu, Yu-Xia, Zhang, Xi, Xu, Xiao-Pan, Liu, Yang, Zhang, Guo-Peng, Li, Bao-Juan, Chen, Hui-Jun, & Lu, Hong-Bing. (2017). Multi-contrast MRI registration of carotid arteries based on cross-sectional images and lumen boundaries (Vol. 10133): SPIE.

Xie, C., Ouyang, L., Chen, J., Zhang, H., Luo, P., Wang, J., & Huang, H. (2019). The Emerging Role of Mesenchymal Stem Cells in Vascular Calcification. Stem Cells Int, 2019, 2875189. doi:10.1155/2019/2875189

Xu, C., Zhang, L. H., Chen, Y. P., Liu, X., Zhou, G. Q., Lin, A. H., Sun, Y., & Ma, J. (2017). Chemoradiotherapy Versus Radiotherapy Alone in Stage II Nasopharyngeal Carcinoma: A Systemic Review and Meta-analysis of 2138 Patients. J Cancer, 8(2), 287-297. doi:10.7150/jca.17317

Xu, J., & Cao, Y. (2014). Radiation-induced carotid artery stenosis: a comprehensive review of the literature. Interv Neurol, 2(4), 183-192. doi:10.1159/000363068

Yang, Fan, Qian, D., Hu, Dan, Hou, Mengyun, Chen, Sandra, Wang, Pei, He, Lin, Cai, Xinzhao, Feng, Zhangkang, Li, Xinting, Xu, Jiawei, Zhong, Qian, & Fan, Na. (2016). Prevalence of cardiovascular disease risk factor clustering in Chinese adults. Clinical Trials and Regulatory Science in Cardiology, 15, 1-6. doi:https://doi.org/10.1016/j.ctrsc.2016.01.007

Yasmin, McEniery, C. M., Wallace, S., Mackenzie, I. S., Cockcroft, J. R., & Wilkinson, I. B. (2004). C-reactive protein is associated with arterial stiffness in apparently healthy individuals. Arterioscler Thromb Vasc Biol, 24(5), 969-974. doi:10.1161/01.ATV.zhq0504.0173

Yoshizaki, T. (2002). Promotion of metastasis in nasopharyngeal carcinoma by Epstein-Barr virus latent membrane protein-1. Histol Histopathol, 17(3), 845-850. doi:10.14670/HH-17.845

Yoshizaki, T., Endo, K., Ren, Q., Wakisaka, N., Murono, S., Kondo, S., Sato, H., & Furukawa, M. (2007). Oncogenic role of Epstein-Barr virus-encoded small RNAs

(EBERs) in nasopharyngeal carcinoma. Auris Nasus Larynx, 34(1), 73-78. doi:10.1016/j.anl.2006.09.025

Yoshizaki, T., Ito, M., Murono, S., Wakisaka, N., Kondo, S., & Endo, K. (2012). Current understanding and management of nasopharyngeal carcinoma. Auris Nasus Larynx, 39(2), 137-144. doi:10.1016/j.anl.2011.02.012

Young, L. S., & Dawson, C. W. (2014). Epstein-Barr virus and nasopharyngeal carcinoma. Chin J Cancer, 33(12), 581-590. doi:10.5732/cjc.014.10197

Yuan, C., Lai, C. W., Chan, L. W., Chow, M., Law, H. K., & Ying, M. (2014). Cumulative effects of hypertension, dyslipidemia, and chronic kidney disease on carotid atherosclerosis in Chinese patients with type 2 diabetes mellitus. J Diabetes Res, 2014, 179686. doi:10.1155/2014/179686

Yuan, C., Wu, V. W., Yip, S. P., Kwong, D. L., & Ying, M. (2014). Predictors of the extent of carotid atherosclerosis in patients treated with radiotherapy for nasopharyngeal carcinoma. PLoS One, 9(12), e116284. doi:10.1371/journal.pone.0116284

Yuan, C., Wu, V. W., Yip, S. P., Kwong, D. L., & Ying, M. (2015). Ultrasound Evaluation of Carotid Atherosclerosis in Post-Radiotherapy Nasopharyngeal Carcinoma Patients, Type 2 Diabetics, and Healthy Controls. Ultraschall Med. doi:10.1055/s-0034-1399293

Yuan, C., Wu, V. W., Yip, S. P., Kwong, D. L., & Ying, M. (2017). Ultrasound Evaluation of Carotid Atherosclerosis in Post-Radiotherapy Nasopharyngeal Carcinoma Patients, Type 2 Diabetics, and Healthy Controls. Ultraschall Med, 38(2), 190-197. doi:10.1055/s-0034-1399293

Zaletel, L. Z., Popit, M., & Zaletel, M. (2018). Is Carotid Stiffness a Possible Surrogate for Stroke in Long-term Survivors of Childhood Cancer after Neck Radiotherapy? Radiol Oncol, 52(2), 136-142. doi:10.2478/raon-2018-0006

Zeiher, A. M., Fisslthaler, B., Schray-Utz, B., & Busse, R. (1995). Nitric oxide modulates the expression of monocyte chemoattractant protein 1 in cultured human endothelial cells. Circ Res, 76(6), 980-986. doi:10.1161/01.res.76.6.980

Zeisberg, E. M., Tarnavski, O., Zeisberg, M., Dorfman, A. L., McMullen, J. R., Gustafsson, E., Chandraker, A., Yuan, X., Pu, W. T., Roberts, A. B., Neilson, E. G., Sayegh, M. H., Izumo, S., & Kalluri, R. (2007). Endothelial-to-mesenchymal transition contributes to cardiac fibrosis. Nat Med, 13(8), 952-961. doi:10.1038/nm1613

Zeng, Mu-Sheng, & Zeng, Yi-Xin. (2010). Pathogenesis and Etiology of Nasopharyngeal Carcinoma. In J. J. Lu, J. S. Cooper, & A. W. M. Lee (Eds.), Nasopharyngeal Cancer: Multidisciplinary Management (pp. 9-25). Berlin, Heidelberg: Springer Berlin Heidelberg.

Zeng, Y. X., & Jia, W. H. (2002). Familial nasopharyngeal carcinoma. Semin Cancer Biol, 12(6), 443-450. doi:10.1016/s1044579x02000871

Zhang, W., Chen, Y., Chen, L., Guo, R., Zhou, G., Tang, L., Mao, Y., Li, W., Liu, X., Du, X., Sun, Y., & Ma, J. (2015). The clinical utility of plasma Epstein-Barr virus DNA assays in nasopharyngeal carcinoma: the dawn of a new era?: a systematic review and meta-analysis of 7836 cases. Medicine (Baltimore), 94(20), e845. doi:10.1097/MD.0000000000000845

Zhou, Q. S., Zhao, Y. M., Li, P. X., Bai, X., & Ruan, C. G. (1992). Thrombomodulin as a Marker of Radiation-Induced Endothelial Cell Injury. Radiation Research, 131(3), 285-289. doi:10.2307/3578417

Zimmerman, Guy A., Elstad, M. R., Lorant, D. E., McIntyre, Thomas M., Prescott, S. M., Topham, Matthew K., Weyrich, Andrew S., & Whatley, Ralph E. (1996). Platelet-activating factor (PAF): signalling and adhesion in cell-cell interactions. In Platelet-Activating Factor and Related Lipid Mediators 2 (pp. 297-304): Springer.

Zingg, S., Collet, T. H., Locatelli, I., Nanchen, D., Depairon, M., Bovet, P., Cornuz, J., & Rodondi, N. (2016). Associations Between Cardiovascular Risk Factors, Inflammation, and Progression of Carotid Atherosclerosis Among Smokers. Nicotine Tob Res, 18(6), 1533-1538. doi:10.1093/ntr/ntv255